

Final Report

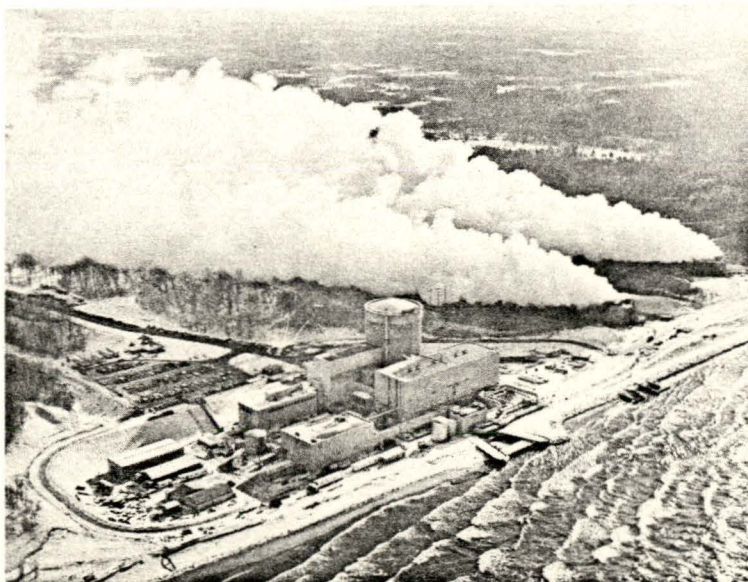
*An Investigation of the
Meteorological Impact of
Mechanical-Draft Cooling Towers
at the Palisades Nuclear Plant*

by

EDWARD RYZNAR
DENNIS G. BAKER
MICHAEL R. WEBER
DENNIS F. KAHLBAUM
MICHAEL ST. PETER

Under contract with:
Consumers Power Company
Jackson, Michigan

January 1980



College of Engineering
Department of Atmospheric and Oceanic Science

Docket # 5000 255
Control # 8003140 240
Date 8/03/10 of Document:
REGULATORY DOCKET FILE

8003140 242

The University of Michigan
College of Engineering
Department of Atmospheric and Oceanic Science

Final Report

AN INVESTIGATION OF THE METEOROLOGICAL IMPACT
OF MECHANICAL-DRAFT COOLING TOWERS AT THE
PALISADES NUCLEAR PLANT

by

Edward Ryznar
Dennis G. Baker
Michael R. Weber
Dennis F. Kahlbaum
Michael St. Peter

DRDA Project 320158

under contract with:

CONSUMERS POWER COMPANY
JACKSON, MICHIGAN

administered through:
The Division of Research Development and Administration

January 1980

PREFACE

This is the final report of the investigation under Contract Number 72-1221-KB2 between Consumers Power Company and the University of Michigan. It discusses and summarizes aspects of the work described briefly in quarterly letter reports submitted since July 1972 and in detail in six annual reports submitted since 1973. Additional results have been published in six data reports which contain summaries and tabulations of all temperature, humidity, precipitation, wind velocity, visibility and solar radiation data recorded by the project's 13 meteorological stations from 1972 through 1977. A final data report for the period 1 December 1978 through the end of the measurement phase in March 1979, is in preparation.

A large number of present and former University of Michigan staff and students have participated in the investigation since it began. Former participants have been individually acknowledged in previous reports and the authors once again would like to thank them. Particular thanks are given to Donald Pearson for maintaining data collection and monitoring equipment performance throughout the entire measurement phase of the investigation. Those who made important contributions to data processing in the last year are Will Beaton, Randy Bliss, Mark Casper, Dennis Hodges, Ken Kurdziel and Bruce Wattle.

Many personnel at the Palisades Plant itself also were extremely helpful. Larry Kenaga and his colleagues maintained the time lapse camera system on the roof of the turbine building and oversaw the plume observation program. The observation program involved both plant security and engineering personnel, who took time to observe the plume and note their observations on plume questionnaires. They completed 2238 questionnaires in 1040 days of cooling tower operation.

The study could not have been conducted at all if several property owners hadn't sacrificed enough of their property for the installation of a precipitation gage and a weather shelter for the duration of the measurement program. In the case of a main station located at the U.S. Department of Agriculture Office in Bangor, not only were we allowed to locate meteorological equipment in a large area outside the building, but all recording equipment was accommodated inside. The cooperation of Mrs. Krohn, Mrs. Johnson and the other USDA employees there is very much appreciated.

Our special appreciation is expressed to Dr. Harry Moses of the U.S. Department of Energy for providing valuable ideas, comments and suggestions concerning all aspects of the project. The advice and cooperation of Dr. Norton Strommen, former NOAA climatologist for Michigan, Dr. Fred Nurnberger of the Michigan Weather Service and all other members of the advisory committee for the study are gratefully acknowledged.

Mrs. Barbara Walunas typed this and other reports, memoranda and correspondence and handled many administrative details. Sincere thanks are expressed for her capable help.

ABSTRACT

Final analyses, summaries and conclusions regarding the meteorological effects of the Palisades cooling towers are presented and discussed. Topics include (1) statistical analyses of operational and nonoperational visibility, temperature, relative humidity, dew point and precipitation data, (2) cooling tower plume effects on fog, icing, snowfall and solar radiation as determined from measurements and visual and photographic plume observation programs, (3) characteristics of true lake breezes and their effects on the cooling tower plume and (4) a comparison of operational and nonoperational occurrences of meteorological conditions conducive to apple scab infections.

CONTENTS

Preface	page
	ii
Abstract	v
List of Figures	vii
List of Tables	x
I. INTRODUCTION	1
PART A. PLUME BEHAVIOR AND EFFECTS	
II. Observations of fog, icing, drift and precipitation	15
III. Shadowing and effects on measured solar radiation	23
IV. Effects of true lake breezes and their characteristics	26
PART B. STATISTICAL ANALYSES AND COMPARISONS OF OPERATIONAL AND NONOPERATIONAL DATA FROM THE 13 METEOROLOGICAL STATIONS	
V. Fog occurrences and visibility reductions at stations P03A and P07A	39
VI. Temperature, relative humidity and dew point	59
VII. Precipitation	107
VIII. Potential apple scab infection conditions	119
PART C. CONCLUSIONS	
IX. Summary of findings	129
REFERENCES	133
Appendix A Project Publications and Reports	135
Appendix B Percent Data Recovery by Month and Variable	137

LIST OF FIGURES

	page
1.1 Aerial view of Palisades Nuclear Plant and mechanical-draft cooling towers prior to operation.	2
1.2 Aerial view of Palisades Nuclear Plant and mechanical-draft cooling towers during operation on 23 December 1977.	4
1.3 Locations of special meteorological stations comprising the Palisades and Cook networks.	7
1.4 Locations of meteorological stations in the Palisades network.	8
5.1 The frequency of hours with a visibility reduction to 3 km or less and the results for a chi-square test for the winter season.	53
5.2 The frequency of hours with a visibility reduction to 3 km or less and the results of a chi-square test for the spring season.	55
5.3 The frequency of hours with a visibility reduction to 3 km or less and the results of a chi-square test for the summer season.	56
5.4 The frequency of hours with a visibility reduction to 3 km or less and the results of a chi-square test for the autumn season.	57
6.1 Diurnal variation of the average temperature difference between coastal and inland stations for spring.	64
6.2 Diurnal variation of the average relative humidity difference between coastal and inland stations for spring.	65
6.3 Diurnal variation of the average dew point difference between coastal and inland stations for spring.	66
6.4 Diurnal variation of the average temperature difference between coastal and inland stations for summer.	69
6.5 Diurnal variation of the average relative humidity difference between coastal and inland stations for summer.	70
6.6 Diurnal variation of the average dew point difference between coastal and inland stations for summer.	71
6.7 Diurnal variation of the average temperature difference between coastal and inland stations for autumn.	73
6.8 Diurnal variation of the average relative humidity difference between coastal and inland stations for autumn.	74
6.9 Diurnal variation of the average dew point difference between coastal and inland stations for autumn.	75

LIST OF FIGURES (cont.)

	page
6.10 Diurnal variation of the average temperature difference between coastal and inland stations for winter.	77
6.11 Diurnal variation of the average relative humidity difference between coastal and inland stations for winter.	78
6.12 Diurnal variation of the average dew point difference between coastal and inland stations for winter.	79
6.13 Deviation of 1600 EST network station temperatures from network average temperature for spring.	83
6.14 Probability that spring 1600 EST network station temperatures for the operational period exceed those for the nonoperational period.	85
6.15 Probability that spring 1600 EST network station relative humidities for the operational period exceed those for the nonoperational period.	86
6.16 Probability that spring 1600 EST network station dew points for the operational period exceed those for the nonoperational period.	87
6.17 Probability that winter 1600 EST network station temperatures for the operational period exceed those for the nonoperational period.	90
6.18 Probability that winter 1600 EST network station dew points for the operational period exceed those for the nonoperational period.	93
6.19 Probability that average winter temperature, relative humidity and dew point for the operational period exceed those for the nonoperational period at P01A.	95
6.20 Probability that average winter temperature, relative humidity and dew point for the operational period exceed those for the nonoperational period at P02A.	96
6.21 Probability that average winter temperature, relative humidity and dew point for the operational period exceed those for the nonoperational period at P03A.	97
6.22 Probability that average 0100 EST winter relative humidity and dew point for the operational period exceed those for the nonoperational period.	100

LIST OF FIGURES (cont.)

	page
6.23 Probability that average 1900 EST winter relative humidity and dew point for the operational period exceed those for the nonoperational period.	101
6.24 Average 0100 EST winter operational minus nonoperational relative humidity and dew point.	102
6.25 Average 1900 EST winter operational minus nonoperational relative humidity and dew point.	103
7.1 Precipitation differences and hypothesis rejection probabilities for winter.	111
7.2 Precipitation differences and hypothesis rejection probabilities for spring.	113
7.3 Precipitation differences and hypothesis rejection probabilities for summer.	114
7.4 Percent frequency of occurrence of mean daily operational and nonoperational precipitation amounts for summer.	116
7.5 Precipitation differences and hypothesis rejection probabilities for autumn.	117

LIST OF TABLES

	page
1.1 Network instrumentation and calibration schedule.	10
2.1 Plume questionnaire results by quarter.	16
2.2 Summary of plume questionnaire reports by quarter.	17
4.1 Monthly occurrences of true lake breezes for 1973 through 1978.	30
4.2 Number of true lake breezes reaching various distances inland.	32
4.3 Values of $T_{55} - T_9$ for true lake breezes.	35
4.4 Changes in $T_{55} - T_9$ with passage and retreat of true lake breezes.	35
5.1 Hours of advection-radiation fog by month and year.	41
5.2 Example of 2 x 2 contingency table.	44
5.3 Contingency tables of hours of advection-radiation fog at P03A and P07A for visibility ≤ 3 km.	46
5.4 Ratios of hours of a-r fog at one station to total hours of a-r fog at one or both stations.	47
5.5 Visibility contingency table.	50
6.1 Statistically significant differences in temperature, relative humidity and dew point between operational and nonoperational data.	81
8.1 Degrees of apple scab infections for various temperatures.	121
8.2 Number of occurrences of potential apple scab infection conditions.	123

I. INTRODUCTION

Background

The investigation was initiated in 1972 under separate contracts with Consumers Power Company and Indiana & Michigan Electric Company for a joint study of meteorological effects of cooling systems at two nuclear power plants near Lake Michigan in southwestern Lower Michigan. The investigation was concerned with Consumers Power Company's Palisades Nuclear Plant, which uses mechanical-draft cooling towers, and Indiana & Michigan Electric Company's Donald C. Cook Nuclear Plant, which uses a once-through cooling system. Both cooling systems were under construction at the time the investigation began.

The Palisades Nuclear Plant has 36 cooling tower cells as shown in Fig. 1.1. The two blocks are 198 m long, 15.2 m wide, 19.8 m high and about 100 m apart. They are parallel to each other in a west-east line extending inland from near the Lake Michigan shoreline. Sand dunes that rise up to 61 m above Lake Michigan extend inland 0.6 km from near the towers, which are located in an interdunal depression.

In the operation of the Palisades mechanical-draft cooling towers, ambient air is drawn past cascading heated water drops which lose heat to the air by sensible and latent heat transfer processes. The result is that the air leaving a cell is usually a saturated mixture of air and water vapor which is warmer than the ambient

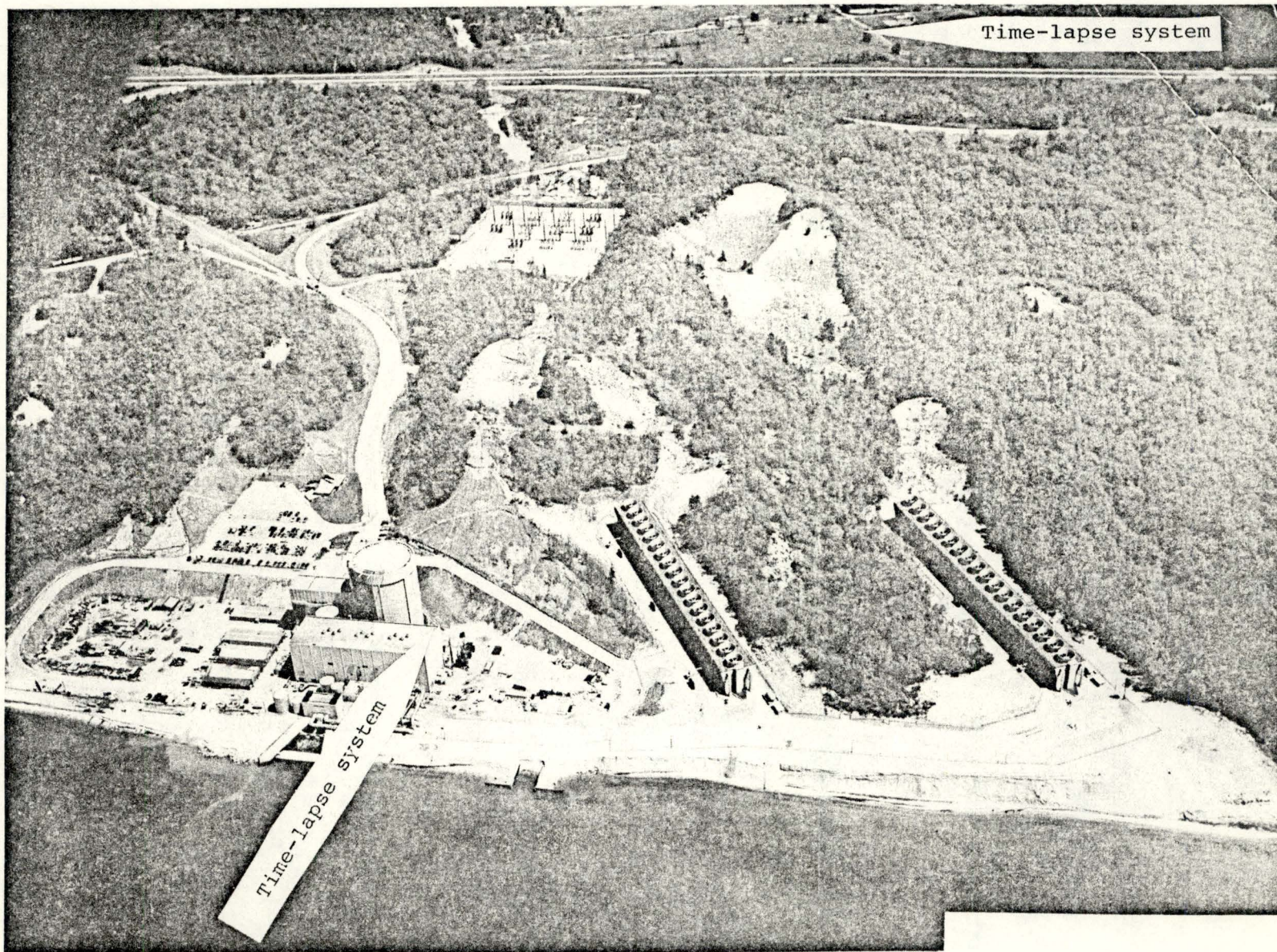


Fig. 1.1: Aerial view of the Palisades Nuclear Plant and mechanical-draft cooling towers prior to operation (Consumers Power Company photo).

air. Condensation of the water vapor occurs as the air leaves the cell and a visible plume usually forms. If the generation load of the nuclear plant is at its full capacity of about 700 megawatts, as many as 12,000 gallons of water per minute may enter the atmosphere directly, both as small droplets which comprise the plume and large drops which fall out as drift. An aerial photograph showing the cooling towers during operation on 23 December 1977 is shown in Fig. 1.2.

In the operation of the once-through system at the Cook Nuclear Plant, water is taken from Lake Michigan at a rate of about 1,645,000 gallons per minute (USAEC, 1973). It becomes heated in cooling the condensers, and the heated water is returned to Lake Michigan. An area of warm water, or thermal plume, spreads out from the discharge point and heat and moisture are lost by conductive, radiative and turbulent transfer processes. According to Carson (1976) the energy flux per unit area into the atmosphere with a lake cooling method is about 3 orders of magnitude less than the energy flux from the top of a cooling tower.

The planning of the joint study took into account that even though meteorological effects of the two methods of cooling were expected to be different, a study of the effects of one system could supplement the other study in many ways, since both cooling systems were located on the Lake Michigan shoreline and separated by a distance of only 33 km. The two investigations were set up as similar

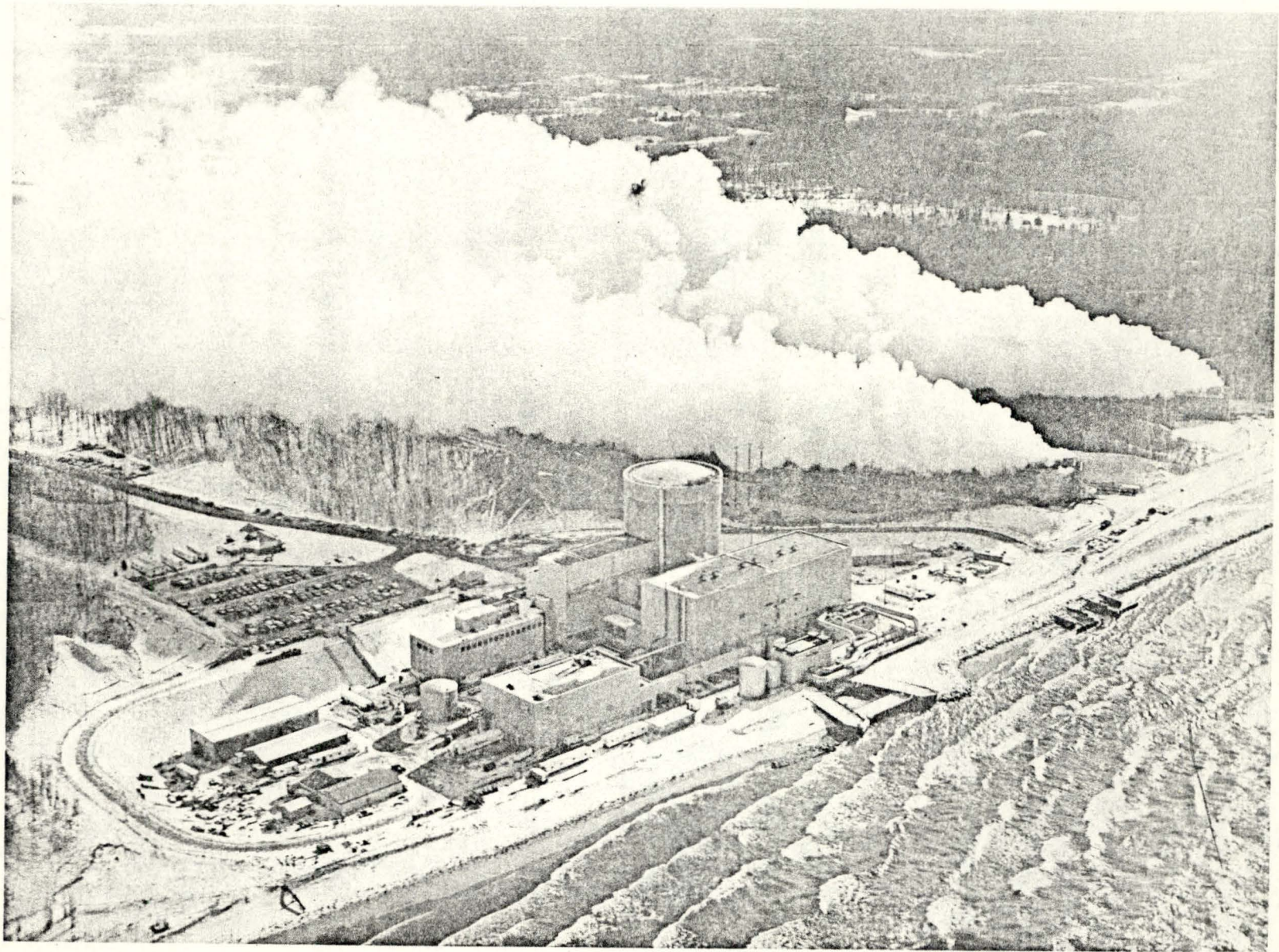


Fig. 1.2: Aerial view of the Palisades Nuclear Plant and mechanical-draft cooling towers during operation on 23 December 1977 (Photo by Hann Photo Service).

5-year projects, therefore, and work on them began in April, 1972, when orders for equipment were placed and locations for meteorological stations were chosen.

Purpose and Approach

The goal of the cooling tower investigation was to determine (1) if the heat and moisture added to the atmosphere affect meteorological conditions inland and (2) if so, to what extent several meteorological variables would be affected. Of major interest and concern, for example, was the possibility that when the cooling tower plume was moving inland it could, under certain atmospheric conditions, increase the humidity near the ground for prolonged periods and, in addition, cause or enhance not only fog and/or icing at the surface, but also cloud growth and precipitation. Humidity increases, if large enough, could seriously impact spraying operations for disease prevention in the fruit belt inland from the cooling towers, for example, and icing could deleteriously affect the trafficability of the I-196 Freeway located about 0.8 km from the cooling towers.

An observational approach was taken in the study which was designed to provide basic information on possible cooling tower effects on fog, solar radiation, precipitation, temperature, and humidity by direct measurements. To the extent possible, information on cloudiness and icing was obtainable from special observations and photographs.

The nearest National Weather Service station which could provide adequate and somewhat representative information on some of these variables was at Muskegon. Because the station was located about 112 km north of the cooling towers, however, it was out of range of their influence. The necessary information closer to the towers was obtained by establishing a special network of 13 meteorological stations extending from near the cooling towers to about 19 km inland (Ryznar, et. al., 1976).

A map showing locations of the stations comprising both the Palisades and Cook networks and stations having other types of meteorological data is shown in Fig. 1.3. Most of the National Weather Service (NWS) cooperative stations shown have valuable long-term temperature and precipitation data. These were used in the study to determine natural variability. Of particular relevance to the Palisades study is the station at South Haven, which is only about 9 km north of the cooling towers and has over 40 years of temperature and precipitation data representative of shoreline conditions. These data were analyzed in detail by Baten and Eichmeier (1955) in terms of climatological characteristics.

A map showing locations of the Palisades network stations in greater detail is given in Fig. 1.4. Temperature, relative humidity and precipitation were measured at all stations. At the two main stations, called P03A

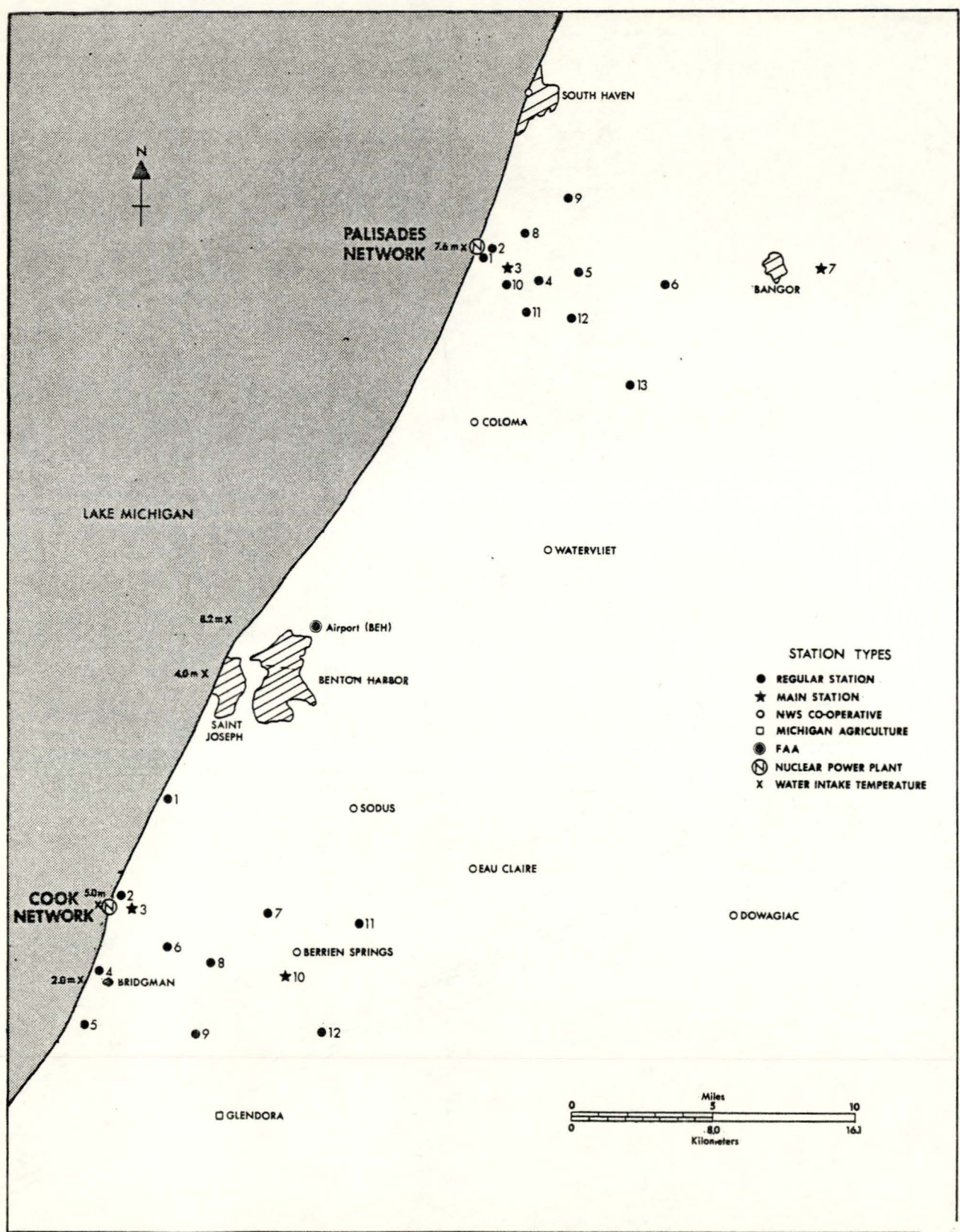


Fig. 1.3: Locations of special meteorological stations comprising the Palisades and Cook networks and other stations from which data were obtained.

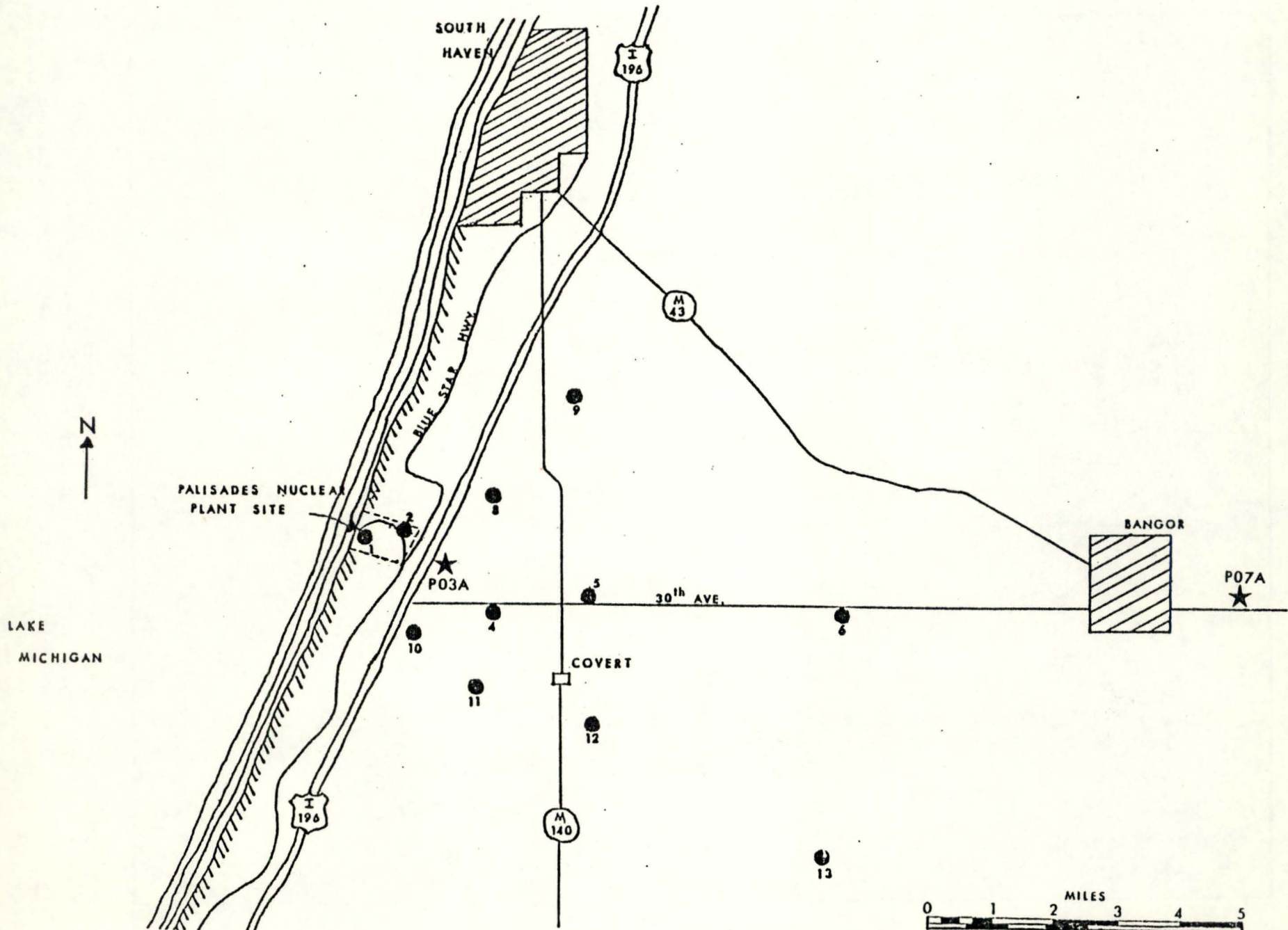


Figure 1.4 Locations of meteorological stations in the Palisades network.

and P07A in this report, wind velocity, visibility, and global solar radiation, consisting of direct plus diffuse solar on a horizontal surface were also measured. The network instrumentation and calibration schedules are given in Table 1.1.

Station P03A was located in a flat field about 1 km ESE of the cooling towers and near the I-196 Freeway. Time-lapse photographs of the plume were made from this station as well as from the roof of the turbine building on-site. In addition to providing general information on plume behavior, the time-lapse photographs were especially helpful in determining occurrences of plume downwash and its downwind extent. Station P07A had the same equipment as P03A except for the time-lapse camera, but because it was about 19 km inland, it was assumed to be out of range of direct cooling tower effects. In this way, it acted as a control station.

The nuclear plant and cooling towers began test operations on 1 April 1975. Plant load was gradually increased to 80% of capacity later that month. Outages lasting from a few hours to a few days were experienced, but the plant remained on line until 20 December 1975, when it was shut down for about five months for refueling and steam generator eddy current testing. It resumed continuous operation on 18 May 1976 and, except for occasional outages lasting from several hours to several days, it maintained an average generator load of about

Table 1.1: Network Instrumentation and Calibration schedule

<u>Variable</u>	<u>Instrument and Source</u>	<u>Height above ground (meters)</u>	<u>Date installed</u>	<u>Months between calib.</u>	<u>Calibration technique</u>
Precipitation	Weighing gage Belfort Inst. Co.	1	10/72	6	Static weights
Temperature Rel. Hum.	Hygrothermograph Model 5-594 Belfort Inst. Co.	1.5	2/73	6	Calib. chamber
Wind Speed	Gill 3-cup Anem. Model 12101 R.M. Young Co.	3	2/73	6	Wind tunnel
Wind Direction	Wind Vane Model 104 WeatherMeasure Corp.	3	2/73	6	Circular linearity
Visibility	Visiometer Model 1580 Meteorology Research Inc.	1.5	10/72 (P03A) 3/73 (C03A) 5/73 (P07A)	12-18	Manufact.
Solar. Rad.	Pyranometer Model R411 WeatherMeasure Corp.	1	10/72 (P03A) 12/72 (C03A) 3/73 (P07A) 12/72 (C10A)	12	Comparison with standard

700 MW(e) until 6 January 1978 when it was shut down for refueling. Testing resumed in April and the cooling towers resumed operation on 21 April 1978. Several prolonged outages were experienced from that time until the end of the measurement program on 26 March 1979.

In keeping with the original plan of the investigation, the final evaluation of the meteorological impact of the cooling towers contained herein is based on (1) an analysis and statistical comparison of nonoperational and operational meteorological data and (2) case studies, observations, and photographs of plume behavior and effects. Lake breezes, which play a major role in determining plume behavior during the spring and summer seasons, are also analyzed in terms of their effects on the plume, frequency of occurrence and penetration inland. The question of cooling tower impact on the fruit industry is addressed directly in terms of a comparison of occurrences of meteorological conditions conducive to potential apple scab infections for nonoperational and operational periods.

PART A. PLUME BEHAVIOR AND EFFECTS

II. OBSERVATIONS OF FOG, ICING, DRIFT AND PRECIPITATION

Introduction

From the time the cooling towers began operation in April 1975 until the measurement program was terminated in March 1979, visual and photographic observations of the cooling tower plume were made. Most of the visual observations were made on-site within about 300 meters of the towers by plant engineering and security personnel, who completed questionnaires concerning characteristics and effects of the plume. Examples of completed questionnaires were given and discussed in each annual report since 1976. Time lapse photographs of the plume were taken from the roof of the turbine building and from station P03A. Final results of the visual and photographic observations are described below.

Visual observations

Table 2.1 lists the number of plume questionnaires completed in each quarter, the number of days of cooling tower operation and the number of observations of plume downwash, fog and icing reported since the cooling towers began operation. The number of days of cooling tower operation was determined from log books of plant operations and from the time lapse photographs.

In the 1042 days of cooling tower operation from April 1975 through 31 March 1979, 2238 questionnaires were

Table 2.1
Plume Questionnaire Results by Quarter

<u>Quarter</u>	<u># Quest.</u>	<u>Days of Operation</u>	<u># Downwash</u>	<u># Plume fog</u>	<u># Icing</u>
4/1/75 - 6/30/75	216	78	75	48	12
7/1/75 - 9/30/75	141	77	27	19	0
10/1/75 - 12/31/75	181	77	79	46	16
1/1/76 - 3/31/76	0	0			
4/1/76 - 6/30/76	85	43	22	14	0
7/1/76 - 9/30/76	69	79	18	28	0
10/1/76 - 12/31/76	226	80	100	127	67
1/1/77 - 3/31/77	402	86	181	147	134
4/1/77 - 6/30/77	271	79	73	68	6
7/1/77 - 9/30/77	161	81	47	57	0
10/1/77 - 12/31/77	174	88	93	108	32
1/1/78 - 3/31/78	6	6	2	5	6
4/1/78 - 6/30/78	66	59	15	29	0
7/1/78 - 9/30/78	119	57	49	63	0
10/1/78 - 12/31/78	71	65	36	55	3
1/1/79 - 3/31/79	50	87	26	38	24

completed. Table 2.2 summarizes the results shown in Table 2.1 in terms of the total number of observations of downwash, plume fog and icing for each of the four quarters. Given in parenthesis is the corresponding percent of the number of questionnaires that reported these effects.

Table 2.2

Summary of Plume Questionnaire Reports by Quarter

<u>Quarter</u>	<u># Quest.</u>	<u>Downwash</u>	<u>Plume Fog</u>	<u># Icing</u>
1/1 - 3/31	458	209 (46%)	190 (41%)	164 (37%)
4/1 - 6/30	638	185 (39%)	159 (25%)	18 (3%)
7/1 - 9/30	490	141 (29%)	167 (34%)	0
10/1 - 12/31	652	308 (47%)	336 (52%)	118 (18%)

Fog. Seasonal changes in reported plume effects on fog are evident in Table 2.2. The percentages of affirmative responses to the question asked concerning downwash, worded as: "did the plume contact the ground?", for example, increased from 29% to 47% from the warm to the cold seasons. A similar increase can be noted in the affirmative responses concerning fog caused by the plume. Combining these results with information obtained from the time lapse photographs shows that between November and March, fog in the form of a downwashing plume occurs near the towers nearly half the time.

Six observations of the plume occasionally descending to ground level near the Blue Star Highway were reported. The highway is 0.7 km from the east end of the cooling towers and is nearly coincident with the east boundary of the Palisades site. Although only six reports of this type were received, it is reasonable to believe that more occurrences took place but were undetected because (1) most visual observations were made in daytime within site boundaries and (2) time lapse photographs showed the plume in limited fields of view and in daytime only.

Icing. Icing due to freezing drift and plume was reported frequently whenever temperatures were below freezing. It was confined mainly to the site itself except for the south boundary, which is about 250 m south of the southernmost block of cooling towers. It was reported as late in the spring as 9 April and as early in the autumn as 12 November. No reports of icing off-site were received. On-site, however, icing due to freezing drift caused damage to vegetation (Rochow, 1978a). Slippery driving conditions on the access road were frequently reported.

Characteristically, the heaviest icing occurred near the towers and consisted of a dense, nearly transparent, type of glaze ice caused by the freezing of the largest and heaviest drift droplets which were the first to fall. Farther downwind, the type of ice changed from glaze ice

to a less dense type of rime ice caused by freezing of the plume rather than of the larger droplets comprising drift.

A case study of a severe icing episode which took place on 18-19 December 1975 was submitted for inclusion in the Fifth Annual Report of Operation for the Palisades Plant submitted by Consumers Power Company to the Nuclear Regulatory Commission in March 1976. Synoptic meteorological conditions which led to the icing were discussed in detail. In addition, a climatological study of the average frequency of occurrence of potential icing conditions for Palisades was described in the Fifth Annual Report (1977).

Drift. Various intensities of drift were always present during cooling tower operation (Rochow, 1978b). In three cases it was observed on the Blue Star Highway at distances of 0.9, 1.2 and 1.4 km east of the cooling towers. In the first two cases, the wind speed measured at station P03A at a height of 3 meters was only about 2 m sec^{-1} and in the third case it was 4 m sec^{-1} .

The downwind transport of drift at Palisades, as illustrated above by the seemingly large distances in spite of light wind speeds, has a complex dependency on wind speed and direction, temperature and humidity and their variations with height. Further complicating the drift transport problem is that the cooling towers are located in an area with higher sand dunes about 50 m east and south of them. With onshore winds, for example,

orographic lifting of air by the dunes takes place which enhances plume rise and adds to the downwind transport. For wind speeds exceeding about 4 m sec^{-1} , however, downwash occurs. These complexities are only pointed out; the present study was not designed to include the special measurements necessary for a more detailed analysis of drift transport.

Precipitation from the plume. Apart from drift, precipitation from the plume in the form of snow was reported on four separate occasions. The first occurred on 19 December 1975 and was described in the report to the NRC cited above. The second occurred on 17 February 1977 with a cloudless sky, a temperature of -14°C and a south wind. Light snow from the plume was reported falling near the visitor's center. The third occurred on 12 January 1979 with a 3000 ft overcast and a temperature of -11°C . The plume was moving northwestward toward Lake Michigan. No natural snow was occurring at the time, but very light snow was reported falling from the plume as it passed across the shoreline. The fourth occurred on 17 February 1979 when the sky was cloudless and the temperature was -23°C . Again, an easterly wind caused the plume to move lakeward, with light snow reported falling from it as it passed across the shoreline.

Observations of this type were corroborated by additional communications with the observers who reported the snow. No reports of snow from the plume offsite

were received nor was any significant accumulation reported on site.

Time-lapse photographs

The time-lapse photographs were made every 90 seconds from station P03A beginning in April 1975 and, in addition, from the top of the turbine building beginning in October 1975 (see Figure 1.1). Components of the time-lapse systems and examples of plume photographs in a lake breeze condition were discussed in the Fourth Annual Report (1976). The system at P03A provided information on plume behavior above the sand dunes, which obscure the cooling towers from the camera site. The site had the advantage of being far enough away from the cooling towers that about 0.5 km of the I-196 Freeway was in the camera's field of view. In addition, the field of view for the 1300 m distance to the cooling towers was about 1300 m horizontally and 1000 m vertically. With winds from W through NW the behavior of the plume was photographed as it moved over the freeway. The least information was obtained with east winds or with strong winds from a general southerly or northerly direction which caused downwash. The latter kept the downwashing plume low enough to be obscured by the dunes as it moved nearly parallel to the shoreline. The plume was usually not visible at all with east winds which took it lakeward.

The camera on the roof of the turbine building was located near the southeast corner and faced inland (east).

Its field of view included (1) a section of the parapet of the turbine building, (2) four cooling tower cells at the east end of the north block of towers and (3) the utility-line corridor extending from the turbine building as far as the first supporting tower on top of a sand dune. Because the camera faced in a general easterly direction it was able to provide information on plume diffusion and occurrences of downwash for wind directions from south-southeast clockwise through west-northwest.

All time-lapse films were reviewed and the characteristics of the plume were determined from the photographs from both locations. Notes were taken on plume characteristics such as its direction of movement, if it evaporated and where, if it fragmented or remained as a dense plume, if it downwashed, if it encountered wind direction shear as it rose and if it stimulated cloud development when there were no other clouds visible. The above information was used to document both the results obtained from the plume questionnaires and the plume effects on solar radiation discussed in the next section.

All questionnaires and time-lapse films are on file at the University of Michigan. The information extracted from each questionnaire was entered individually in a master log book and is documented with meteorological data.

III. SHADOWING AND EFFECTS ON SOLAR RADIATION

The time lapse films of the cooling tower plume discussed in the previous section show that the plume often resembles a stratocumulus type of cloud which, for a cloudless sky, shadows an area on the ground as it moves downwind. If more than 7/10 of the sky is already covered by opaque cloudiness, the shadowing is hardly discernible and any additional diminution by the plume of solar radiation reaching the ground is insignificant. If the sky is cloudless except for the plume, however, and if no abnormally large attenuation of solar radiation by atmospheric particulates and/or aerosols is occurring, the plume simultaneously diminishes solar radiation directly where its shadow falls and enhances it on both sides. Examples were discussed briefly in the Fifth (1977) and Sixth (1978) Annual Reports. Evaluations of these effects as well as the seriousness of the shadowing problem in general are described below.

The results are based on case studies for times when an observer was near the pyranometer at station P03A to verify that the sky was cloudless and that the cooling tower plume was the only cause of the variations in solar radiation recorded. The recordings included times when the plume was close to and occasionally intersected an imaginary line connecting the sun and the pyranometer. The plume was fragmenting during these times and produced

frequent brief decreases as well as increases in measured solar radiation. It was found that the mean of each of the 4-hour recordings analyzed was about 6% greater than that which would have occurred with a completely cloudless sky.

The reason for the increase is that the plume reflects solar radiation in a way similar to that of a cumulus-type of cloud. The reflections occur not only back to space from the plume's upper surface but, more importantly, toward the ground from its sides. As a result, ground locations within a certain distance on either side of its main shadow receive not only the direct and diffuse solar radiation they would normally receive with a cloudless sky but also the additional amount reflected by the plume. The reason that the effects of a plume differ from those of cumulus clouds is that cumulus clouds are usually randomly distributed. A plume, however, can move in a relatively constant direction downwind if the wind direction variability is small. Over a matter of hours, therefore, whereas cumulus clouds normally decrease solar radiation compared to its cloudless value, a plume can enhance it at certain locations.

Several factors determine which locations receive smaller or larger than cloudless amounts of solar radiation. The most important is the geometry involving the position and direction of movement of the plume in relation to the position of the sun. A dense plume moving parallel to the shoreline (north or south), for example, can be expected

to increase solar radiation in an inland (east) direction just after sunrise and in a lakeward (west) direction just before sunset. Near solar noon, areas on both sides of the plume receive additional solar radiation regardless of the plume's direction of movement. The steadier the wind direction, the more prolonged will be the time that (1) the area shadowed completely by the plume receives less solar radiation at the same time that (2) areas on each side of it receive more.

Regarding shadowing effects by the plume in general, cloudiness information obtained from climatological summaries for Muskegon shows that except for the summer season, shadowing by the plume does not significantly add to that produced by natural daytime cloudiness. For example, natural daytime cloudiness covers an average of 8.5 tenths of the sky in winter, 6.6 tenths in spring, 5.2 tenths in summer and 6.7 tenths in autumn (Michigan Department of Agriculture, 1971). Even in summer, shadowing is usually not pronounced except in the early part of the day. Time lapse photographs show that after 1100 local time, on most summer days the plume evaporates within a short distance of the cooling towers unless a lake breeze forms. In this case abrupt changes in plume characteristics and behavior can take place, as discussed in the following section.

IV. EFFECTS OF TRUE LAKE BREEZES AND THEIR CHARACTERISTICS

Introduction

Because the Palisades cooling towers are located on the shore of Lake Michigan, the behavior of the cooling tower plume in the warm seasons is often determined by diffusion characteristics associated with lake and land breeze circulations. Time lapse photographs show, for example, that the plume's behavior and characteristics undergo significant changes during and immediately after the passage of a true lake breeze and during the more gradual passage of a land breeze.

The importance of lake breezes in affecting plume behavior caused their characteristics to be studied since the measurements comprising this investigation began in 1973. Analysis of recordings of temperature and humidity at each station and of wind velocity at the four main stations for the 6-year period of recordings provided information on lake breeze occurrences, penetration inland and speed of movement inland. These characteristics were studied in relation to other meteorological variables such as cloudiness and offshore wind speed. Each annual report since 1974 contains an updated summary of findings. Final results are discussed below.

Types of lake breezes

A true lake breeze, abbreviated in this discussion as TLB, is defined here as air from over Lake Michigan moving onshore and inland and displacing warmer air moving toward the lake. Because the air along the leading edge of a TLB is

displacing warmer air, it has many of the characteristics of a cold front, or TLB front in this case.

Whereas the offshore wind preceding a TLB is caused by the large-scale pressure distribution as indicated by isobars on a weather map, the TLB itself is a daytime wind caused by a lake-to-land pressure difference generated by the land becoming warmer than the water. The Michigan shoreline in the vicinity of the cooling towers is oriented approximately north-northeast to south-southwest, so a TLB moves inland against an existing wind direction which is between northeast clockwise through south. Its passage is best characterized and detected by a shift in wind direction from a general easterly to a westerly one.

Although it is not considered here, another type of lake breeze occurs more frequently than the TLB at the Palisades location. It is a type which occurs when the existing wind is already onshore and similar thermal differences between land and water develop. This type of lake breeze adds an impetus to the existing onshore wind and is detectable mainly as an increase in wind speed. Changes in temperature, humidity, wind direction and thermal stability are generally less than those caused by a TLB. As a result, even though it is more common than the TLB along the eastern shore of the lake (because westerly winds are more common than easterly winds in the warm seasons), its overall effects on the cooling tower plume are also less.

Effects on the plume

A well-developed TLB front passing over the cooling tower site causes the plume to change from one which is moving lake-ward and has significant vertical development near the shore to one which is moving inland, is more dense, and has less vertical development. These changes, which may take place in as short a time as 10 minutes, are due to the following meteorological changes accompanying the passage of the TLB and the transition from land air to lake air at the cooling tower site:

- (1) a shift in wind direction from offshore to onshore,
- (2) a decrease in temperature which decreases the wet bulb depression and acts to increase plume density and length,
- (3) an increase in humidity which also decreases the wet bulb depression and acts to increase plume density and length,
- (4) an increase in wind speed which bends the plume over and in many cases leads to downwash, and
- (5) a change in vertical temperature structure to a more stable stratification, which acts to decrease the buoyancy of the plume.

The largest changes in temperature and humidity caused by a TLB front usually occur during times of the greatest land to water temperature contrast. For example, if a TLB does not develop until early afternoon, which is usually the time of maximum temperature and lowest relative humidity, a decrease in temperature of 2°C and an increase in relative humidity of about

20% are common changes.

The following is an example of the relevance of these changes to the behavior of the cooling tower plume. If the air temperature remains near 24°C, but if the relative humidity increases from a value of 40% to 60% due to a TLB frontal passage the wet-bulb temperature increases from about 15°C to 19°C and decreases the wet-bulb depression. The smaller the wet-bulb depression, the less the amount of water that can be evaporated into the air. The effects on the plume are increases in its density and length.

Effects of cloudiness and wind speed on TLB

A total of 187 TLB occurrences in the 6-year period were analyzed to determine how cloudiness and wind speed control the formation and behavior of the TLB. It was found that

1) A TLB will form if the sky is cloudless (or nearly so) and if the speed of the existing wind blowing lakeward does not exceed about 5 m sec⁻¹. It is likely to form between 0900 and 1100 local time and move inland at a speed of about 1 to 2 m sec⁻¹. The lighter the offshore wind and the fewer the clouds, the earlier it will form and the faster and farther it will move inland.

2) If the sky is cloudless and the offshore wind speed is near 6 m sec⁻¹, a TLB is likely to form, but later in the day near the time of maximum land-lake temperature difference. It is not likely to penetrate more than 5 km inland. There is also a strong possibility that it will be forced to retreat, often back to the shoreline itself.

3) A TLB will not form if more than about 7/10 of the sky is covered by clouds or if the existing offshore wind exceeds 7 m sec^{-1} even if the sky is cloudless. In the first case it will not form for the following reason: the greater the cloudiness, the less chance that a large enough land-to-lake temperature difference will develop to enable a TLB to form. In the second case, enhanced turbulent exchange of heat and momentum associated with an offshore wind of about 7 m sec^{-1} does not allow the land-to-lake temperature difference to become large enough near the shoreline to create the pressure field necessary to initiate a lake breeze circulation.

Occurrences from 1973 through 1978

Table 4.1 shows the number of occurrences of true lake breezes by month for each year from 1973 through 1978.

Table 4.1

Monthly Occurrences of True Lake Breezes for
1973 through 1978

	M	A	M	J	J	A	S	O	N	TOT
1973	5	3	2	2	2	3	1	3	0	21
1974	3	1	4	5	7	10	5	0	0	35
1975	1	3	4	4	5	7	3	1	2	30
1976	2	2	5	4	4	8	4	1	0	30
1977	1	6	6	6	4	5	3	2	0	33
1978	0	6	7	3	7	9	5	0	1	38
Tot	12	21	28	24	29	42	21	7	3	187

It can be noted from Table 4.1 that an average of about 31 TLB occur between March and November each year and that July and August have the largest number of occurrences. The fact that the TLB is most frequent in these two months can be explained in terms of average air and water temperatures, cloudiness and wind speeds which occur in combination along the eastern shore of Lake Michigan. Compared to average conditions for the other months shown, July and August have the highest maximum temperatures (about 26°C), the least daytime cloudiness (about 4/10 coverage) and the lowest wind speeds (about 4 m s⁻¹). The average water temperature near the surface is about 21°C. The overall result is that the land to water temperature difference, which is the driving force of the TLB, is enhanced in these months by the small amount of daytime cloudiness, which allows the land to warm and by the low wind speeds, which remove proportionately less heat from the land by turbulent exchange than do the higher wind speeds of the other months shown.

Penetration inland

Table 4.2 shows the 187 occurrences in terms of the number that reached various maximum distances inland.

Table 4.2

Number of True Lake Breezes Reaching
Maximum Distances Inland

	<u><1</u> km	1-5 km	5-11 km	11-19 km	>19 km
1973	4	2	4	3	8
1974	3	3	6	10	13
1975	2	7	7	5	9
1976	1	3	7	7	12
1977	2	1	10	5	15
1978	3	6	5	5	19
Total	15	22	39	35	76

It can be noted from Table 4.2 that a total of 76 of the 187 TLB, or nearly every second one, moved at least as far inland as the farthest station, which was P07A at 19 km. On the other hand, 15 passed the shoreline stations but were just barely discernible when they passed stations near 1 km inland.

Although they are not shown explicitly in Table 4.2, 50 TLB reached some maximum distance inland but were then forced to retreat lakeward by the existing offshore wind and/or by an increase in cloudiness which decreased the land-to-lake temperature difference. Of the 50 TLB fronts which returned lakeward, 24 were forced back to the shoreline itself. For these occurrences, the meteorological changes which were associated with the TLB moving inland were reversed, with corresponding changes in the characteristics of the cooling tower plume.

Vertical temperature structure

The availability of meteorological tower data for 1975 through 1978 enabled a total of 129 TLB occurrences to be analyzed to determine their effects on thermal stability. The analysis was based on hourly averages of temperature data obtained from Meteorological Evaluation Services Inc., Amityville, New York, which has the responsibility for processing and tabulating wind and temperature data from the meteorological tower located at the Donald C. Cook Nuclear Plant. The tower is located on top of a sand dune about 300 m from Lake Michigan. In addition to wind sensors, the tower contains temperature sensors at 9 and 55 m. For 1978, similar data were provided by Consumers Power Company from a newly installed meteorological tower at the Palisades site.

Although there are many variations of the TLB, a typical behavior of wind direction throughout the day associated with the TLB consists of a morning wind shift to onshore, a gradual clockwise veering of the wind throughout the day due to the effect of Coriolis force and an evening wind shift to an offshore wind direction as the land cools to the water temperature (Weber, 1978). Effects of the various wind directions on temperature differences between 9 and 55 meters were determined using hourly values (1) prior to TLB passage, (2) covering the time of TLB passage, (3) for the period of onshore wind, (4) covering the time of the evening wind shift from onshore to offshore and (5) after the wind shift and subsequent return to land air had occurred.

Results of the analysis are shown in Table 4.3 and Table 4.4. Table 4.3 shows averages of $T_{55}-T_9$ for the hour prior to, during the TLB period, and for the hour after the passage of a TLB front. Table 4.4 shows averages of the changes that took place with TLB passage and retreat. In all cases actual, and not potential, temperatures were used.

It can be noted from Table 4.4 that in 114 cases, the average temperature difference for the hour prior to TLB passage was negative (thermally unstable stratification, or lapse) with an average of -1.4°F . This is equivalent to a height decrease in temperature of about $1.7^{\circ}\text{C}/100\text{ m}$, or nearly twice the adiabatic lapse rate. With moderate wind speeds, such a temperature difference is conducive to rapid vertical and horizontal diffusion of the cooling tower plume. During the daytime period with onshore winds, the average temperature difference for 114 cases was nearly the same as above. One hour after the evening wind shift from onshore to offshore, however, 63 of 120 cases had changed to an inversion (thermally stable stratification), 45 retained a lapse and 12 had the same temperature at 9 and 55 m.

From Table 4.4, it can be noted that with the passage of a TLB, an increase in stability occurred in 68 cases, a decrease occurred in 28, and 27 showed no change. With the evening wind shift, the predominant change was toward increasing stability as shown by the 103 positive changes. Some of the 17 negative and zero changes were associated with lake breezes which were forced to retreat lakeward during the afternoon when there was still a pronounced temperature lapse over land.

Table 4.3
Values of $T_{55}-T_9$ for True Lake Breezes*

$T_{55}-T_9$	Hour Prior		During Onshore Winds		Hour After	
	# Cases	Ave. °F	# Cases	Ave. °F	# Cases	Ave. °F
Neg. (lapse)	114	-1.4	114	-1.3	45	-0.9
Pos. (inversion)	5	+2.9	6	+0.9	63	+1.5
Zero	4	0	1	0	12	0

Table 4.4
Changes in $T_{55}-T_9$ with Passage and Retreat of
True Lake Breezes*

Sign of Change	With Passage		With Evening Windshift With Retreat	
	# Cases	Ave. °F	# Cases	Ave. °F
Pos. (incr. inversion or decr. lapse)	68	+0.8	103	+1.1
Neg. (decr. inversion)	28	-0.8	12	-0.6
Zero	27	0	5	0

* Differences in the total number of cases in the various categories are caused by missing data

A comparison of 1978 results was made using data for both the Palisades and Cook meteorological towers. Actual values were slightly different, but both showed (1) instability for the hour prior to TLB passage, (2) an increase in stability with passage, (3) instability during the period of onshore winds and (4) an increase in stability accompanying the wind shift from onshore to offshore. For the hour after this wind shift, however, the Cook data showed an average lapse of -0.4°C but the Palisades data showed an inversion of about $+0.4^{\circ}\text{C}$. One of the main factors responsible is that comparatively flat homogeneous terrain is upwind from the Palisades tower for offshore winds. Wooded inhomogeneous terrain is upwind of the Cook tower, however, which delays the formation of inversions compared to that over flat and level terrain.

PART B. STATISTICAL ANALYSES AND COMPARISONS OF
OPERATIONAL AND NONOPERATIONAL DATA
FROM THE 13 METEOROLOGICAL STATIONS

V. FOG OCCURRENCES AND VISIBILITY REDUCTIONS AT STATIONS P03A AND P07A

Introduction

The possibility that moisture from the cooling towers may increase fog at locations other than those close to the cooling towers, where downwash occurs, was studied with both nonoperational and operational visibility measurements from visimeters at stations P03A and P07A. In the first part of the study, the approach was to determine which episodes of visibility reductions to less than 3 km were caused by advection-radiation fog (abbreviated in this report as a-r fog) and then to compare occurrences and durations at the two stations when the cooling towers were operational and nonoperational. Meteorological conditions conducive to a-r fog formation as they might be affected by cooling tower operation were discussed in detail in the Fourth Annual Report (1976).

In the second part of the study, statistical methods and tests were applied to the number of hours with visibilities reduced to 3 km or less by meteorological obstructions other than snow. The purpose was to determine if an increase in the number of hours of visibility reductions occurred during cooling tower operation and if so, whether the increase was statistically significant.

Advection-radiation fog

The basic assumption in this study was that station P07A, because it was located about 19 km inland from the

cooling towers, was out of range of tower influence on a-r fog, so occurrences there were due to natural causes only. A-r fog at P03A, which was located about 1 km from the cooling towers, however, was also due to natural causes, but occurrences and durations there could be enhanced by moisture from the cooling towers. Non-operational and operational occurrences of a-r fog at both stations were compared, therefore, to determine if significant increases occurred at P03A which were not attributable to natural causes.

Nonoperational and operational occurrences. The number of hours with a-r fog at both stations is given by month and year in Table 5.1 for the preoperational years of 1973-74 and the operational years of 1975 through 1978. The corresponding percentages of available data recorded in each month are also listed. These data comprise the basis for the contingency analysis discussed below.

Contingency Tabulation. The statistical method found to be effective in analyzing the data in Table 5.1 for a possible cooling tower effect is the 2 x 2, or tetrachoric, contingency table applied to individual episodes of a-r fog at each station. The reason that the method is useful is that if there are two events, a and b, only one of which must occur, and two other events, c and d, only one of which must occur, a determination can be made concerning

Table 5.1 Hours of advection-radiation fog by month and year

	<u>P03A</u>		<u>P07A</u>	
	Avail. Data (%)	Hours Fog	Avail. Data (%)	Hours Fog
<u>1973</u>				
	(Preop.)			
J	74	0	0	-
F	58	0	0	-
M	0	-	0	-
A	0	-	0	-
M	72	34.4	51	13.1
J	100	59.2	91	18.5
J	100	78.6	98	38.2
A	97	103.5	61	26.7
S	100	61.9	61	13.6
O	99	87.5	100	26.3
N	100	5.7	100	5.4
D	97	0	100	0
<u>1974</u>				
	(Preop.)			
J	0	-	97	0
F	55	0	94	10.7
M	60	5.5	66	5.9
A	0	-	0	-
M	43	6.6	75	13.8
J	100	51.5	99	25.9
J	100	78.1	100	30.6
A	86	93.8	68	23.9
S	93	123.8	0	-
O	100	14.2	0	-
N	100	31.9	0	-
D	100	0	0	-

Table 5.1 (cont.)

	P03A		P07A	
	Avail. Data (%)	Hours Fog	Avail. Data (%)	Hours Fog
			<u>1975</u>	
J	99	0	0	-
F	99	0	34	0
M	100	19.5	100	0
A	100	9.4	73	0.2
M	78	26.5	100	11.9
J	94	74.6	100	32.6
J	81	120.3	100	31.0
A	96	60.2	89	31.9
S	87	51.2	95	43.3
O	100	45.5	100	28.6
N	88	25.4	69	26.9
D	87	0	0	-
			<u>1976</u>	
J	100	0	0	-
F	100	0	0	-
M	93	1.4	85	0
A	89	16.8	99	4.9
M	91	20.5	100	21.3
J	98	42.6	100	22.4
J	81	26.1	89	30.0
A	100	113	100	67.6
S	100	38	90	35.1
O	90	20	100	12.4
N	97	0	98	0
D	21	0	84	0

Table 5.1 (cont.)

	P03A		P07A	
	Avail. Data (%)	Hours Fog	Avail. Data (%)	Hours Fog
<u>1977</u>				
J	20	0	81	0
F	40	0	93	0
M	77	0	100	0
A	87	3.2	99	0.2
M	100	28.8	98	3.1
J	96	17.7	92	7.5
J	100	29.7	99	7.1
A	90	18.8	100	3.7
S	100	18.4	100	13.6
O	83	11.9	100	8.5
N	97	0	96	0
D	79	0	71	0
<u>1978</u>				
J	33	0	0	-
F	87	0	0	-
M	100	0	0	-
A	100	4.2	0	-
M	100	29.1	95	5.6
J	93	27.5	80	12.8
J	99	29.6	100	8.1
A	87	53.0	99	7.5
S	88	67.9	99	22.5
O	85	36.8	100	13.5
N	100	8.9	100	13.7
D	93	0	85	0

any association between the occurrence of events a and c (Brooks and Carruthers, 1953). The frequencies of (a,c) (a,d) (b,c) and (b,d) are set out in the form of a 2 x 2 contingency table (Snedecor, 1956). An example with stations P03A and P07A is shown in Table 5.2 in which the letters are used as defined below.

Table 5.2 Example of 2 x 2 contingency table

		P03A		Total
		fog	no fog	
P07A	fog	a	b	a + b
	no fog	c	d	c + d
Total		a + c	b + d	a + b + c + d = n

a = hours with fog at both P03A and P07A

b = hours with fog at P07A but not at P03A

c = hours with fog at P03A but not at P07A

d = hours with no fog at either station for days with fog.

One of the main advantages of this method is that recorded data must be available for both stations in order for them to be included in the contingency table. For example, if a-r fog were occurring at one station but data were missing from the other because of equipment malfunction, the occurrence was not counted at all.

As a result, even though the overall totals for a station may be somewhat less than actual, missing data in most cases do not cause the results for one station to be biased with respect to the other.

Table 5.3 consists of contingency tables which give a breakdown of the hours with a-r fog for 1973-74, which were preoperational years, and 1975 through 1978, which were operational years. Relative changes in the number of hours with a-r fog at the two stations can be seen more clearly by incorporating results of Table 5.3 in terms of ratios for individual years. For those days on which fog occurred at a station, ratios of hours of fog at one station alone (b for P07A and c for P03A in Table 5.2) to the total number of hours of fog at one or both stations ($b/a+b+c$ and $c/a+b+c$ as defined above) are shown in Table 5.4.

Table 5.3

Contingency tables of hours of advection-radiation fog at P03A and P07A for visibility \leq 3 km.

1973-1974
(nonoperational)

		P03A		Total
		fog	no fog	
P07A	fog	159	44	203
	no fog	338	2579	2917
Total		497	2623	3120

1975 through 1978
(operational)

		P03A		Total
		fog	no fog	
P07A	fog	465	250	715
	no fog	844	7490	8334
Total		1309	7740	9049

Table 5.4 Ratios of hours of a-r fog at one station to total hours of a-r fog at one or both stations.

	1973-74	1975	1976	1977	1978
P07A alone	$\frac{44}{541} = 8\%$	$\frac{55}{493} = 11\%$	$\frac{68}{341} = 20\%$	$\frac{44}{232} = 19\%$	$\frac{84}{492} = 17\%$
P03A alone	$\frac{338}{541} = 62\%$	$\frac{288}{493} = 58\%$	$\frac{165}{341} = 48\%$	$\frac{129}{232} = 56\%$	$\frac{263}{492} = 53\%$

Table 5.4 shows that station P07A alone had fog about 8% of the total a-r fog hours in the preoperational years of 1973-74 and about 16% of them during the operational years. The corresponding ratios for P03A are 62% and 54%. In general, the much greater number of hours during which P03A alone had a-r fog are real in both cases, but the comparatively small ratio for P07A in the preoperational years is caused mainly by missing data. There were frequent visiometer malfunctions at the beginning of visibility measurement program. It can be noted from Table 5.1, for example, that data recovery for the months of August and September, when a-r fog is most frequent, was 68% or less for P07A but greater than 85% for P03A for both years. The ratios for 1975 through 1978 are probably more representative of the actual difference in a-r fog between the two stations.

The differences in a-r fog between P03A and P07A as well as the small changes from preoperational to operational conditions are due to natural causes and variabilities. Among the most important causes are the naturally higher humidities at P03A resulting from (1) the proximity of that station to Lake Michigan and (2) the slight terrain depression in which it is located. Particularly on cloudless summer evenings with light winds, the coolest air settles into the lowest elevations such as those at P03A. Because the air is already moist, slight cooling increases the relative humidity enough to cause a-r fog frequently to form earlier in the evening and last longer in the morning at P03A than at P07A, which is at a slightly higher elevation.

In summary, the results for the a-r fog study showed that regardless of whether or not the cooling towers were operating,

- (1) July, August and September had the most hours of a-r fog and November through March had the least, and
- (2) station P03A had about twice as many hours of a-r fog as station P07A in the summer when a-r fog was most frequent.

The cooling towers did not increase either the number of a-r fog occurrences or their duration at either station.

Visibility Reductions

To augment the study of a-r fog occurrences described above, a similar study was made of whether the cooling towers affect surface visibilities in general. Choosing an effective technique to determine if natural reductions in visibility are enhanced by the cooling towers is complicated by the fact that, like many meteorological variables, the statistical distribution of visibility data is highly u-shaped. Because of this non-normality, statistical methods which assume normality could not be used. A statistical method which was independent of the sample distribution was required. A method which met this criterion consisted of a 2 x 2 contingency table and a chi-square test to determine independence of the elements in the table (Dixon and Massey, 1979). This method was applied to the visibility data from stations P03A and P07A to determine if an increase in the number of hours of visibility reductions occurred during cooling tower operation and, if so, whether the increase was statistically significant.

For the purpose of this analysis, only complete days of observation from the beginning of visiometer measurements at the two stations until they ended in March, 1979, were used. The data set was categorized according to season and by hour of the day. The number of hours in which the visibility was reduced to 3 km or less (instrument threshold) by obstructions other than snow was then tabulated according to

cooling tower status (operational or nonoperational) and entered into a 2 x 2 contingency table as shown in Table 5.5

Table 5.5. Visibility contingency table

	Vis > 3 km	Vis ≤ 3 km	Total
NONOP	A	B	A+B
OP	C	D	C+D
	A+C	B+D	A+B+C+D=N

where: A and C are the hours in which the visibility was greater than 3 km for the operational and nonoperational periods, respectively. B and D are the hours in which the visibility was less than or equal to 3 km for the nonoperational and operational periods, respectively. N is the total hours of instrument operation.

The chi-square statistic was then generated from this table using the following equation.

$$x^2 = \frac{N(AD-BC - 0.5N)^2}{(A+B)(A+C)(B+D)(C+D)} \geq \chi^2(1)_{1-\alpha},$$

where: A,B,C,D, and N are given above,

0.5 is Yate's Constant, which provides for a better fit between the test statistic (x^2) and a chi-square distribution with 1 degree of freedom, $\chi^2(1)_{1-\alpha}$ is the $1-\alpha$ percentile of a chi-square distribution with 1 degree of freedom and

α is the probability of detecting a change in the frequency of hours of visibility ≤ 3 km when in fact there has not been a statistically significant change. On the tests performed here, α is taken as 0.05.

The hypothesis (H_0) being tested by this method was as follows:

H_0 : the occurrence of fog with visibility ≤ 3 km is independent of the cooling tower operational status.

This hypothesis can be rejected in the classical sense if the minimum expected value (E) is ≥ 5 and if the value of x^2 is $\geq \chi^2(1)1-\alpha$. The value of E is given by the product of the marginal frequencies divided by N. For B, the nonoperational hours of reduced visibility, the expected value E_B may be written

$$E_B = (A+B)(B+D)/N$$

However, Snedecor (1956) in his analysis indicates that this requirement of E_B being ≥ 5 to reject the hypothesis is too strict and that meaningful results can be obtained when E_B is less than 5 by multiplying the value of $\chi^2(1)1-\alpha$ by 1.5. Thus a second criterion for rejecting the hypothesis of independence occurs whenever

$$E_B < 5 \text{ and } x^2 \geq (1.5)(\chi^2(1)1-\alpha).$$

From the 2 x 2 contingency tables, the frequency distribution of hours containing a visibility reduction to 3 km or less was computed for each station and season. These frequency distributions were then plotted for both the operational and nonoperational periods and are shown in Figs. 5.1 to 5.4. In these figures, the frequency of occurrence for each period and hour of the day is equal to

$\frac{\text{the number of observations with a visibility reduction}}{\text{the number of complete days in the operational or nonoperational period}} \times 100$

The number of complete days used in each period and season is also given. Periods of possible cooling tower effects are indicated by the shaded areas between the operational and nonoperational curves.

Below the frequency distribution are shown the results of the chi-square test of independence. The value of x^2 for each hour of the day is represented by the height of the bar; the number above the bar is the minimum expected value (E_B) for that test. The solid horizontal line is the value which x^2 must equal or exceed to reject the hypothesis of independence when $E_B \geq 5$. The dashed line, on the other hand, corresponds to the value x^2 must equal or exceed to reject the hypothesis when $E_B < 5$.

Seasonal variations. Results for the winter season are shown in Fig. 5.1. The nonoperational curve for P03A is higher than the operational curve for all hours except 1100, 1300, 1700, 1800, and 2300, when the operational curve is either concurrent or higher, indicating that cooling tower effects are possible. However, the chi-square tests at each of these hours fail to reject the hypothesis of independence; thus no cooling tower effect is likely.

The nonoperational curve for P07A is also higher than its operational counterpart for all hours except between 0800-1000 and 1400-1700. Again, the chi-square tests fail to reject the hypothesis.

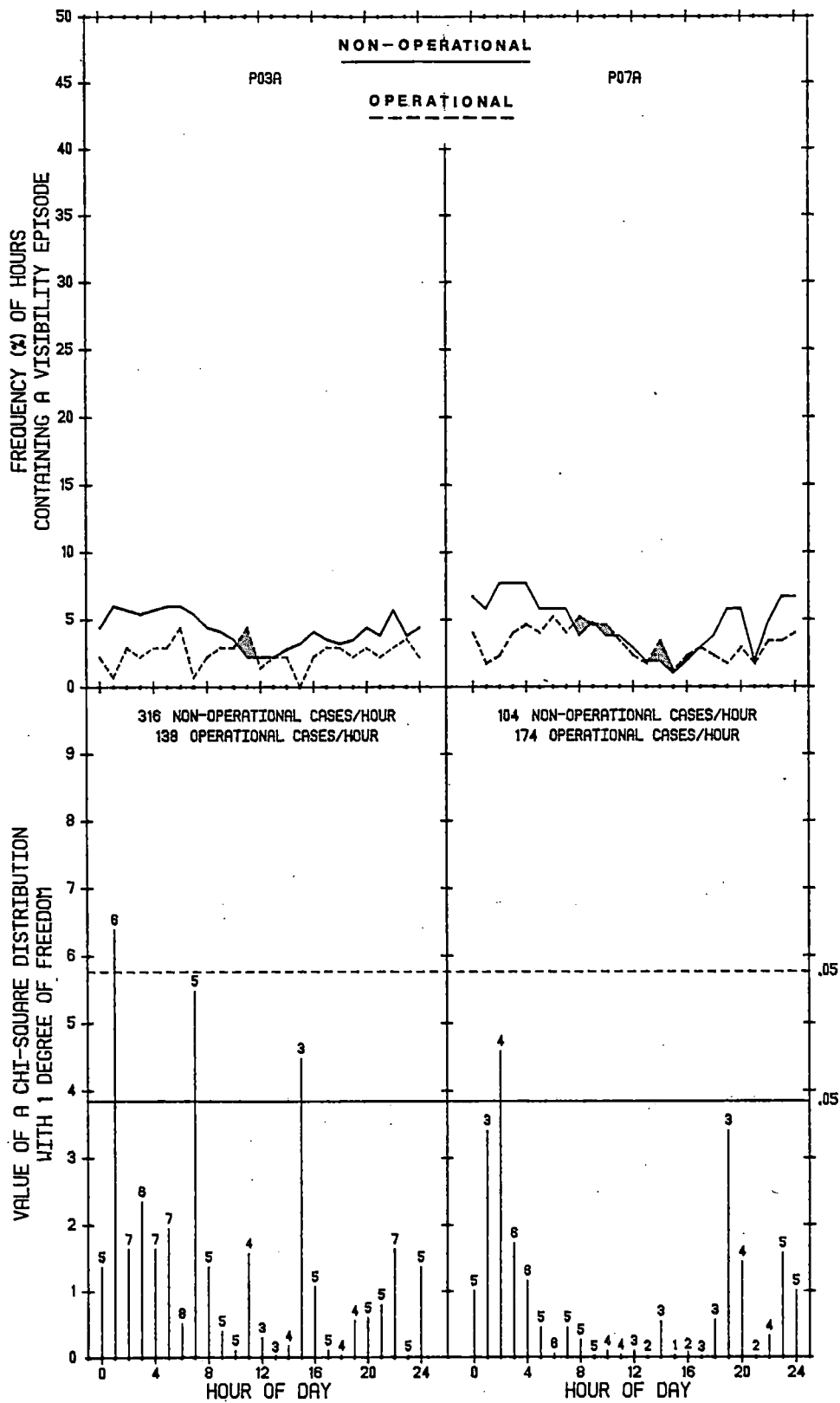


Fig. 5.1: The frequency of hours with a visibility reduction to 3 km or less and the results of a chi-square test for the winter season.

Results for spring are shown in Fig. 5.2. The diurnal variation of visibility is more pronounced for both stations during this season. For P03A, the operational curve exceeds the nonoperational curve for about 15 hours during the morning and afternoon. However, none of the chi-square values is significant at the 5% level. The values at 0900 and 1000 come close to being significant, but they correspond to periods when the operational curve is less than the nonoperational curve.

Similar conditions also occur with the P07A data. Here, the operational curve is higher than the nonoperational curve for 12 hours during the morning and evening. Again, however, none of these differences is statistically significant. Thus, as with the winter season, there is no detectable cooling tower effect.

Results for summer are shown in Fig. 5.3. The diurnal pattern is very pronounced during this season, especially for P03A. Statistically significant results occur for 9 hours for P03A. However, the nonoperational curve for this station is always greater than the operational curve.

For P07A, only two hours (1300, 2000) have significant results. Again, the nonoperational curve is greater than the operational data set at these times.

Results for autumn are shown in Fig. 5.4. The nonoperational curve for P03A is considerably higher than the operational curve during the early morning and late evening hours. Most of these differences are significant at the 5% level.

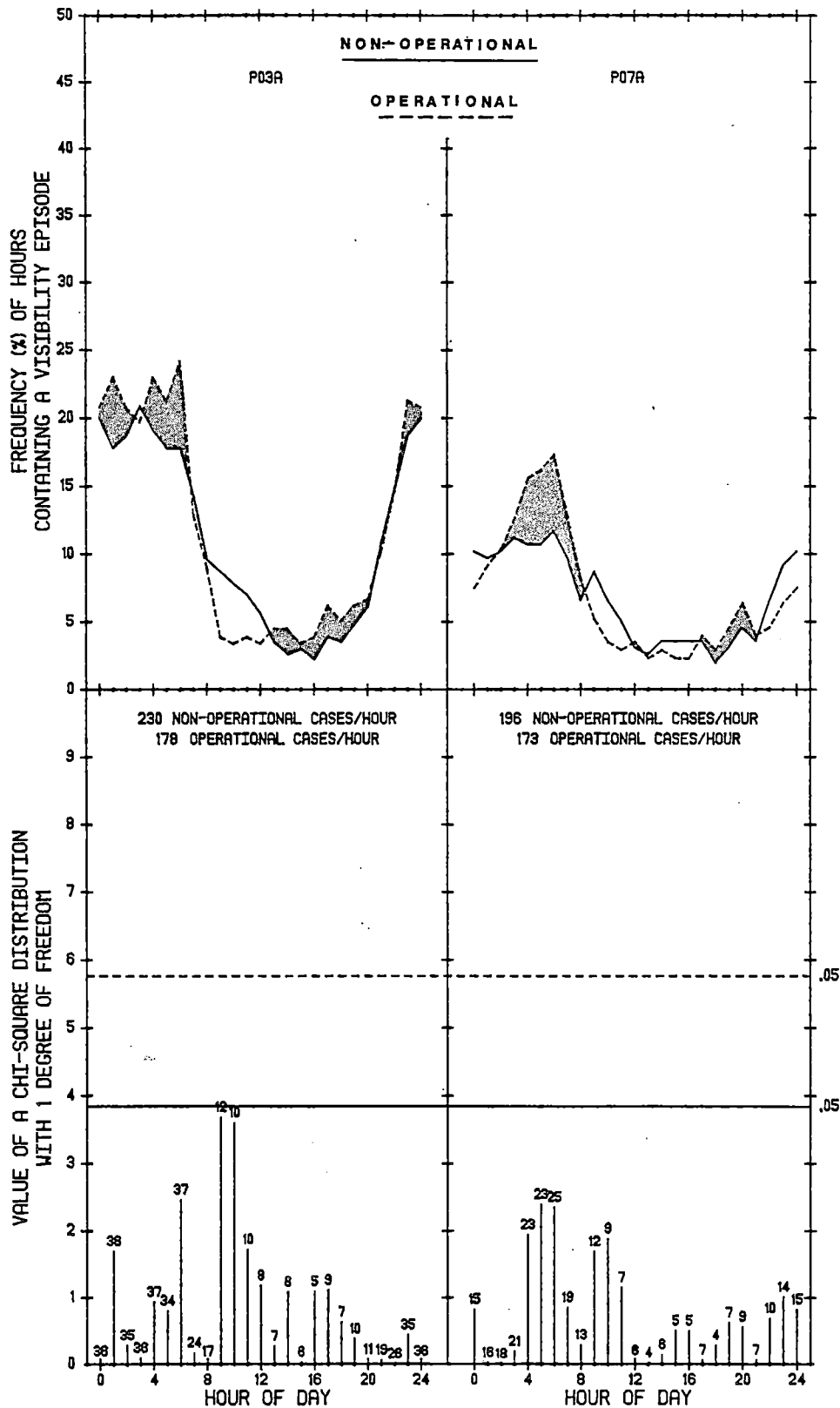


Fig. 5.2: The frequency of hours with a visibility reduction to 3 km or less and the results of a chi-square test for the spring season.

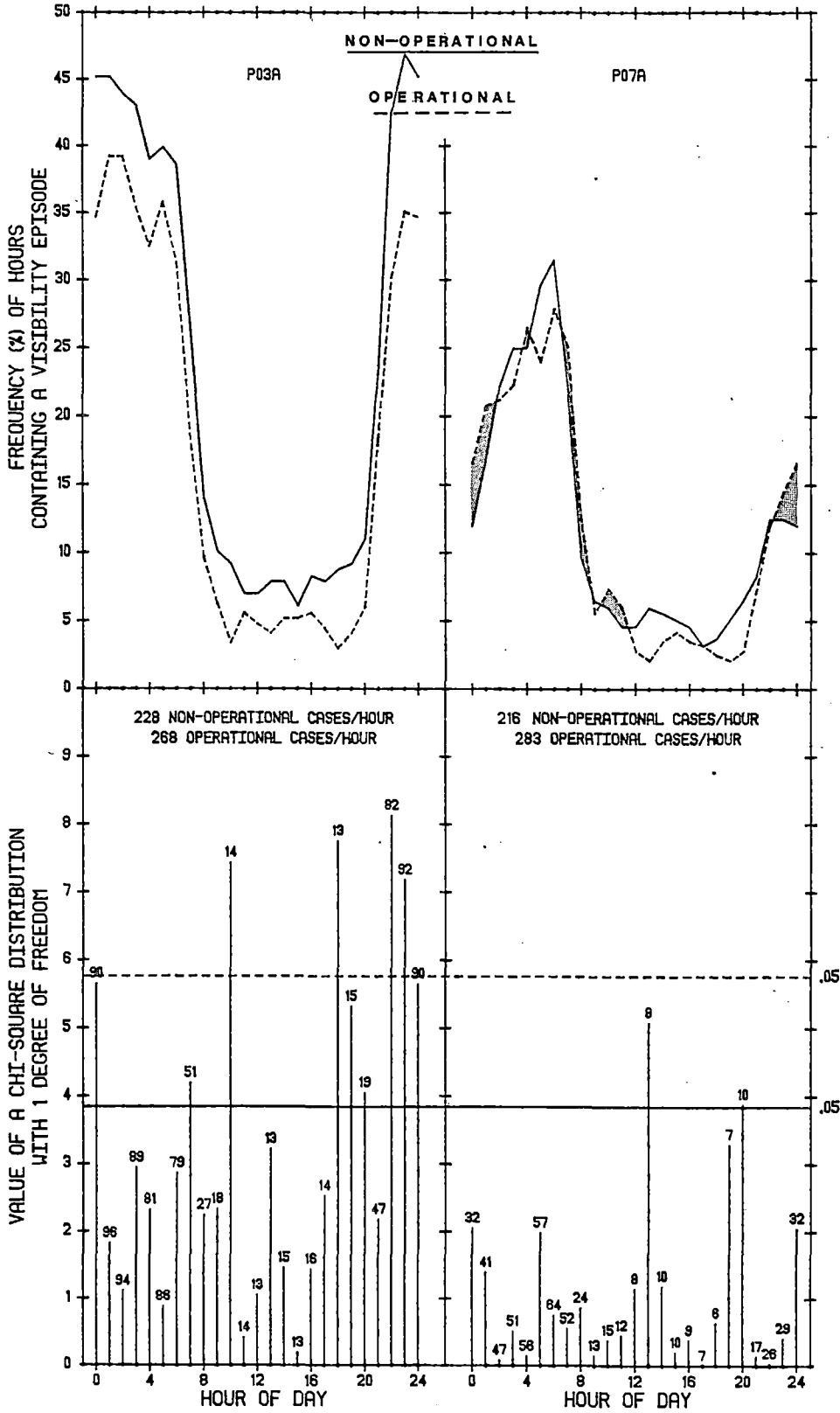


Fig. 5.3: The frequency of hours with a visibility reduction to 3 km or less and the results of a chi-square test for the summer season.

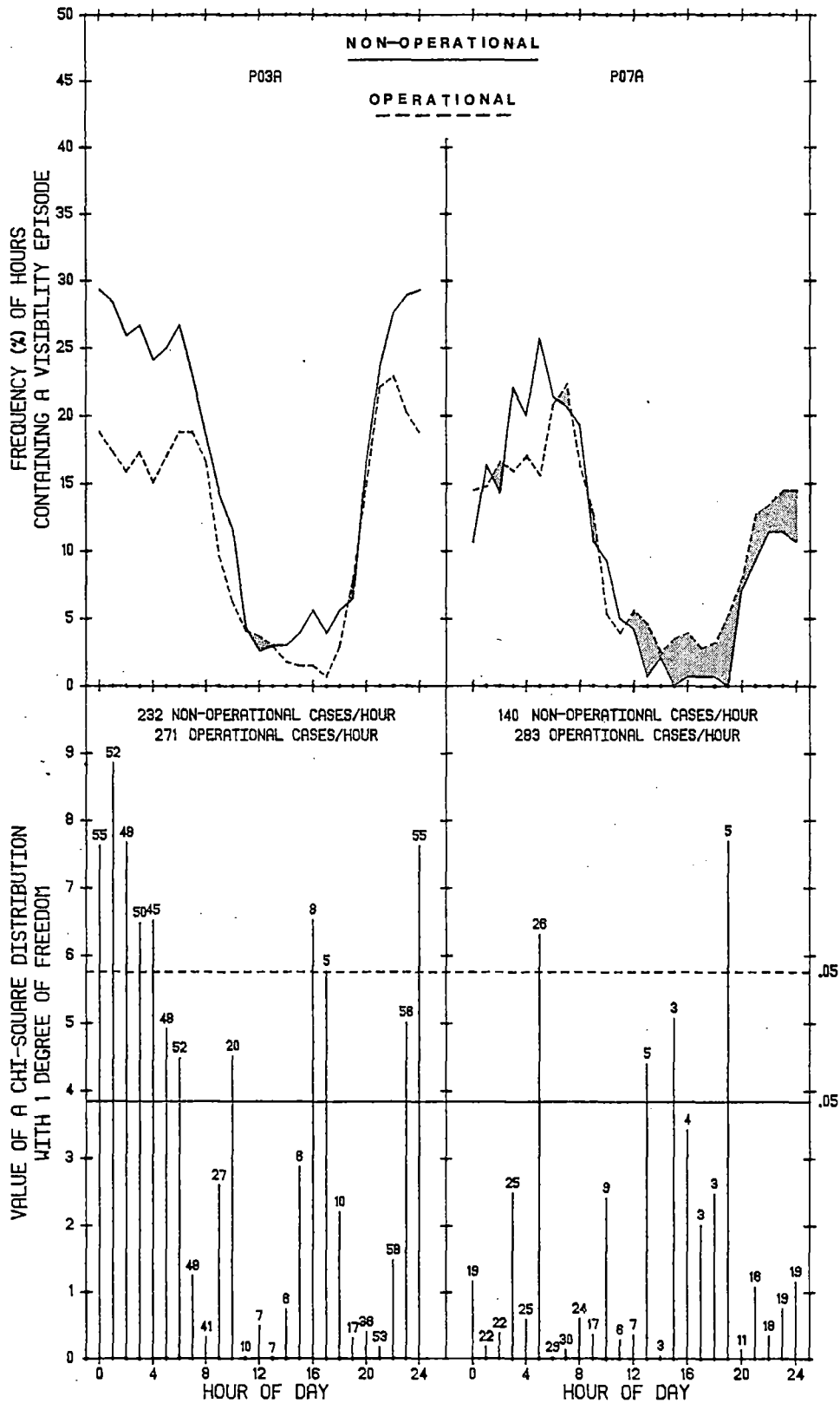


Fig. 5.4: The frequency of hours with a visibility reduction to 3 km or less and the results of a chi-square test for the autumn season.

The operational curve is greater than the nonoperational curve at 1200 and 1900 but the chi-square values for these hours are too low to cause rejection of the hypothesis.

For P07A, the operational curve is above the nonoperational curve for 16 hours (primarily from noon until midnight). However, only two of these hours (1300 and 1900) are significant at the 5% level.

Conclusion. Categorizing visibility reductions according to a 2 x 2 contingency table and applying the chi-square test to determine the significance of these results showed that with the possible exception of occasional periods during the autumn season for station P07A, there is no cooling tower effect on reductions to 3 km or less. Even in these cases, the 19-km distance of P07A from the cooling towers leads to the conclusion that natural causes are responsible.

VI. TEMPERATURE, RELATIVE HUMIDITY AND DEW POINT

Introduction

One of the possible effects of injecting large amounts of heat and water directly into the atmosphere by the cooling towers is an increase in air temperature and/or atmospheric moisture near the towers. The meteorological network established in this study was, in fact, designed to detect such effects if they existed, by means of a before/after comparison of data from the stations near the towers. Such a before/after study has been shown (Lowry, 1977) to be an ideal method for determining the existence of localized effects on climate.

The approach taken in determining possible temperature or humidity effects caused by operation of the cooling towers is to compare operational and nonoperational data for stations near the plant. Since the seasonal average temperature, for example, at those stations can vary greatly from year to year regardless of the operational status of the plant, it is necessary to incorporate additional data into the analysis to take into account such natural variability. The network stations 10-20 km inland, for example, are affected by the same large-scale weather patterns as those near the lake but are far enough away so that there is little chance that their temperatures are affected by the cooling towers. Since, however, data from these inland stations are still representative of conditions near Lake Michigan, they may be used as controls to accommodate natural temperature variations.

Method

The method used in this analysis has been described in detail in previous annual reports, and is summarized below. For each hour, the average temperature for the Palisades inland stations (P06A, P07A, P13A) was subtracted from the average temperature for the stations near the plant (P01A, P02A, P03A, P08A, P10A). After stations were grouped and temperature differences (ΔT) calculated, the data were sorted by wind direction measured at P03A and by the hour of day. The wind direction (WD) sorting was into two categories:

offshore ($55^\circ \leq \text{WD} < 170^\circ$)
and onshore ($235^\circ \leq \text{WD} < 350^\circ$).

Hours with alongshore winds ($350^\circ \leq \text{WD} < 360^\circ$; $0^\circ \leq \text{WD} < 55^\circ$) and ($180^\circ \leq \text{WD} < 235^\circ$) were not used in the analysis. The data were sorted by wind direction because if there is an increase in temperature near the plant, the possibility of detecting it in the station data exists only during periods of onshore winds. In addition, the ΔT data for offshore winds provide a control which may be compared to the ΔT data for onshore winds. The data were finally sorted by hour of day.

Plots of the diurnal variation of the average shoreline minus inland ΔT for each season and wind direction category were made to be able to visually compare the curves for the operational period with those for the nonoperational period. If there is a detectable cooling system effect, one would expect the operational ΔT curves for onshore winds to be

displaced upward (i.e., more positive ΔT) from the nonoperational curves, with no corresponding displacement of the operational curves for offshore winds.

To evaluate the statistical significance of any observed differences, "Student's- t " test was applied. The test requires that the observations in the data sample be independent and approximately normally distributed. With a moderate sample size (30 or more observations), the requirement for normality may be ignored. Hourly observations of most meteorological variables, however, are generally not independent, since the value of a variable for one hour is usually dependent on the value for the previous hour.

To avoid the problem of dependence within a sample, the data were sorted by hour of the day so the observations grouped for any particular hour were separated by at least 24 hours (and often longer, due to the wind direction restriction). The t -test was then applied for each hour of the day. Although the results for any particular hour are closely related to the results for the hours immediately preceding and following it, significant results are separable from the natural diurnal variability in the temperature field.

An identical analysis was performed for relative humidity (RH). In the absence of an increase in temperature near the plant during the operational period, an increase in atmospheric moisture might be detected as a positive displacement of the operational ΔRH curve from the nonoperational curve for onshore winds. ΔRH is defined here as the average coastal minus inland relative humidity. An increase in temperature coupled with an increase in absolute humidity (the actual amount of

water in the air), however, might not be detectable by examination of RH alone, because of the dependence of RH on temperature.

For that reason, the average coastal minus inland dew point (ΔDP) was also analyzed in the same way. The significance of dew point as a moisture variable is that it is a function of the actual amount of water vapor in the air rather than the amount relative to saturation, as is relative humidity. A positive displacement of the operational ΔDP curve from the nonoperational curve for onshore winds would be the expected result if the plant had indeed caused an increase in atmospheric moisture by operation of the the cooling towers.

Discussion

The method described above was used to analyze temperature, relative humidity, and dew point data for December 1973 - March 1979. Results are described by season below. In each of the following figures, the curve made up of open boxes, centered between the "+95%" curve and "-95%" curve represents nonoperational data. Vertical lines show the 95% confidence interval given by the t -distribution. Operational data are plotted as solid circles. The numbers shown at the points plotted at 0600, 1200, 1800, and 2400 EST are the number of observations each of those data points represent.

Spring. Of the 16 months of spring data from March 1974 - March 1979, there were approximately 8 months of nonoperational data, 6 months of operational data, and 2 months (April - May 1978) of no data resulting from the network being de-commissioned from April-November 1978. The diurnal variation of the average difference in temperature, relative humidity and dew point between the coastal and inland stations for both onshore and offshore winds is shown in Figs. 6.1, 6.2 and 6.3, respectively.

In Fig. 6.1 the effect of the relatively cold lake on coastal temperatures is seen in the curves for onshore winds. During the hours of maximum solar heating, inland temperatures averaged about 1.0°C higher than those at the coast during the nonoperational period and 2.0°C higher during the operational period. This may be compared to coastal-inland differences of less than 0.3°C during the same hours, but for offshore winds.

The "+95%" and "-95%" curves show that the magnitude of a statistically significant difference of the operational data from the nonoperational is about $\pm 0.4^{\circ}\text{C}$ for onshore winds and $\pm 0.2^{\circ}\text{C}$ for offshore winds. These values are for the daylight hours, when wind speeds are generally higher, vertical mixing is maximized and local terrain or exposure effects are minimized. As a result, the daytime data are generally made up of more observations and have greater consistency (i.e., smaller variance) than the nighttime data. It can be seen that the operational data for onshore winds fall well outside the lower confidence limit throughout

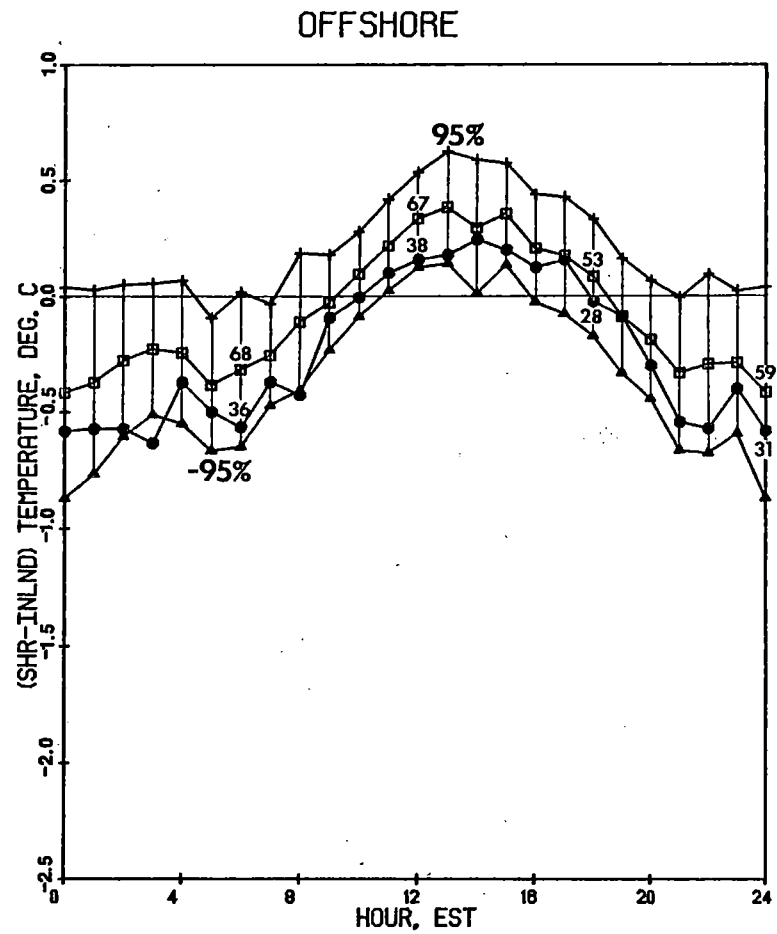
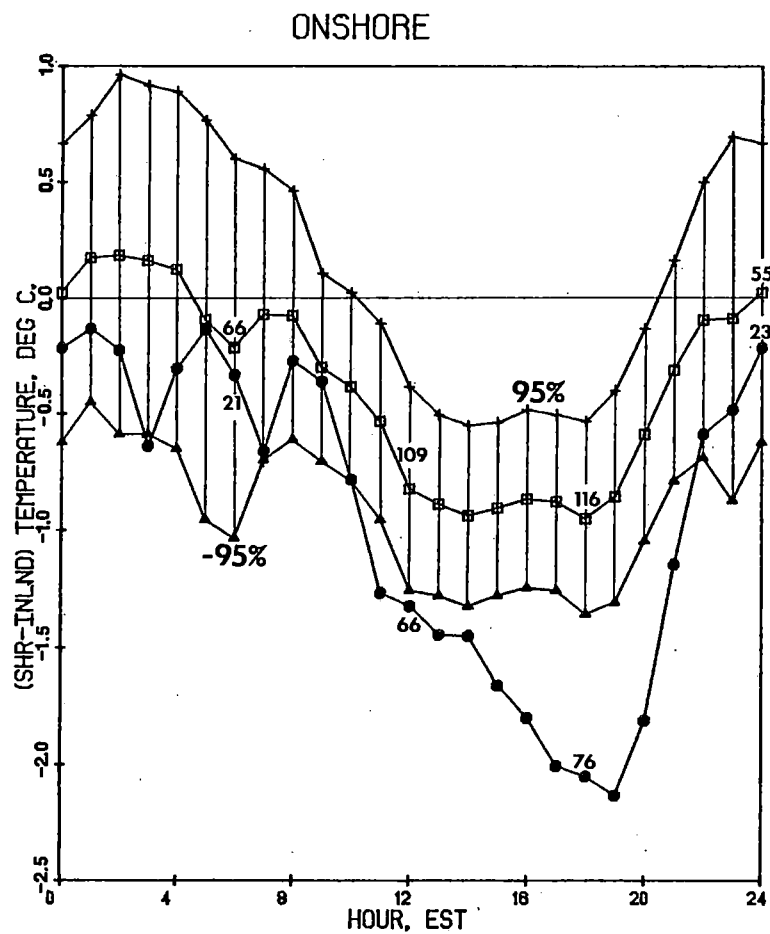


Fig. 6.1: Diurnal variation of the average difference in temperature between coastal and inland stations with onshore and offshore winds, for the spring season.

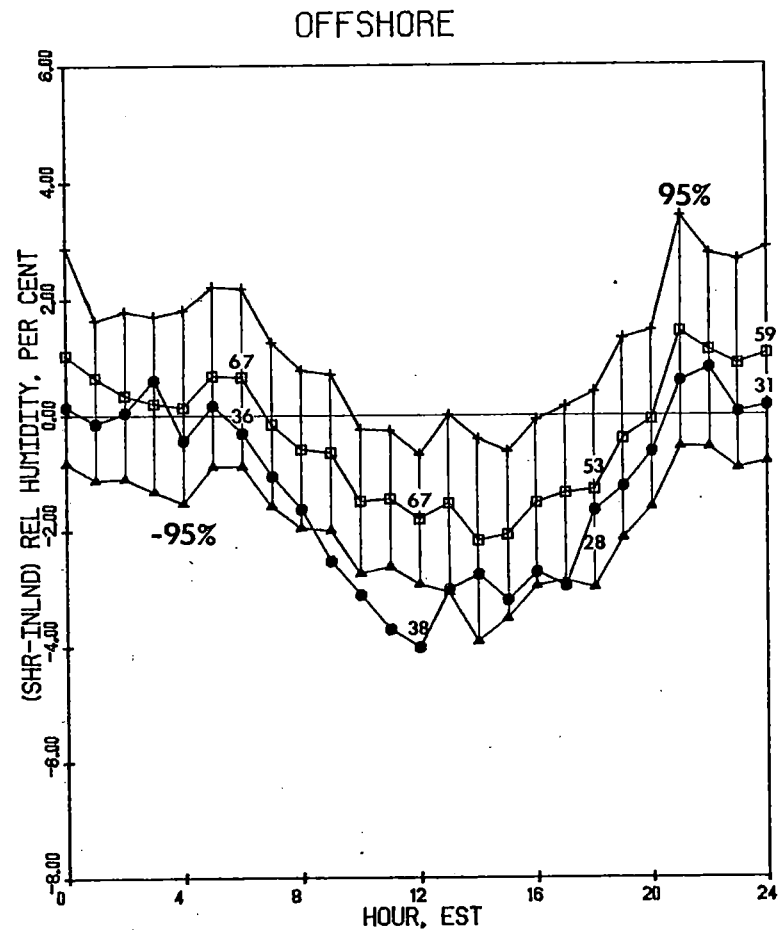
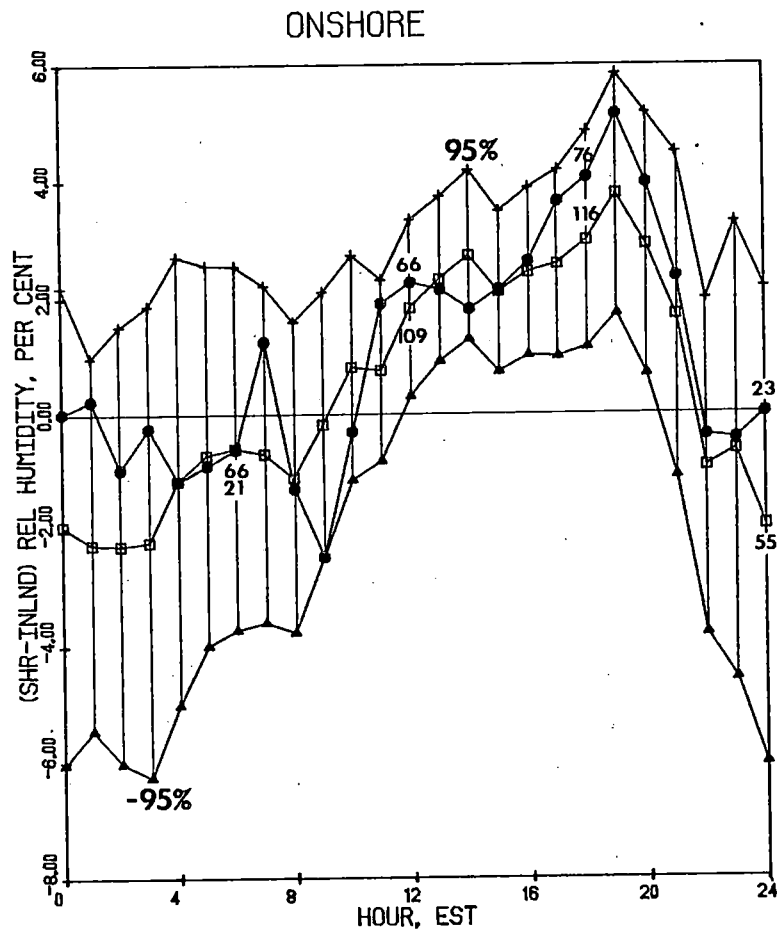


Fig. 6.2: Diurnal variation of the average difference in relative humidity between coastal and inland stations with onshore and offshore winds, for the spring season.

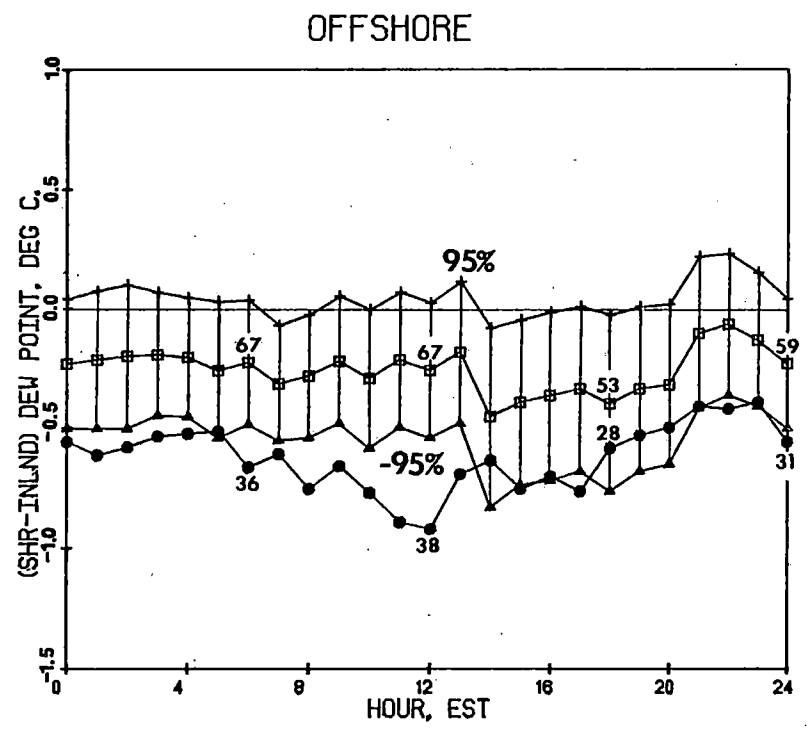
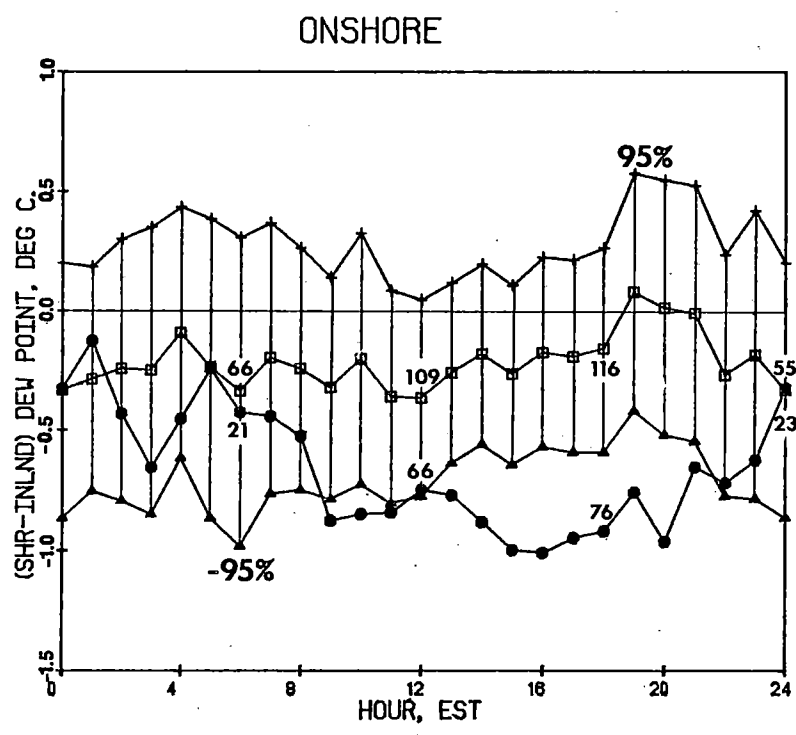


Fig. 6.3: Diurnal variation of the average difference in dew point between coastal and inland stations with onshore and offshore winds, for the spring season.

the afternoon, while operational data for offshore winds are generally within the confidence band. Possible explanations for the observed behavior will be given in the next section, but it may be noted here that the direction of the shift of the operational curve from the nonoperational is exactly opposite to that expected if there were a cooling tower effect.

The ΔRH curves (Fig. 6.2) for onshore winds show a distinct diurnal cycle, which is the inverse of the diurnal ΔT cycle shown in Fig. 6.1. At night, when it is warmer near the coast than it is inland, the relative humidity is lower near the coast. The daytime relative humidity, on the other hand, is higher near the coast mainly because the temperature is lower than it is inland. The combination of these effects is shown in the ΔDP curves (Fig. 6.3). It can be noted that the diurnal cycle of ΔDP is small, implying that there is little diurnal change in the coastal/inland absolute moisture gradient in spring.

The magnitude of a statistically significant difference between operational and nonoperational data is about $\pm 1.5\%$ relative humidity and $\pm 0.4^\circ\text{C}$ dew point for onshore winds and $\pm 1.3\%$ and $\pm 0.3^\circ\text{C}$ respectively, for offshore winds. Operational ΔRH data generally fall within the confidence bands except for the morning hours with offshore winds. Operational ΔDP data are generally lower than the lower limit during the afternoon with onshore winds, as were the corresponding ΔT data. Similarly, the operational ΔDP data for offshore winds are lower than the lower limit during the morning, as were the corresponding ΔRH data.

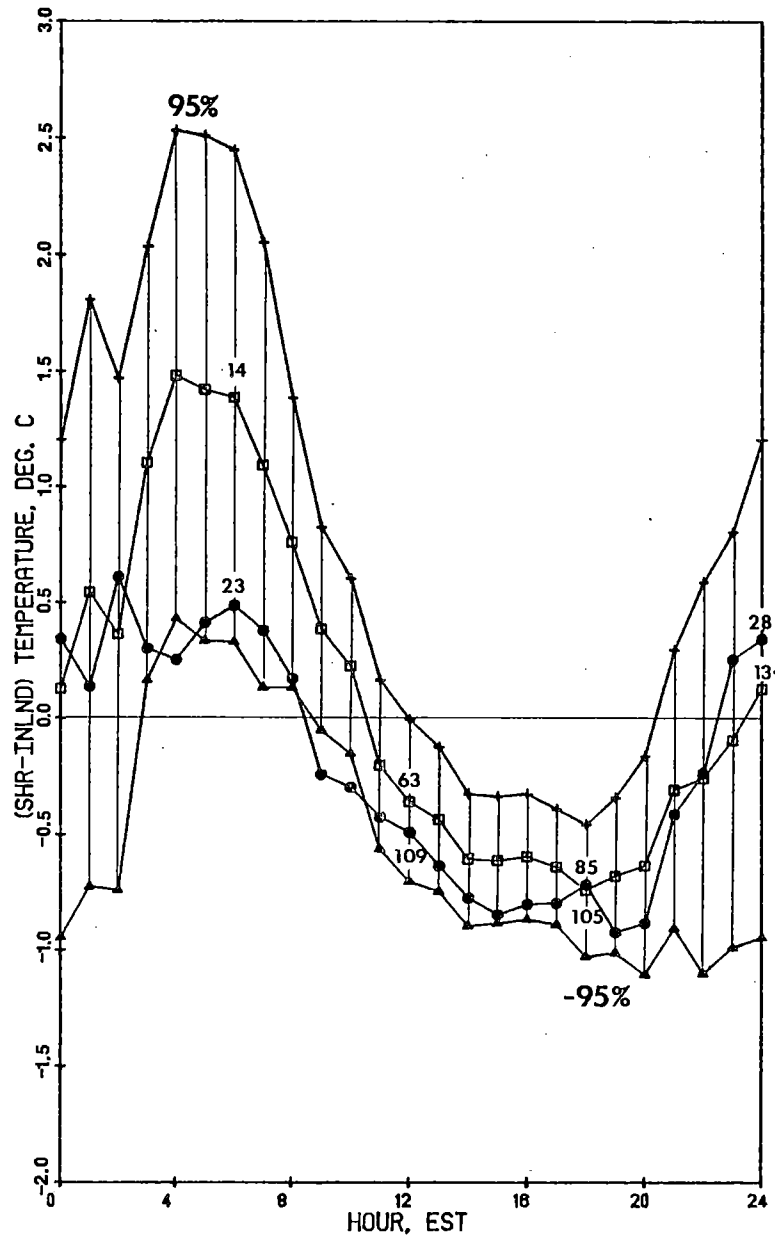
Summer. For the period June 1974 - August 1978, there were approximately 4 1/2 months of nonoperational data, 7 1/2 months of operational data and 3 months of no data (June - August 1978). Summer average diurnal variations of ΔT , ΔRH and ΔDP are shown in Figs. 6.4, 6.5 and 6.6, respectively.

The shapes of the onshore ΔT curves (Fig. 6.4) are similar to those for spring. An effect of the lake being warmer in summer than in spring is seen in the upward shift of the curves (more positive ΔT) on the summer plots. The offshore curves exhibit an unusual diurnal variation which appears to be just the opposite of the onshore variation. Similar plots for stations in the Cook network (not shown here) display little diurnal pattern, with the curves generally matching each other between 1000 and 1900 EST. The surprising result is that ΔT goes negative at night with offshore winds in the Palisades network.

As discussed in previous annual reports, it is believed that this result is due to station locations, since, of the five Palisades shoreline stations, four are located in low-lying terrain. It is likely that temperatures of those stations are affected to a greater degree by local air drainage processes which have been observed to cause large differences in temperature over short distances and could reasonably account for the offshore negative ΔT 's observed at night.

The magnitude of a statistically significant difference in ΔT between the operational and nonoperational periods is

ONSHORE



OFFSHORE

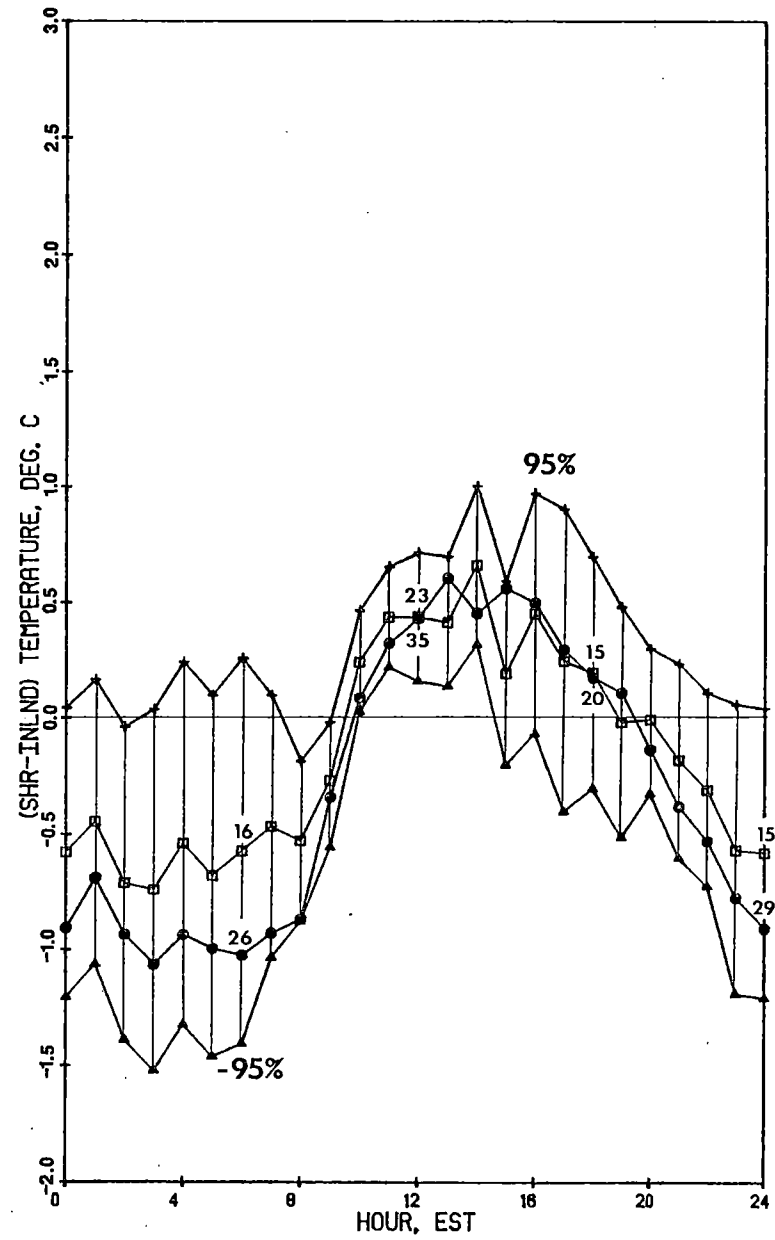
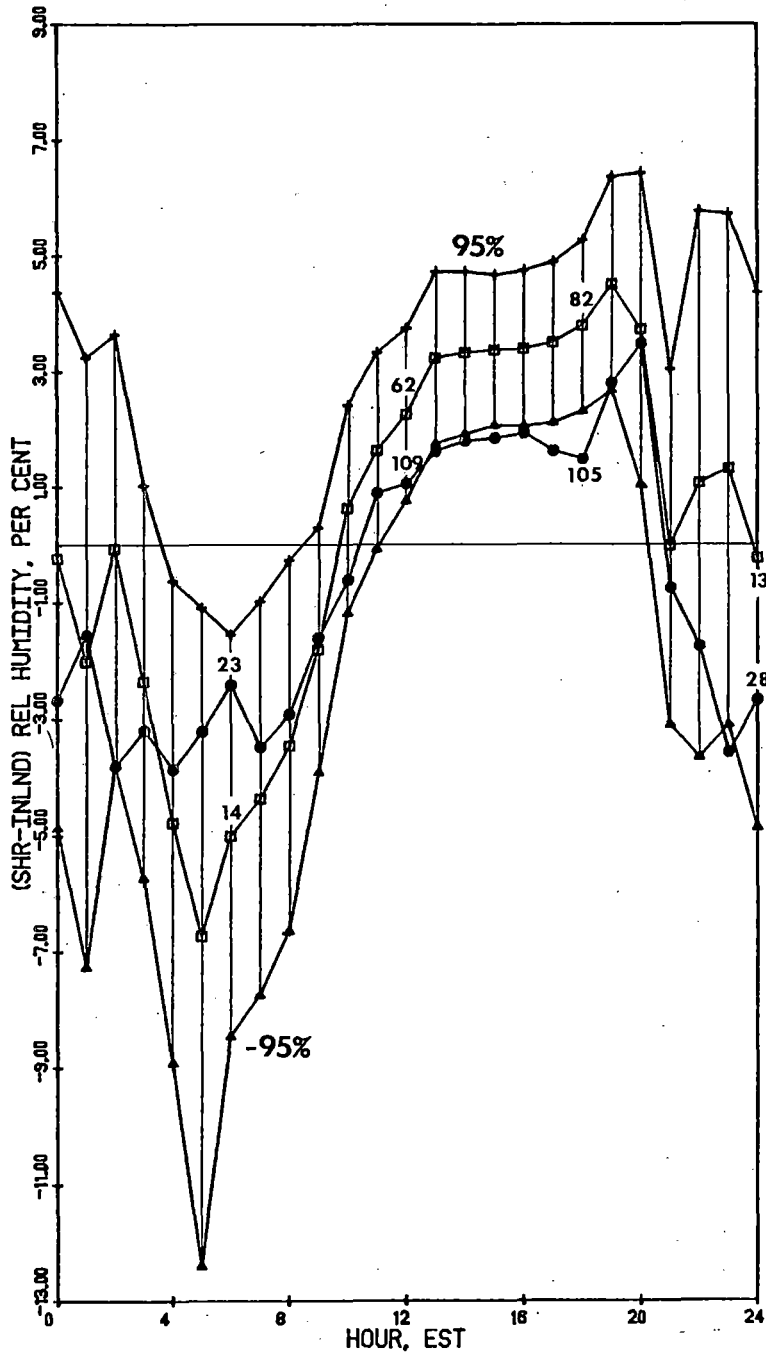


Fig. 6.4: As in Fig. 6.1, for the summer season.

ONSHORE



OFFSHORE

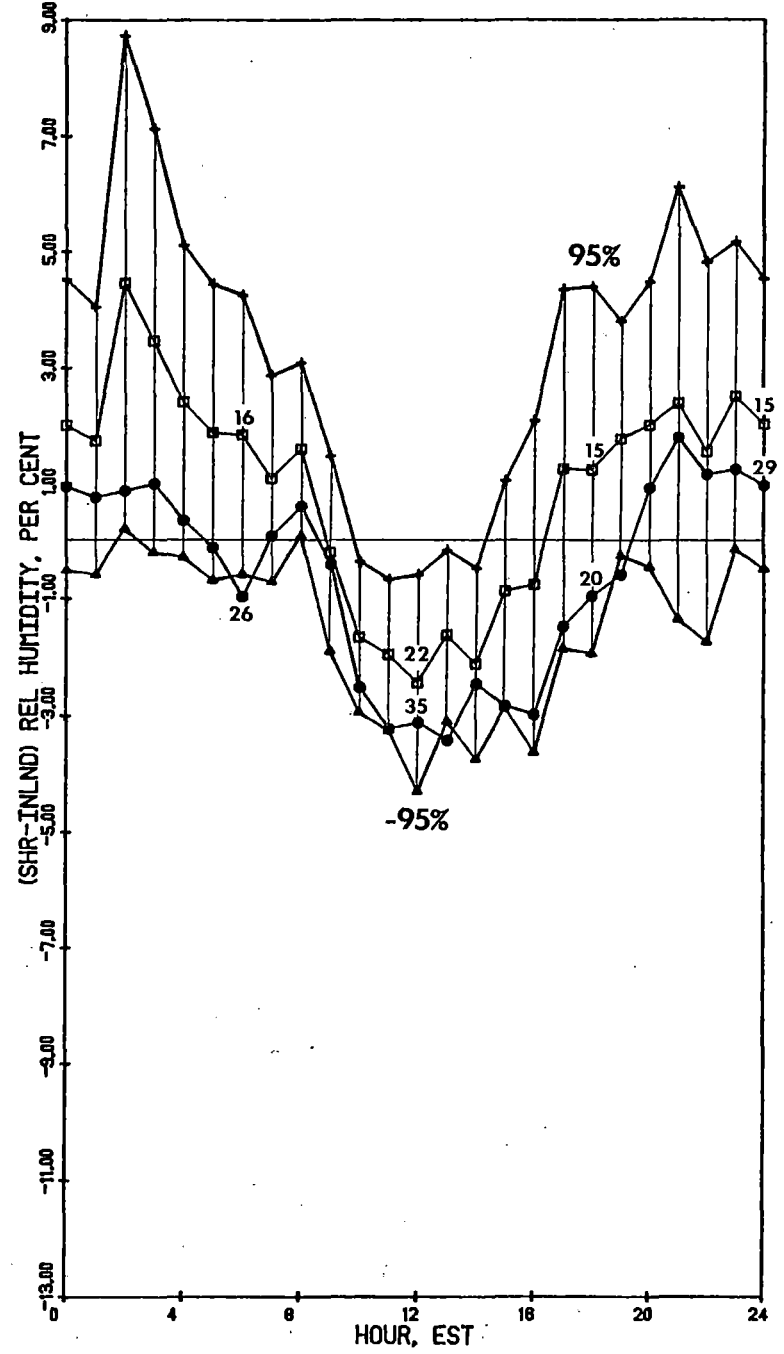


Fig. 6.5: As in Fig. 6.2, for the summer season.

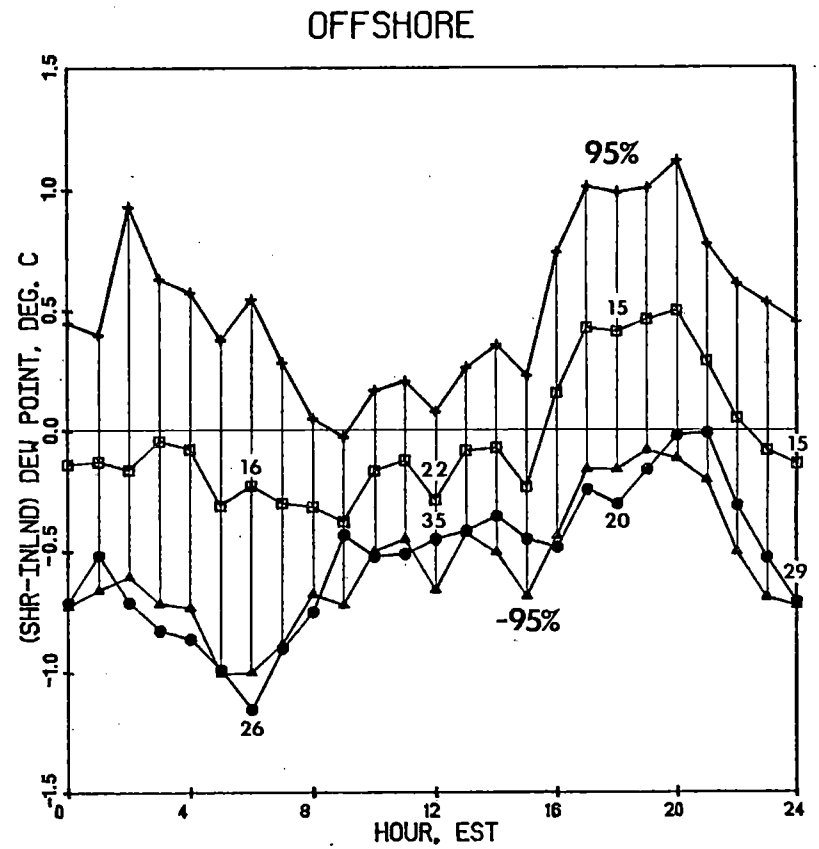
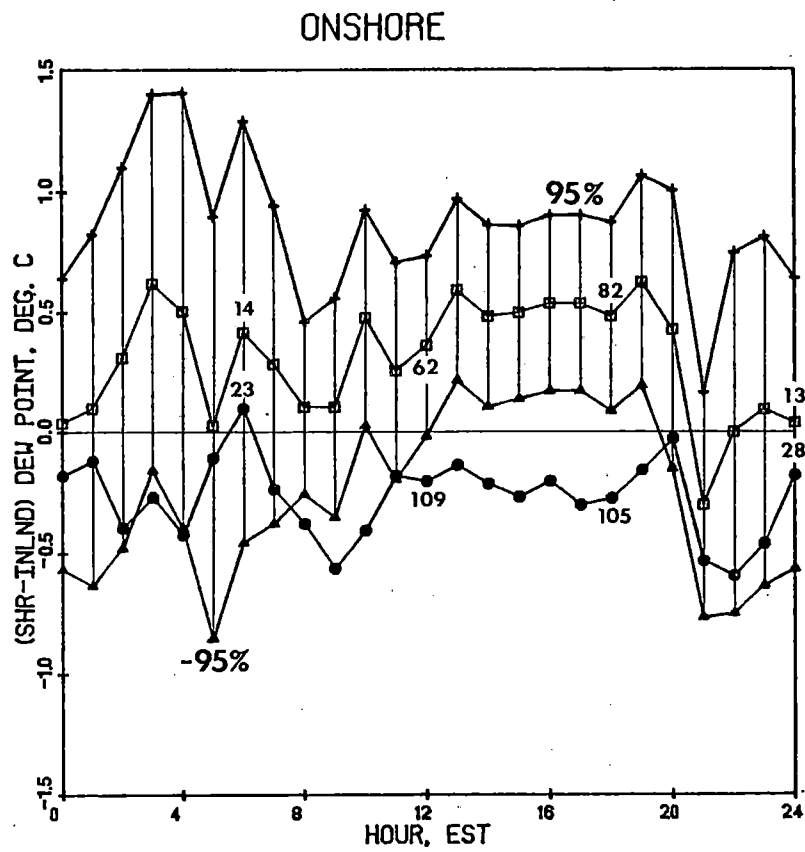


Fig. 6.6: As in Fig. 6.3, for the summer season.

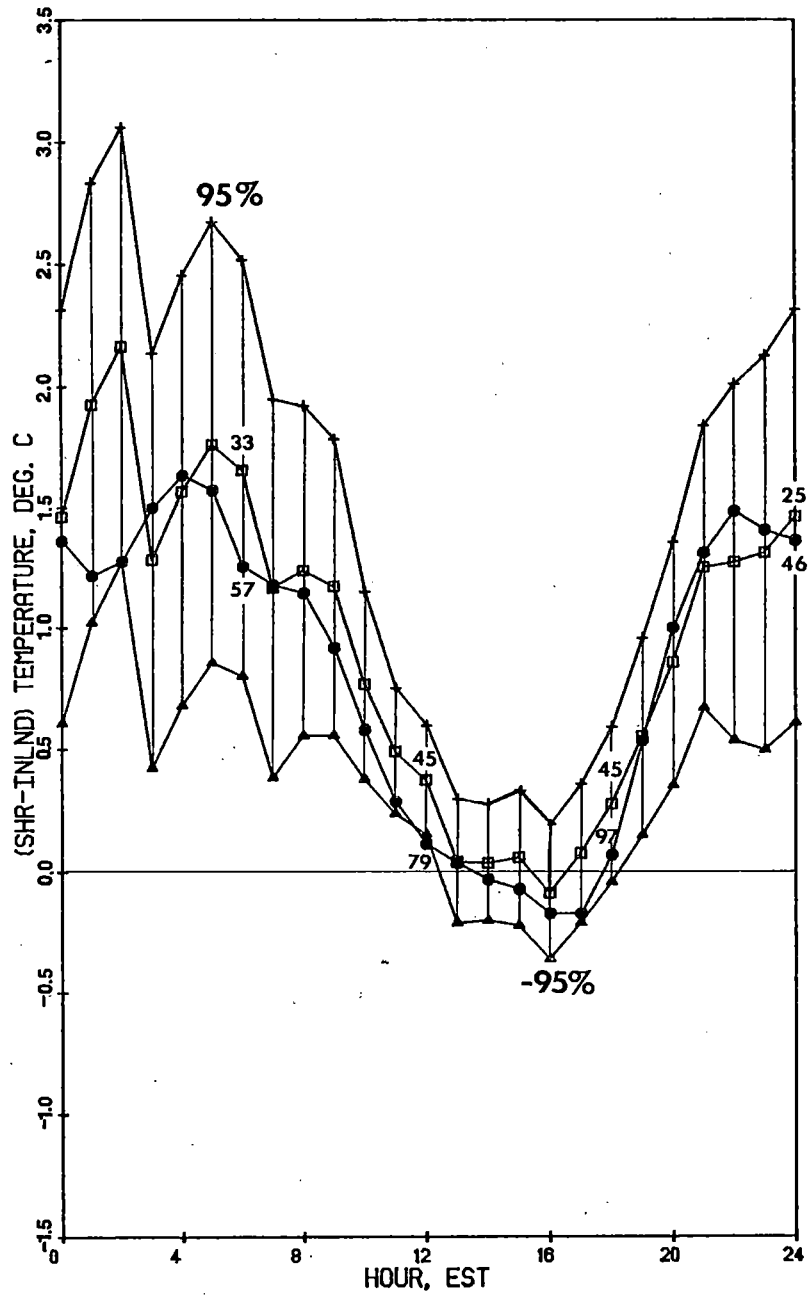
$\pm 0.3^{\circ}\text{C}$ for onshore winds and $\pm 0.2^{\circ}\text{C}$ for offshore winds. The offshore operational curve lies completely within the confidence band, while the onshore operational curve lies near the lower limit of, but generally within the confidence interval.

As in spring, the diurnal cycles of ΔRH (Fig. 6.5) for summer are the inverse of the ΔT cycles. Throughout the daylight hours, the operational data are at or near the lower limit of the confidence intervals on nonoperational data for both onshore ($\pm 1.4\%$) and offshore ($\pm 1.3\%$) winds.

The individual effects seen in the ΔT and ΔRH plots are again combined in the ΔDP plot (Fig. 6.6). With offshore winds, operational ΔDP is at or near the lower limit of the confidence interval ($\pm 0.3^{\circ}\text{C}$). With onshore winds, since both operational ΔT and operational ΔRH curves are at or near the lower confidence limit during the daylight hours, ΔDP is well below the lower limit of the confidence interval ($\pm 0.4^{\circ}\text{C}$).

Autumn. Of the 15 possible months of autumn data from September 1974 - November 1978, approximately 3 1/2 months were nonoperational, 8 1/2 were operational and, again, there were no data for the 3 months of 1978. Plots of ΔT , ΔRH and ΔDP are shown in Figs. 6.7, 6.8 and 6.9 respectively.

ONSHORE



OFFSHORE

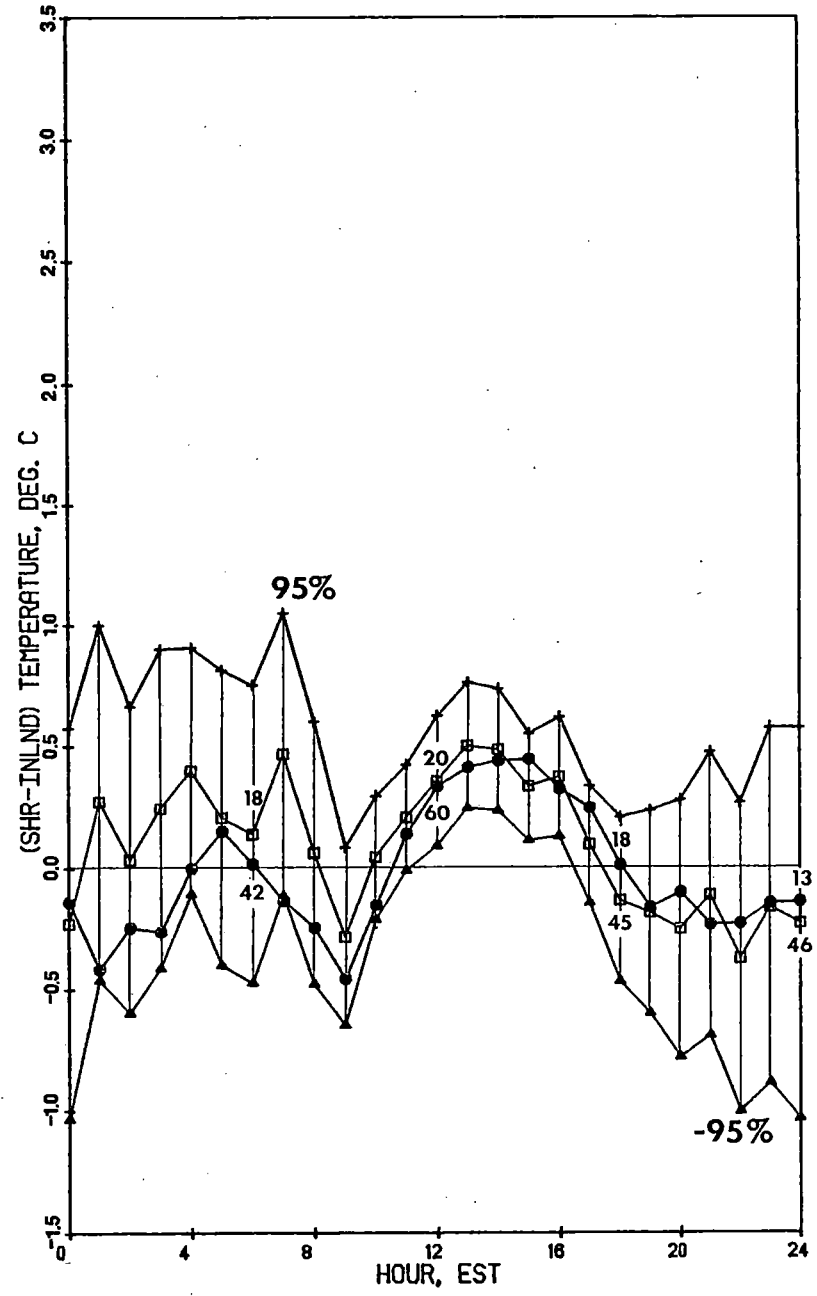


Fig. 6.7: As in Fig. 6.1, for the autumn season.

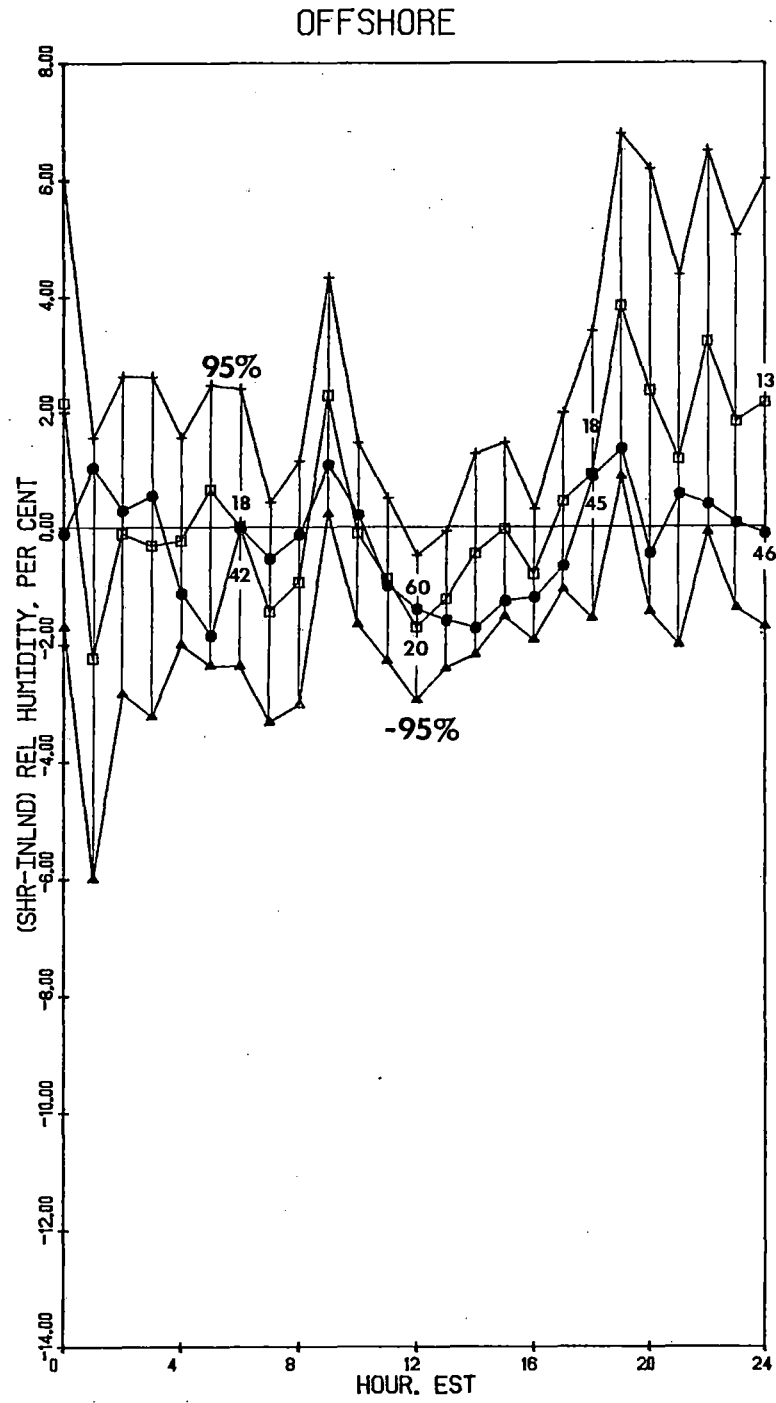
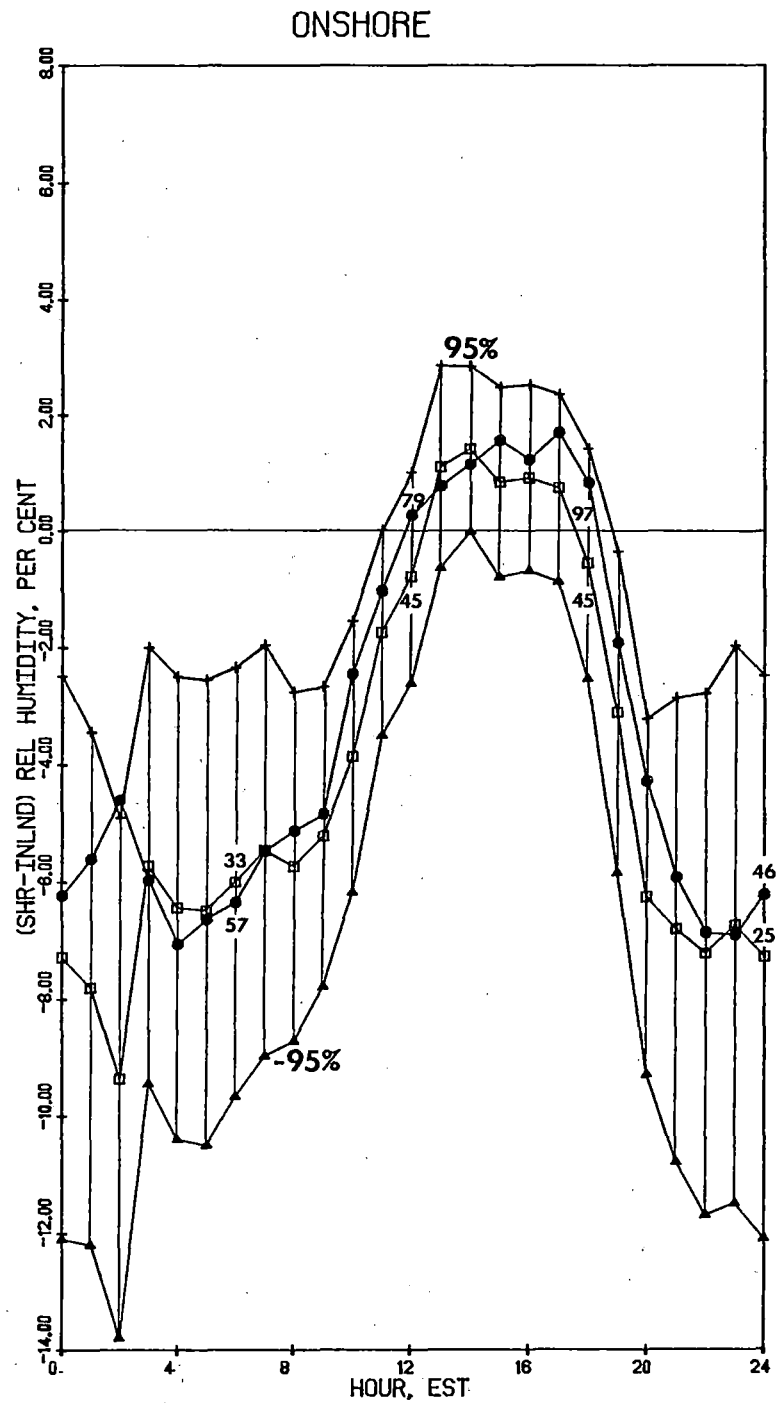


Fig. 6.8: As in Fig. 6.2 for the autumn season.

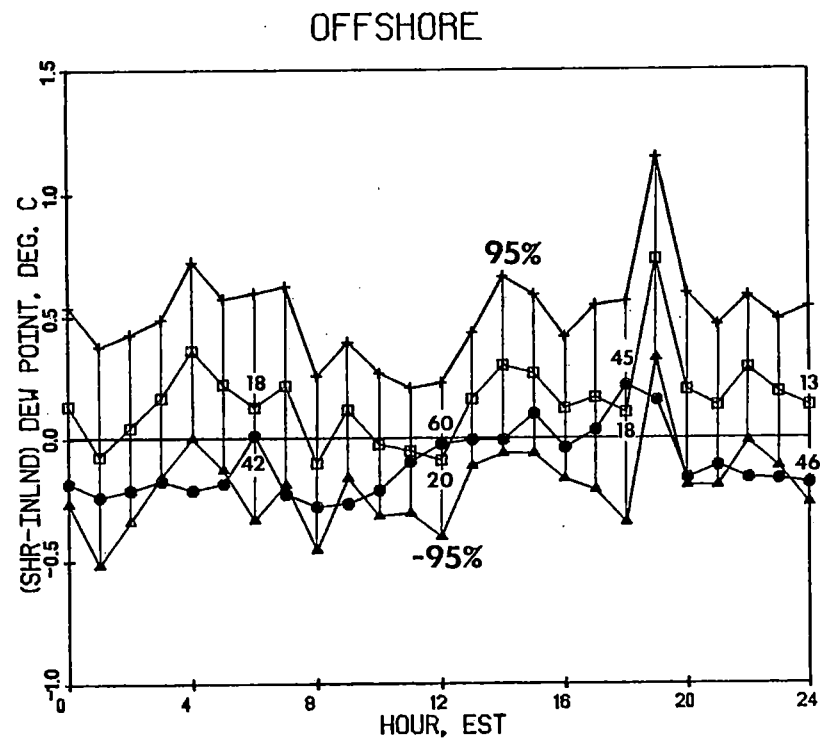
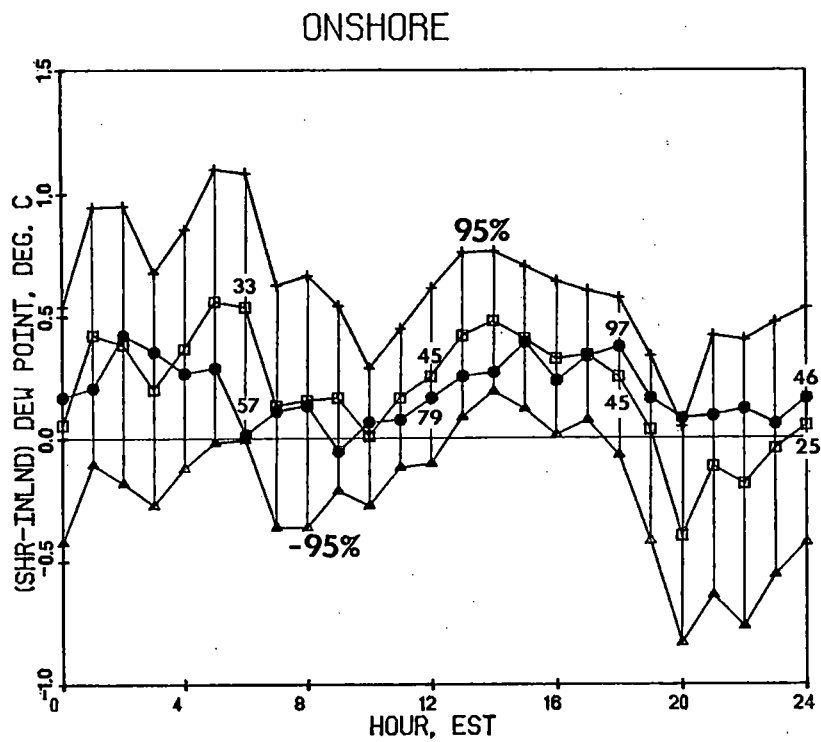


Fig. 6.9: As in Fig. 6.3, for the autumn season.

The upward shift of the ΔT curves for onshore winds noted in summer continues into the autumn season (Fig. 6.7). As colder weather sets in, the land cools much more rapidly than the lake, so temperatures at the coastal stations remain higher than those further inland for nearly the entire day. The magnitude of a statistically significant difference in ΔT between the nonoperational and operational periods is about $\pm 0.2^\circ\text{C}$ for both onshore and offshore winds. Operational data for both wind conditions are generally within those bounds.

As in the other seasons, ΔRH for onshore winds (Fig. 6.8) has a diurnal cycle the inverse of that for ΔT , while ΔDP for onshore winds (Fig. 6.9) shows little diurnal variation whatsoever. Operational ΔRH data fall within the confidence bounds of about $\pm 1.6\%$ for onshore winds and $\pm 1.2\%$ for offshore winds. Operational ΔDP data for onshore winds also fall within the $\pm 0.3^\circ\text{C}$ confidence bounds. Operational ΔDP data for offshore winds are contained within the confidence interval of $\pm 0.3^\circ\text{C}$ during the daylight hours. At night, those data are at or near the lower confidence limit.

Winter. There were 18 months of winter data available from December 1973 - February 1979. The cooling towers were not operational for about 11 months and operational for about 7 months. In addition, there were no relative humidity and dew point data available for December 1973, a nonoperational month. Diurnal plots of the average coastal-inland ΔT , ΔRH and ΔDP are shown in Figs. 6.10, 6.11 and 6.12, respectively.

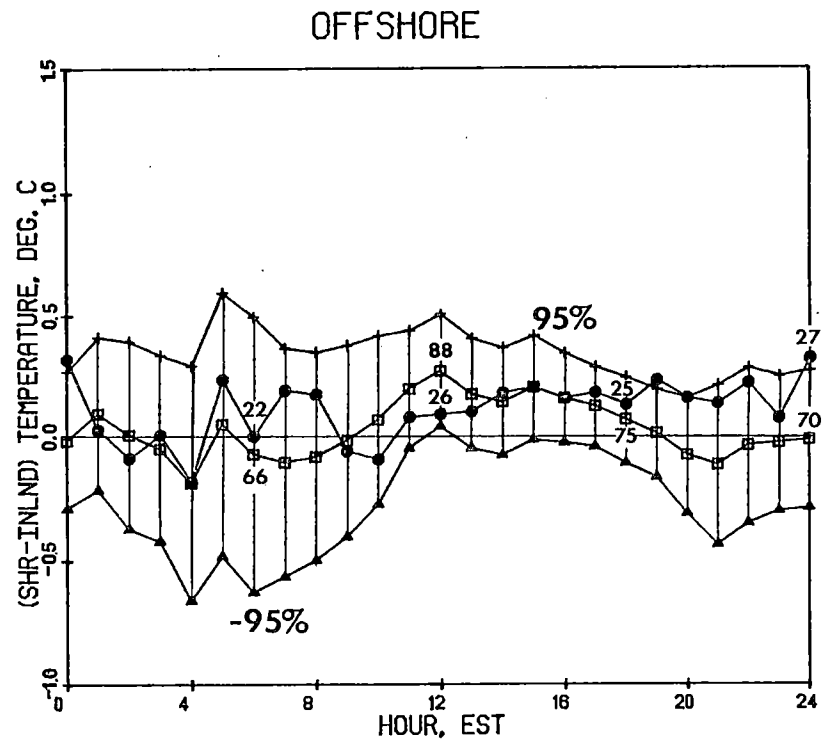
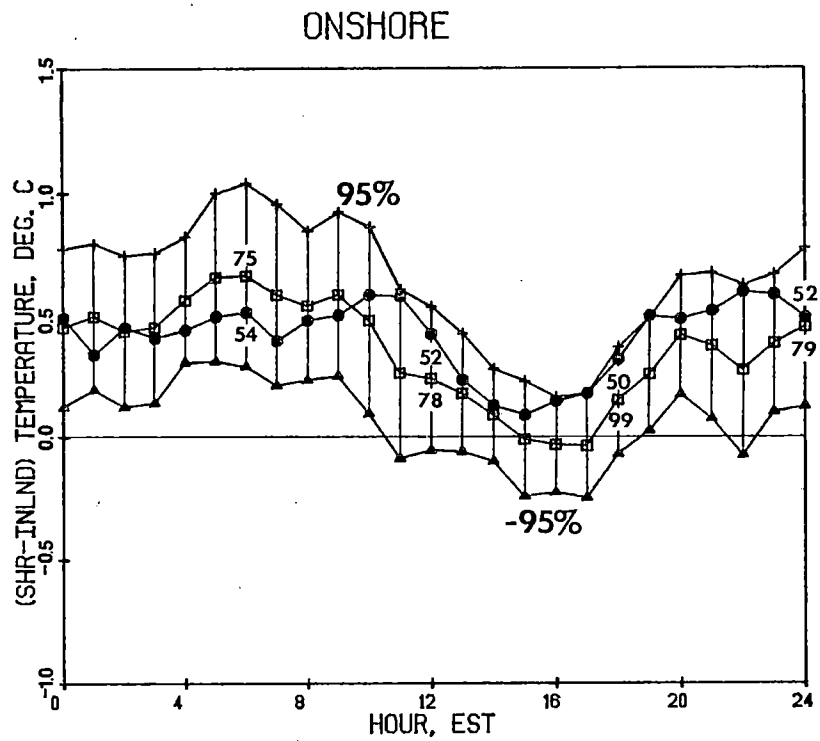


Fig. 6.10: As in Fig. 6.1, for the winter season.

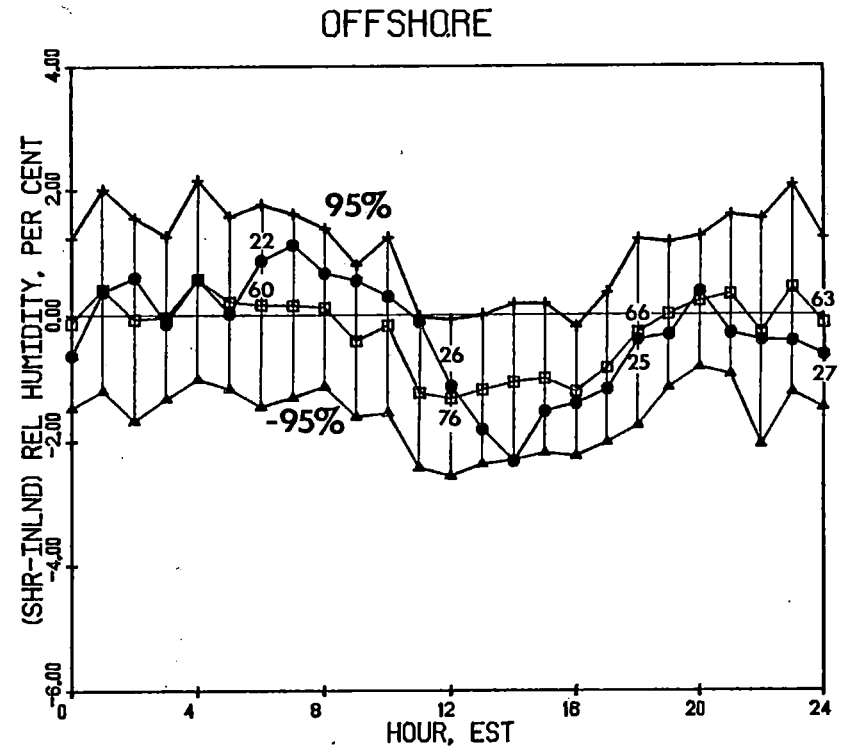
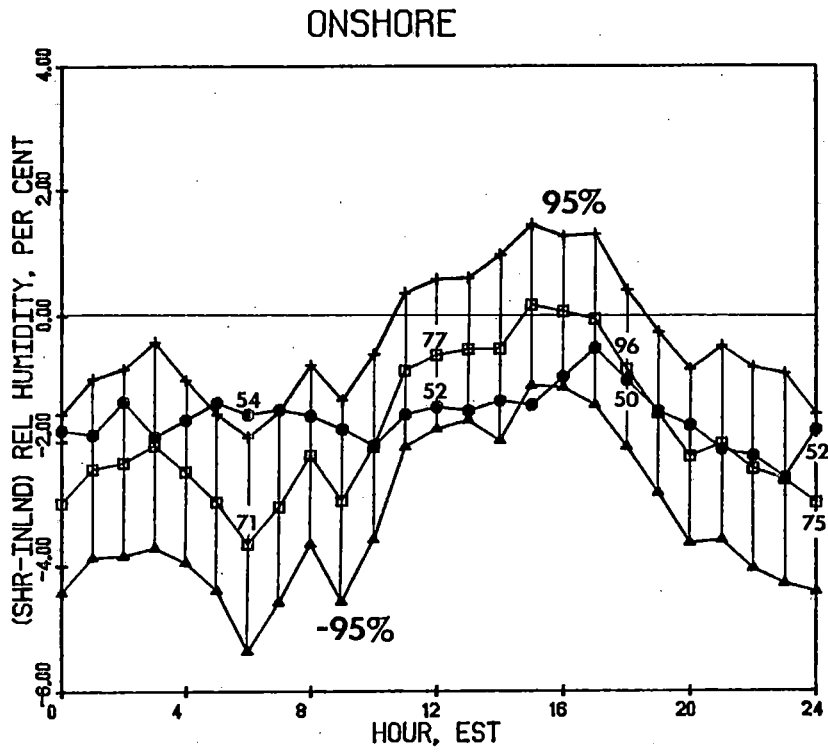


Fig. 6.11: As in Fig. 6.2, for the winter season.

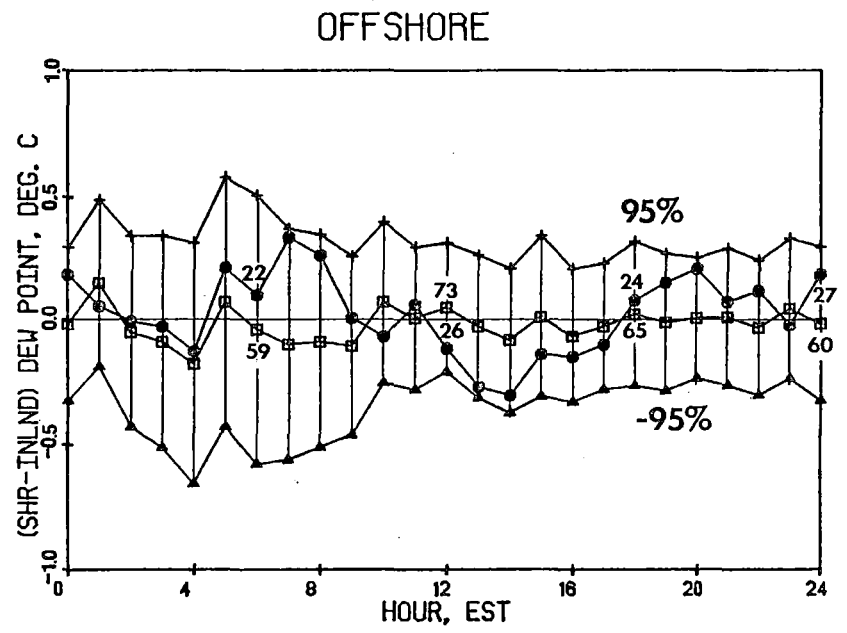
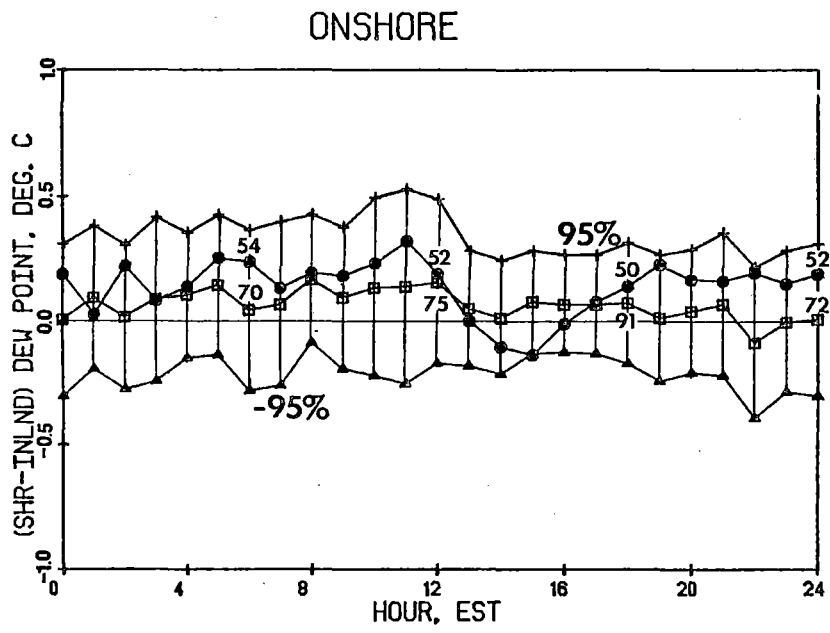


Fig. 6.12: As in Fig. 6.3, for the winter season.

The amplitude of the night-to-day variation of ΔT in winter with onshore winds (Fig. 6.10) is greatly reduced from that of the other seasons, a result of the frequent occurrences of cloudy conditions typical of Great Lakes winters. As in the autumn season, the fact that the lake is generally warmer than the land causes temperatures at the coastal stations to be higher than those further inland throughout the day. The ΔT curves for offshore winds are quite flat. The magnitude of a statistically significant change in ΔT from the nonoperational to the operational period is about $\pm 0.2^\circ\text{C}$ for both onshore and offshore winds. Although operational data generally fall within those bounds, it should be noted that from 1000-1200 EST and 1500-1800 EST, operational data for onshore winds are at or near the upper limit, with no corresponding shift of the operational data for offshore winds.

The amplitude of the diurnal ΔRH variation (Fig. 6.11) is also much smaller than that for the other seasons. Operational data for onshore winds are at or near the lower limit of the $\pm 1.2\%$ confidence interval at the times that ΔT data were near their upper limit noted above. Operational data for offshore winds are generally within the $\pm 1.2\%$ confidence interval.

The ΔDP curves (Fig. 6.12) for both onshore and offshore winds are quite flat. The magnitude of a statistically significant difference in ΔDP from the nonoperational to the operational period is about $\pm 0.2^\circ\text{C}$ for onshore winds and $\pm 0.3^\circ\text{C}$ for offshore winds. Operational data fall within the confidence bands at all hours although both curves approach their respective lower limits during the afternoon.

Evaluation of significant differences

A few statistically significant differences between operational and nonoperational data were noted in the discussion above. Table 6.1 summarizes the magnitude of a change between nonoperational and operational data required for statistical significance at the .05 level.

Table 6.1. Magnitude of statistically significant differences between operational and nonoperational data by season and variable.

	ΔT	ΔRH	ΔDP
Spring	<u>+0.4°C*</u>	<u>+1.5%</u>	<u>+0.4°C*</u>
Summer	<u>+0.3°C</u>	<u>+1.4%</u>	<u>+0.4°C*</u>
Autumn	<u>+0.2°C</u>	<u>+1.6%</u>	<u>+0.3°C</u>
Winter	<u>+0.2°C*</u>	<u>+1.2%</u>	<u>+0.2°C</u>

Values noted with an asterisk (*) were exceeded during the operational period with onshore winds, with no such corresponding occurrence with offshore winds.

The summer ΔDP value which was exceeded was discussed previously and is probably not related to cooling tower operation. The others are evaluated below in terms of possible explanations for the observed behavior.

Spring ΔT , ΔDP . The largest differences between operational and nonoperational ΔT were noted above for the spring season (Fig. 6.1), in which operational ΔT averaged 0.5 - 1.3°C lower than nonoperational ΔT during the daylight hours. It appears that those differences are due mainly to natural

differences in cloudiness between the nonoperational and operational data sets. For example, average sunrise to sunset cloudiness at Muskegon, the nearest representative first-order weather station, was 6% higher in the nonoperational period than in the operational period. It seems likely that the larger number of cloudy days during the nonoperational period resulted in weaker average coastal/inland temperature gradients and the flatter daytime ΔT curve. In fact, those gradients were much weaker in the nonoperational period, as seen in Fig. 6.13, which shows the deviation of each 1600 EST average station temperature from the network average temperature, for onshore winds. The isotherms are much more widely spaced in the nonoperational period, with a maximum coastal/inland difference of about 1.5°C , compared to a maximum difference of about 3.0°C in the operational period.

The statistical significance of such differences between operational and nonoperational data can also be evaluated on a station-by-station basis by use of the t -test. Care must be taken in the interpretation of results for individual stations, since instrument or calibration errors take on greater importance than they do in the data averaged over a group of stations. A plot of the statistical significance data on a network map, however, can show areas of statistically significant differences which may then be relatable to plant operational status and/or meteorological phenomena.

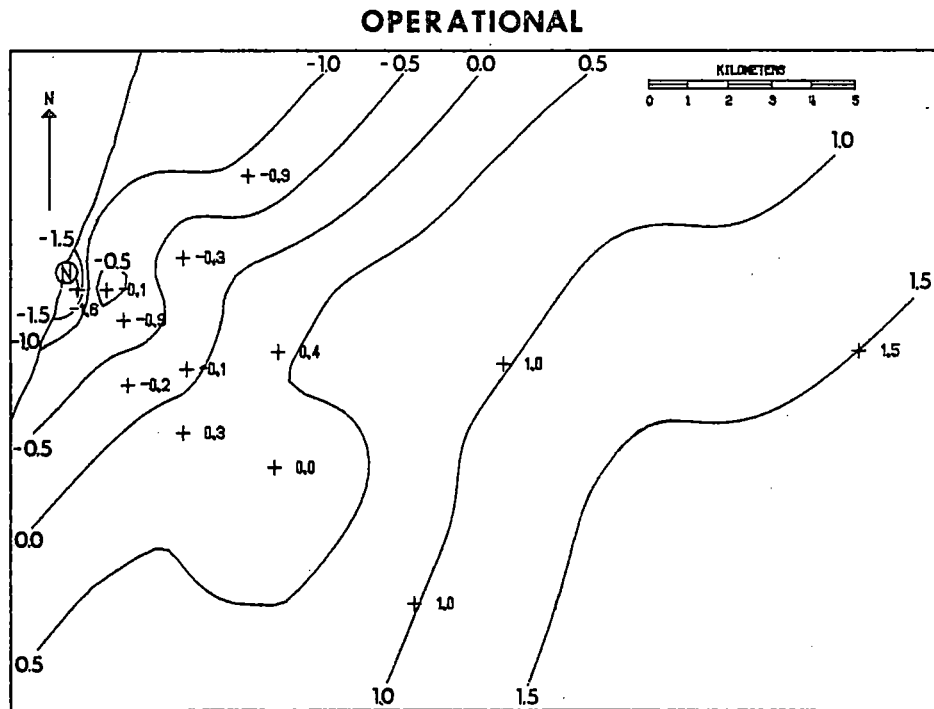
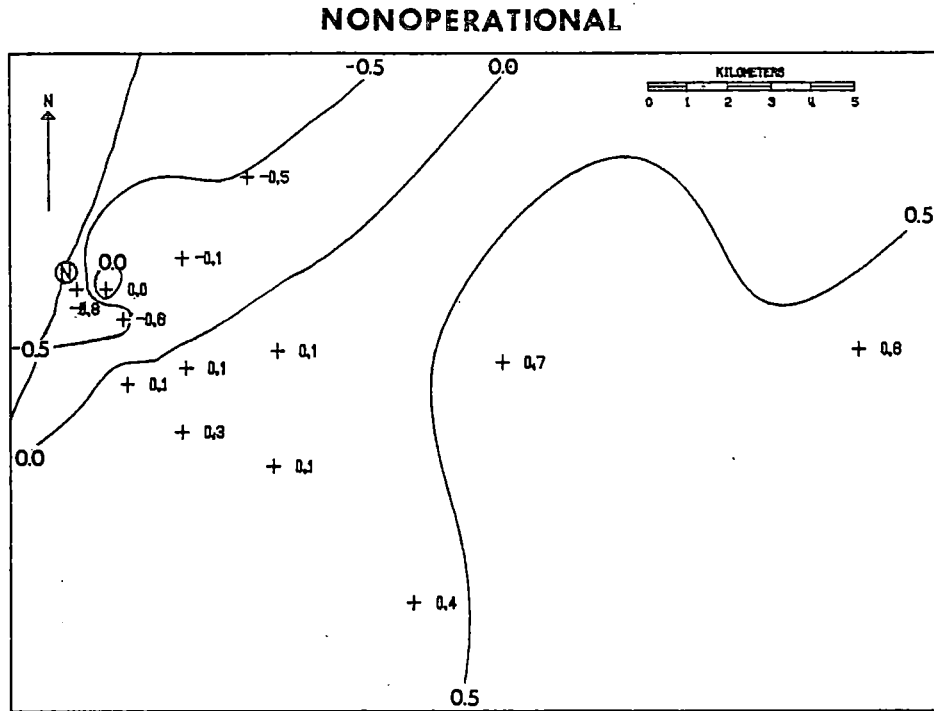


Fig. 6.13: Spring 1600 EST station temperatures minus network average temperature ($^{\circ}\text{C}$) with onshore winds, for nonoperational and operational periods.

An example of such a plot is shown in Fig. 6.14. The data plotted, rather than being t -test values which give no information as to the sign of the difference between the nonoperational and operational means, are Bayesian posterior probabilities (Larson, 1969) that the operational means are greater than the nonoperational means. Values greater than .95 are strong evidence that the operational temperatures are larger than the nonoperational temperatures, while values less than .05 are strong evidence that the operational temperatures are smaller. Data are plotted for both onshore and offshore winds. As seen in the figure, data for offshore winds are distributed rather randomly, while for onshore winds there is a clear pattern of operational temperature lower along the coast and higher inland. These plots lend further support to the analysis above, especially since the dissimilarity between the plots shows that the before/after differences are not simply systematic (i.e., independent of wind direction).

It was noted in the previous section that ΔDP also fell below the lower confidence limit throughout the afternoon with onshore winds, while ΔRH remained generally within its bounds. Spatial displays of the probability that operational relative humidities and dew points exceed nonoperational, corresponding to the temperature plots above, are shown in Figs. 6.15 and 6.16, respectively. The relative humidity plots are very similar to each other, with a mixture of higher and lower operational relative humidities both at the coast and inland. No plant- or lake-induced differences are evident. The pattern for dew point with offshore winds is

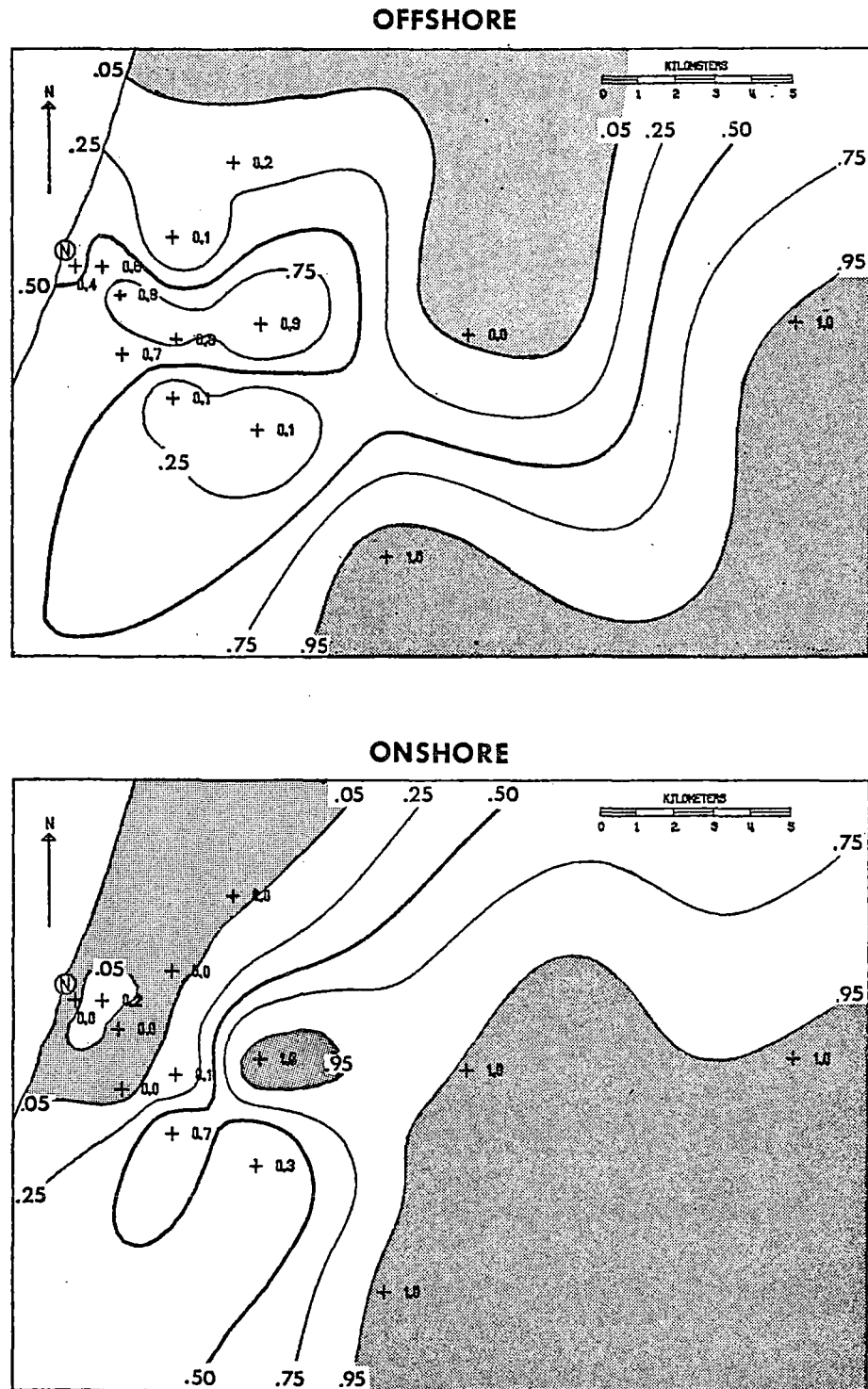


Fig. 6.14: Probability that spring 1600 EST station temperature minus network average temperature is greater in the operational period than in the nonoperational period, for offshore and onshore winds. Values less than .05 shaded light, values greater than .95 shaded dark.

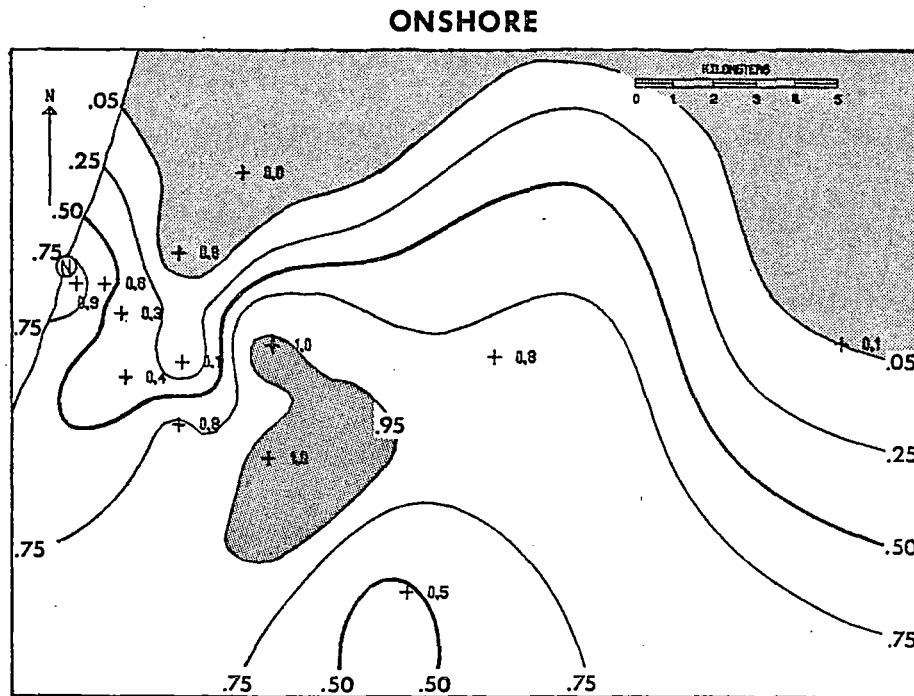
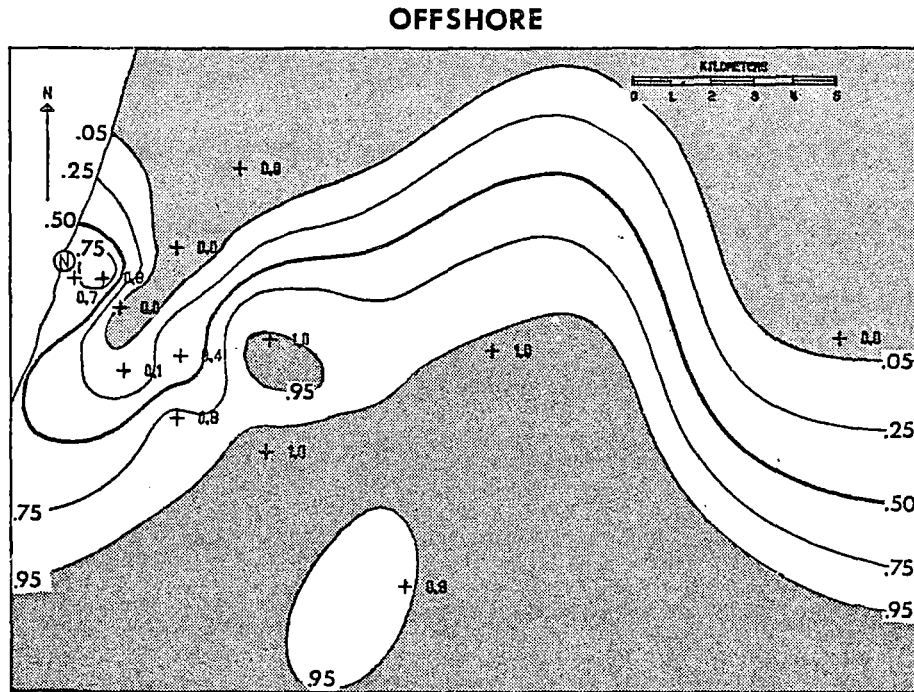


Fig. 6.15: Probability that spring 1600 EST station relative humidity minus network average relative humidity is greater in the operational period than in the nonoperational period, for offshore and onshore winds. Values less than .05 shaded light, values greater than .95 shaded dark.

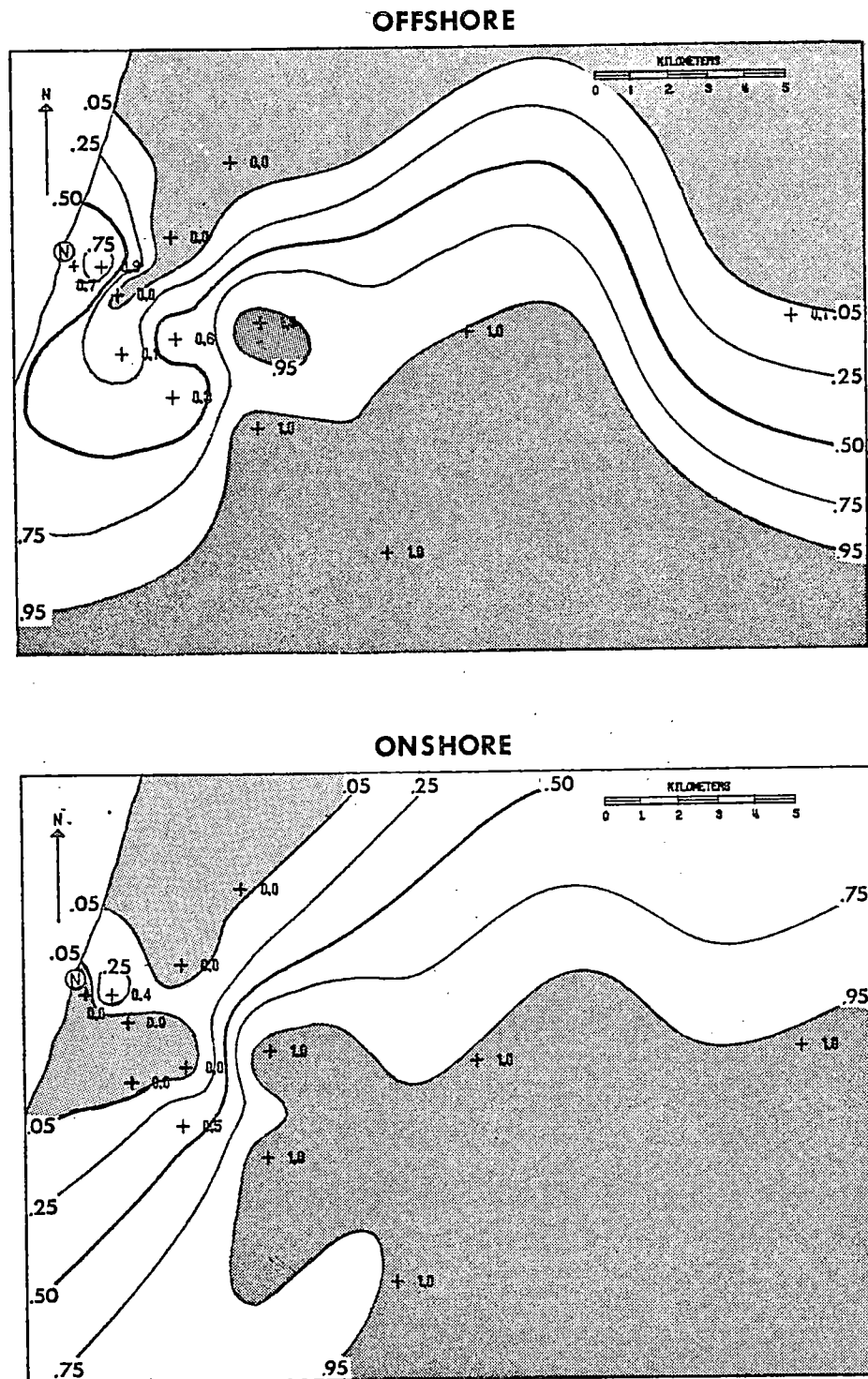


Fig. 6.16: Probability that spring 1600 EST station dew point minus network average dew point is greater in the operational period than in the nonoperational period, for offshore and onshore winds. Values less than .05 shaded light, values greater than .95 shaded dark.

very similar to that for relative humidity, while the pattern for onshore winds is much like the corresponding temperature pattern. Clearly, the pattern of significant differences in temperature combined with the mixture of increases and decreases of relative humidity at both the coast and inland results in significant differences in dew point similar to those for temperature.

The important thing to be noted is that significant differences such as these between data from the operational and nonoperational periods, which have no relation to the operation of the cooling towers, can occur. It is important, then, that such differences be evaluated in light of all available information.

Winter ΔT . It was noted previously that operational ΔT was at or near the upper confidence limit for winter nonoperational ΔT with onshore winds (Fig. 6.10), throughout much of the daylight period. Since the operational data are actually contained within the confidence interval, it is possible that the difference between the two data sets is due simply to random processes. Further examination is necessary, however, since the operational data show a positive displacement from the nonoperational data, and, as noted in previous annual reports, winter is the most likely season in which either a temperature or a moisture effect may occur and be detectable by this statistical approach.

Maps of the probability that the operational mean temperature exceed the nonoperational means at 1600 EST are shown in Fig. 6.17. The plots for onshore and offshore winds are similar to each other in that there is an east-west band of higher operational temperatures stretching from P03A to P06A, bounded by areas of lower operational temperatures on the north (P02A, P08A, and P09A) and east (P07A). The major differences between the plots are at P13A, where operational temperatures are similar to nonoperational temperatures with offshore winds, but significantly lower with onshore winds, and at P01A, where operational temperatures are slightly lower than nonoperational temperatures with offshore winds, but significantly higher with onshore winds. The combination of these effects would, indeed, tend to cause the positive displacement of the operational curve from the nonoperational apparent in Fig. 6.10.

There are no apparent meteorological or physical reasons for the behavior observed at P01A. Operational temperatures with offshore winds averaged 0.1°C lower than nonoperational, but with onshore winds they consistently averaged about 0.3°C higher at all hours of the day. The results are especially puzzling in light of the fact that operational temperatures at P02A, only 400 m away, were lower with both offshore and onshore winds, while operational temperatures at P03A, about 900 m away, were higher with both offshore and onshore winds. A case

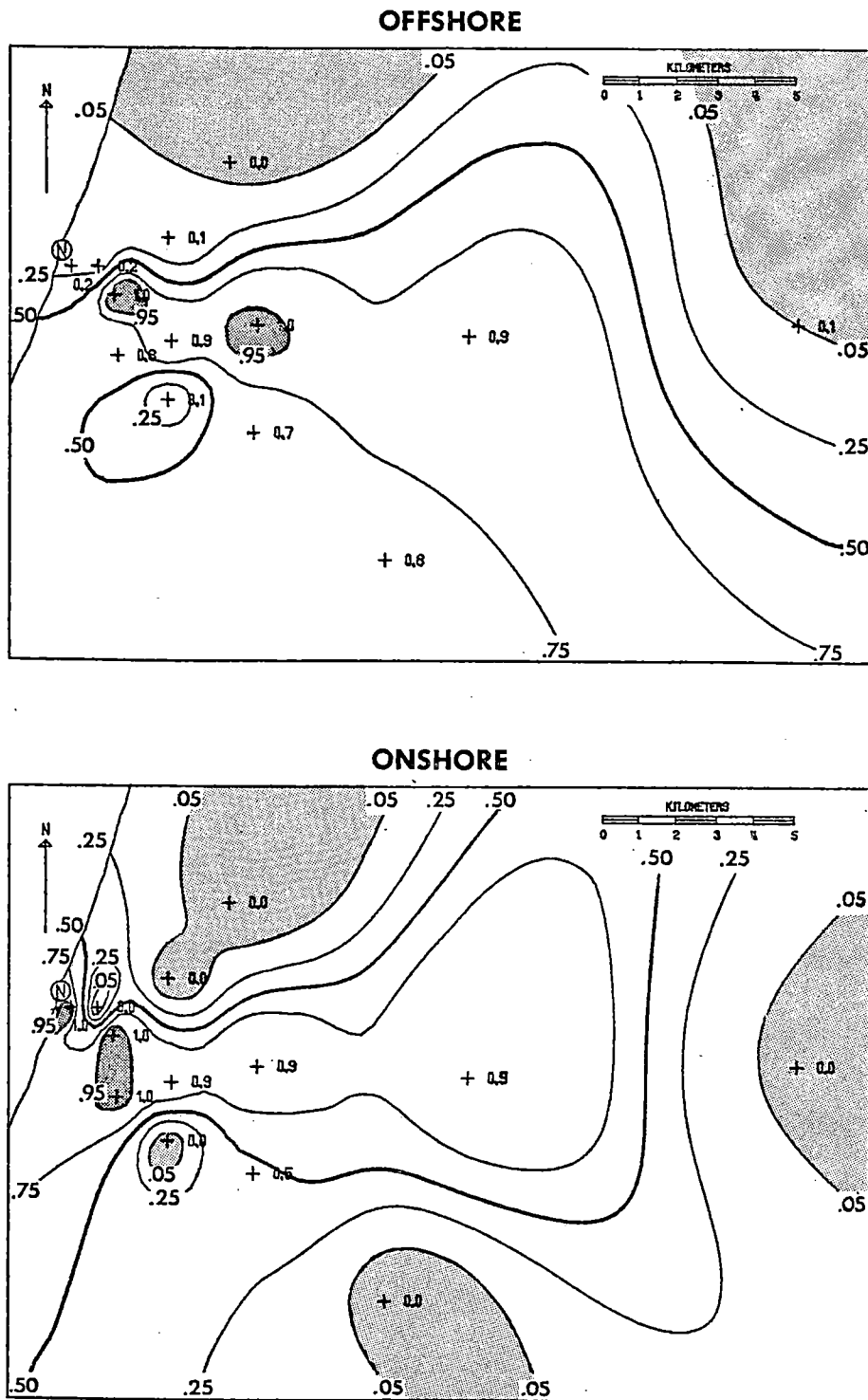


Fig. 6.17: Probability that winter 1600 EST station temperature minus network average temperature is greater in the operational period than in the nonoperational period, for offshore and onshore winds. Values less than .05 shaded light, values greater than .95 shaded dark.

could be made for the onshore wind plot being "reality", with P01A, P03A, P04A, P05A, P06A and P10A being in a spatially unified region of higher operational temperatures, and the offshore wind plot showing unexplainably lower operational temperatures at P01A. On the other hand, this entire analysis is predicated on the fact that data for offshore winds serve as a control, since the stations are all upwind of the cooling towers, and there are no meteorological reasons to expect differences between the operational and nonoperational periods.

It then seems more likely that the plot for offshore winds represents the true state of affairs, with P01A in a spatially unified region of lower operational temperatures which includes P02A, P08A and P09A. The analysis above, combined with consideration of the proximity of the station to the cooling towers, and data obtained from plume observations by plant personnel and examination of time-lapse photographs all point to the operation of the cooling towers as a possible cause of the significantly higher operational temperatures at P01A with onshore winds. The fact that no such difference occurred at the next nearest station (P02A), and that an unexplainable difference between data for offshore and onshore winds also occurred at a station well removed from the vicinity of the cooling towers (P13A) tend to throw doubt on such a conclusion. Nevertheless, operation of the cooling towers cannot be discarded as a possible cause for the

increased operational temperatures at P01A with onshore winds in the winter season.

Relative humidities at P01A and P02A did not differ significantly between the nonoperational and operational periods, so the dew point comparisons (Fig. 6.18) show the same pattern of differences between offshore and onshore winds near the plant that were seen for temperature. While the implied increase in absolute moisture at P01A with onshore winds during the operational period does not prove that plume effects were detectable there, the result is consistent with the temperature increase described above, in that they are both the kinds of impacts originally hypothesized for this cooling system.

Analysis with respect to direction of plume motion

Because the analysis above indicates the possibility of onsite plume-induced effects in winter, the data for that season were examined in greater detail by use of a sorting process which attempts to isolate meteorological situations where effects are likely to be observed. Since the moisture and heat from the cooling towers are released in a plume which extends downwind from the plant, the greatest changes from natural unmodified meteorological conditions should be found under the centerline of the plume and decrease away from the plume axis. Therefore, the analysis below examines the statistical significance of observed changes in temperature,

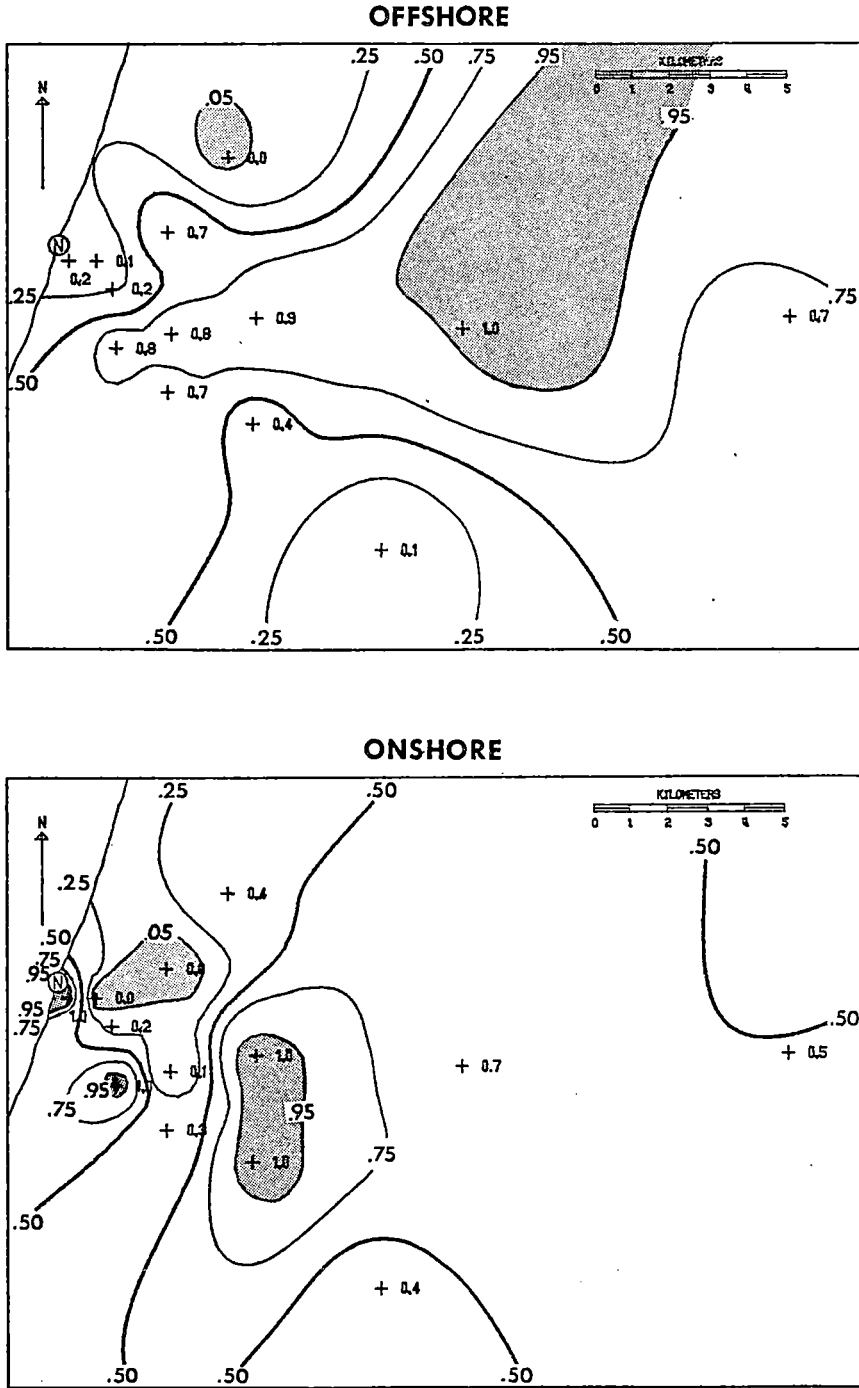


Fig. 6.18: Probability that winter 1600 EST station dew point minus network average dew point is greater in the operational period than in the nonoperational period, for offshore and onshore winds. Values less than .05 shaded light, values greater than .95 shaded dark.

relative humidity and dew point with respect to an estimated position of the plume.

The most representative data available for the direction of the plume is the wind direction observed at P03A. Clearly, orographic effects and/or changes of wind direction with height may contribute to differences between the two, but these are taken into account in analysis of the results. Data with wind directions within 30° intervals are grouped together. The direction from the cooling towers to each station is known and data for the station are analyzed relative to this direction. Computations are made every 15° so there is a 15° overlap in data between adjacent groupings.

As in the above analyses, observations are grouped by the hour of the day to ensure independence of the data values. Four hours were selected for examination: 0100 EST, 0700 EST, 1300 EST, and 1900 EST. These were considered representative of day, night, and transition conditions, and there were sufficient data values in each grouping to ensure the general applicability of the statistical tests applied. Bayesian posterior probabilities are again applied to determine the probability that the operational average is greater than the nonoperational average.

Probabilities for temperature, relative humidity, and dew point are given in Figures 6.19, 6.20, and 6.21 for stations P01A, P02A, and P03A, respectively. In these figures the

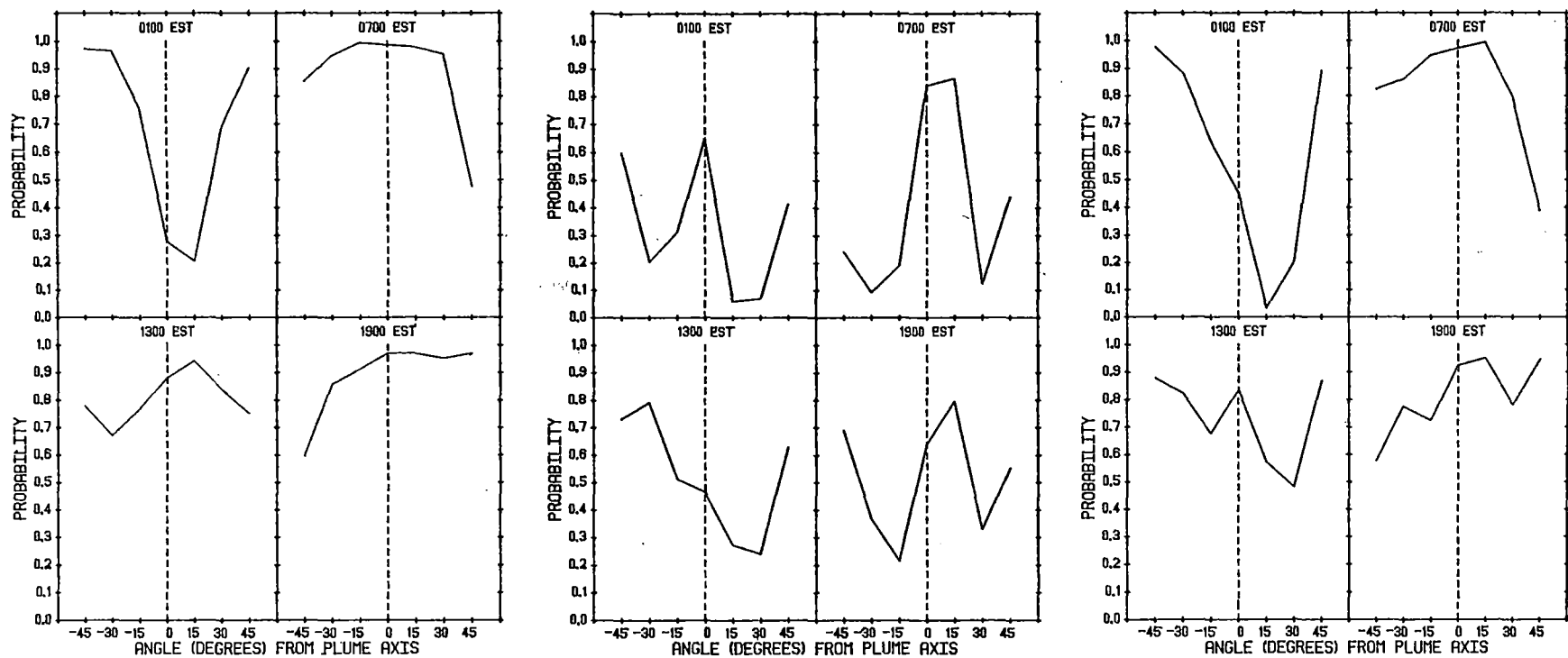


Fig. 6.19: Probability that the average winter temperature (left), relative humidity (middle), and dew point (right) at station P01A were higher for operational data than for nonoperational data as a function of wind direction.

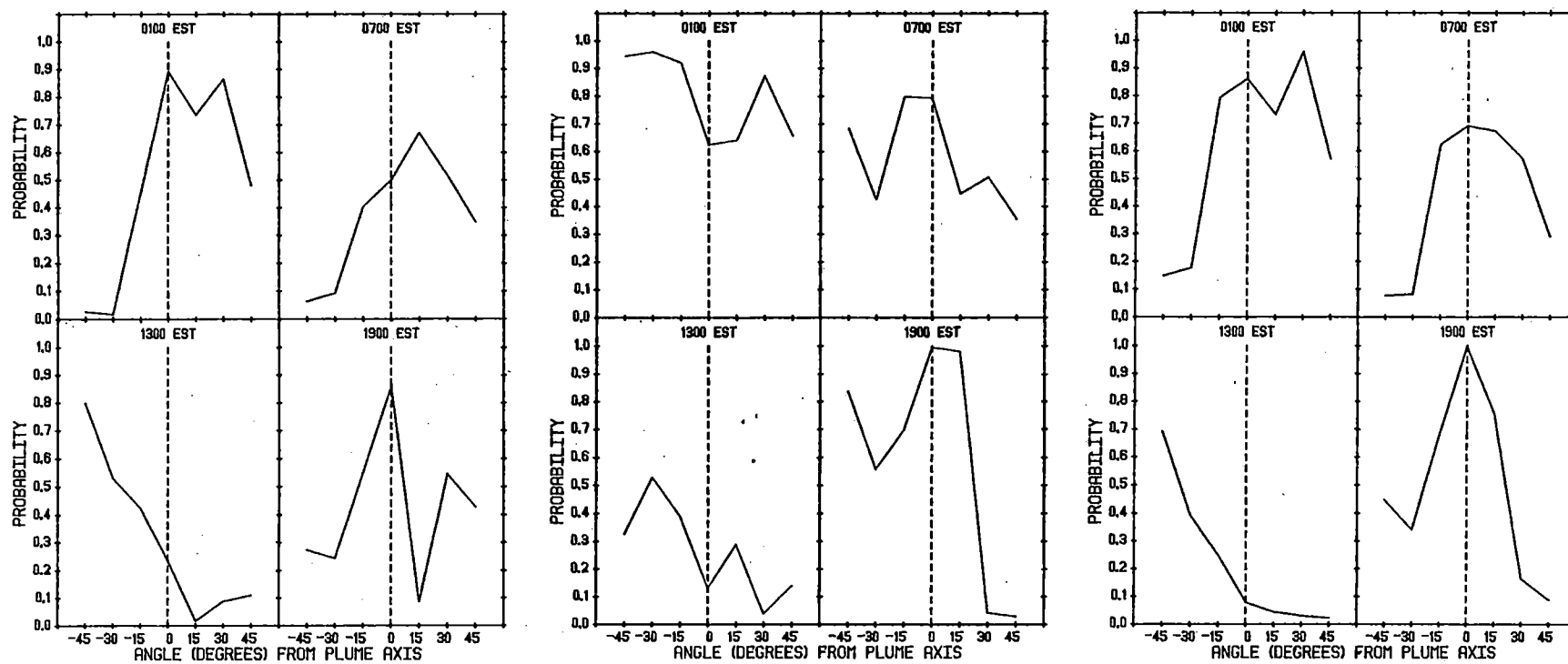


Fig. 6.20: As in Fig. 6.19, for station P02A.

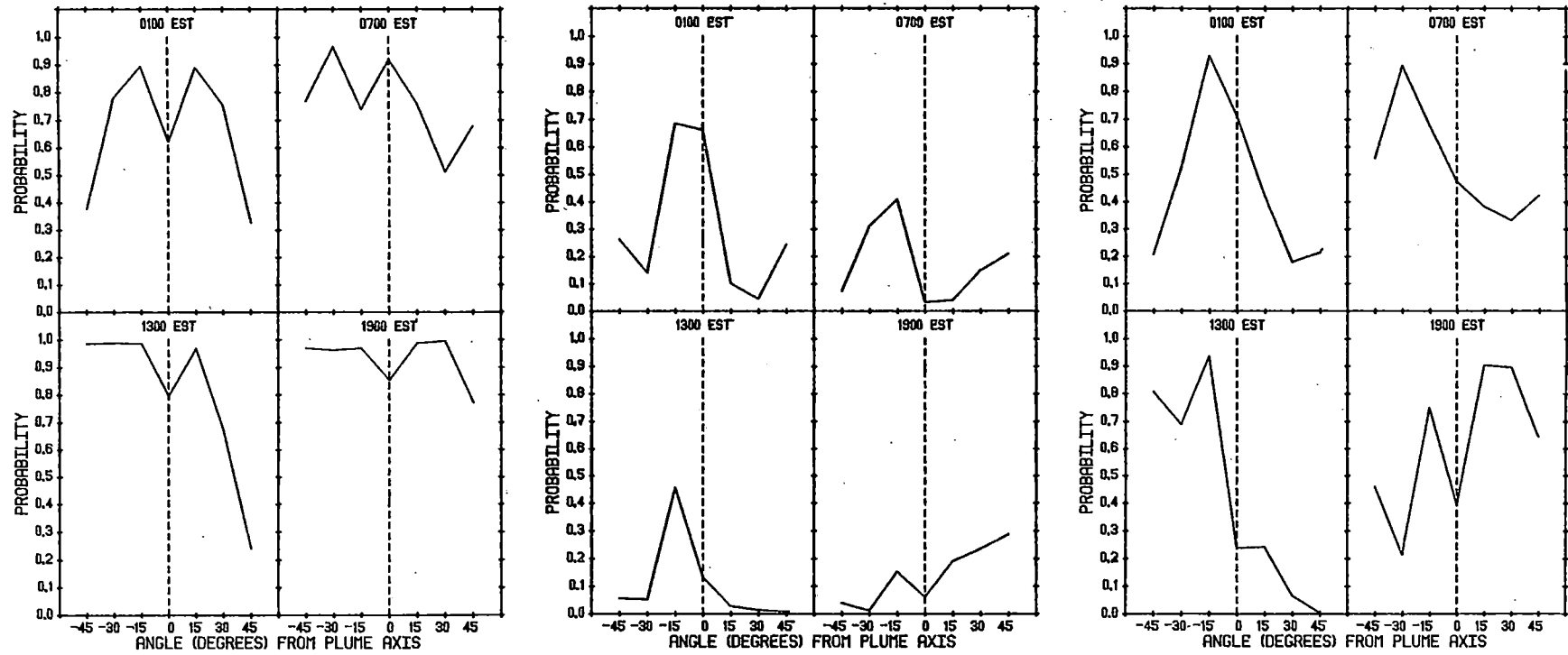


Fig. 6.21: As in Fig. 6.19, for station P03A.

probabilities are plotted as a function of the angle between the plume axis and a line connecting the station and the cooling towers. If the modifications are detectable, symmetric variations of these probabilities about the plume axis should be found, with a maximum on the axis.

Figure 6.19 shows several patterns which meet the above criterion: relative humidity at 0100 EST, 0700 EST, and 1900 EST and dew point at 1300 EST and 1900 EST. However, for several of these the maximum probabilities do not occur on the axis, but 15° off-axis. Although such a displacement suggests that the cooling towers are not the cause of these probability changes, there are several possible reasons why the cooling tower plume could be off-axis. For instance, the wind direction at P03A may not be representative of that at P01A, especially at night. Possibly, orography around P01A funnels the cooling tower plume so it affects the station from a somewhat different wind direction.

According to the Gaussian plume model results described in the Sixth Annual Report (1978), the effect of the plume is to increase the temperature, relative humidity and, consequently, the dew point. Such increases should produce increases in the Bayesian probability levels near the plume axis. Such increases were noted above for relative humidity at 0100 EST, 0700 EST and 1900 EST, and dew point at 1300 EST and 1900 EST. However, temperature and dew point at 0100 EST have the opposite behavior. If this behavior is in fact a result of the plume, its physical explanation is not obvious.

The computations for P02A (Fig. 6.20) and P03A (Fig. 6.21) produce patterns that for some variables and hours are fairly symmetric about the plume axis. In some cases, the patterns are similar to those at P01A, while in other cases the patterns are reversed (such as for temperature at 0100 EST at P02A).

In order to assimilate the computation for each station in an organized fashion, two-dimensional objective analyses of the data were made. All station probabilities were entered on an x-y display, with the x-axis being the distance of the station from the cooling towers projected on the plume axis and the y-axis being the angle between the plume axis and a line connecting the station and cooling towers. It was originally intended to use the transverse distance from the plume to the station for the y-axis, but the objective analysis program was not general enough to handle this type of display where the observation density changes markedly across the analysis region.

Objective analyses were generated by the computer program Surface II (Sampson, 1978) for temperature, relative humidity, and dew point at 0100 EST, 0700 EST, 1300 EST, and 1900 EST. Of the twelve analyses, the majority showed no discernible patterns of plume effects. Only 0100 EST and 1900 EST for relative humidity and dew point have patterns suggestive of modification. Those probabilities are presented in Fig. 6.22 and Fig. 6.23. Regions with probabilities of 0.6 or greater have been shaded to show areas of possible modification. The corresponding actual differences between the operational and nonoperational data sets are given in Fig. 6.24 and Fig. 6.25, respectively.

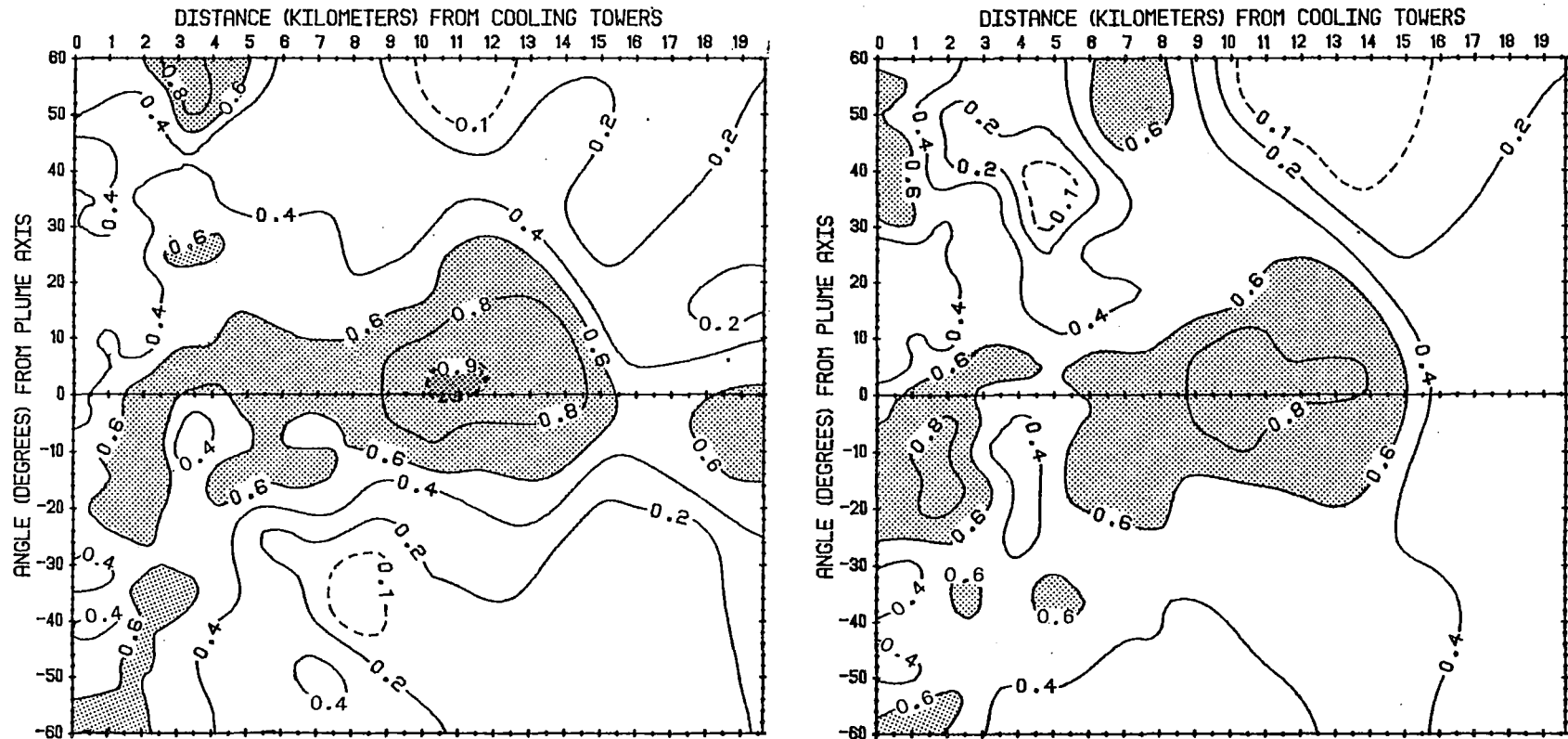


Fig. 6.22: Probability that the average 0100 EST winter relative humidity (left) and dew point (right) were higher for operational data than for nonoperational data as a function of distance from cooling towers and angle from plume axis. Regions with probabilities of 0.6 or greater are lightly shaded and regions with probabilities 0.9 or greater have darker shading.

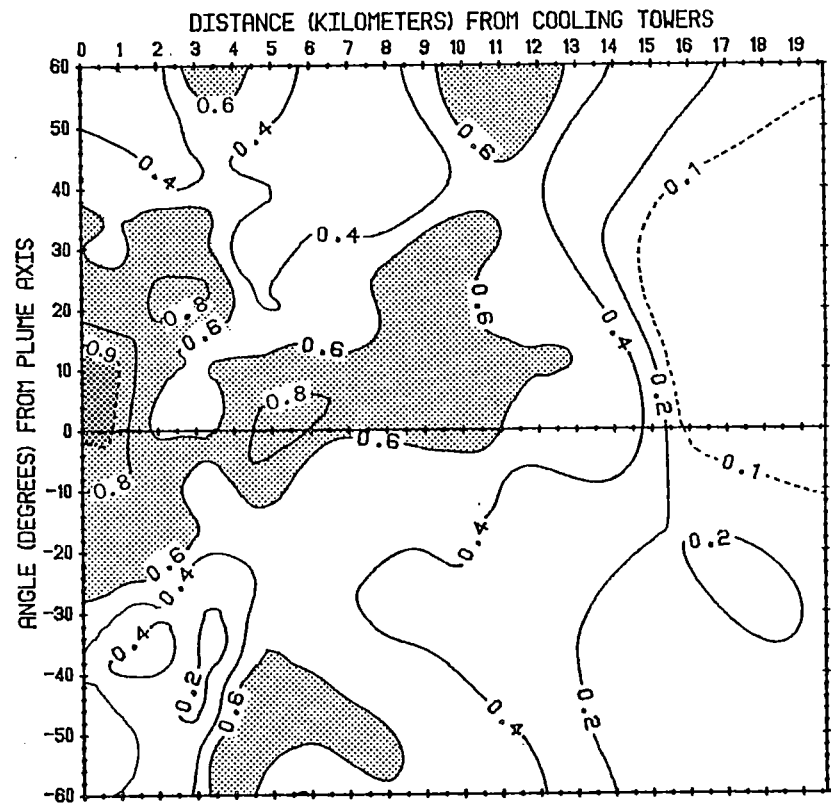
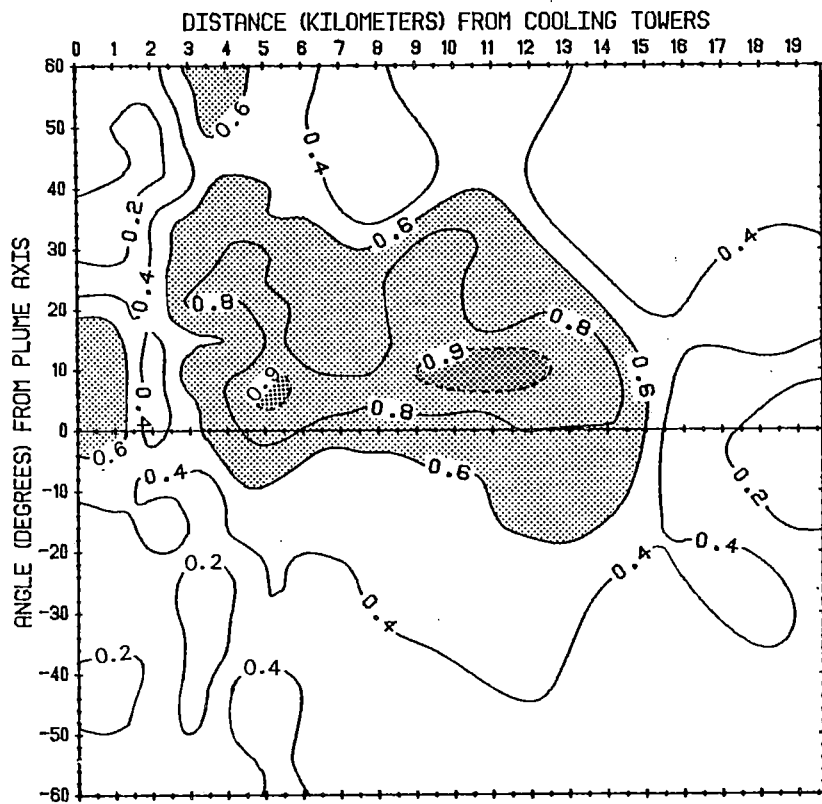


Fig. 6.23: As in Fig. 6.22, for 1900 EST.

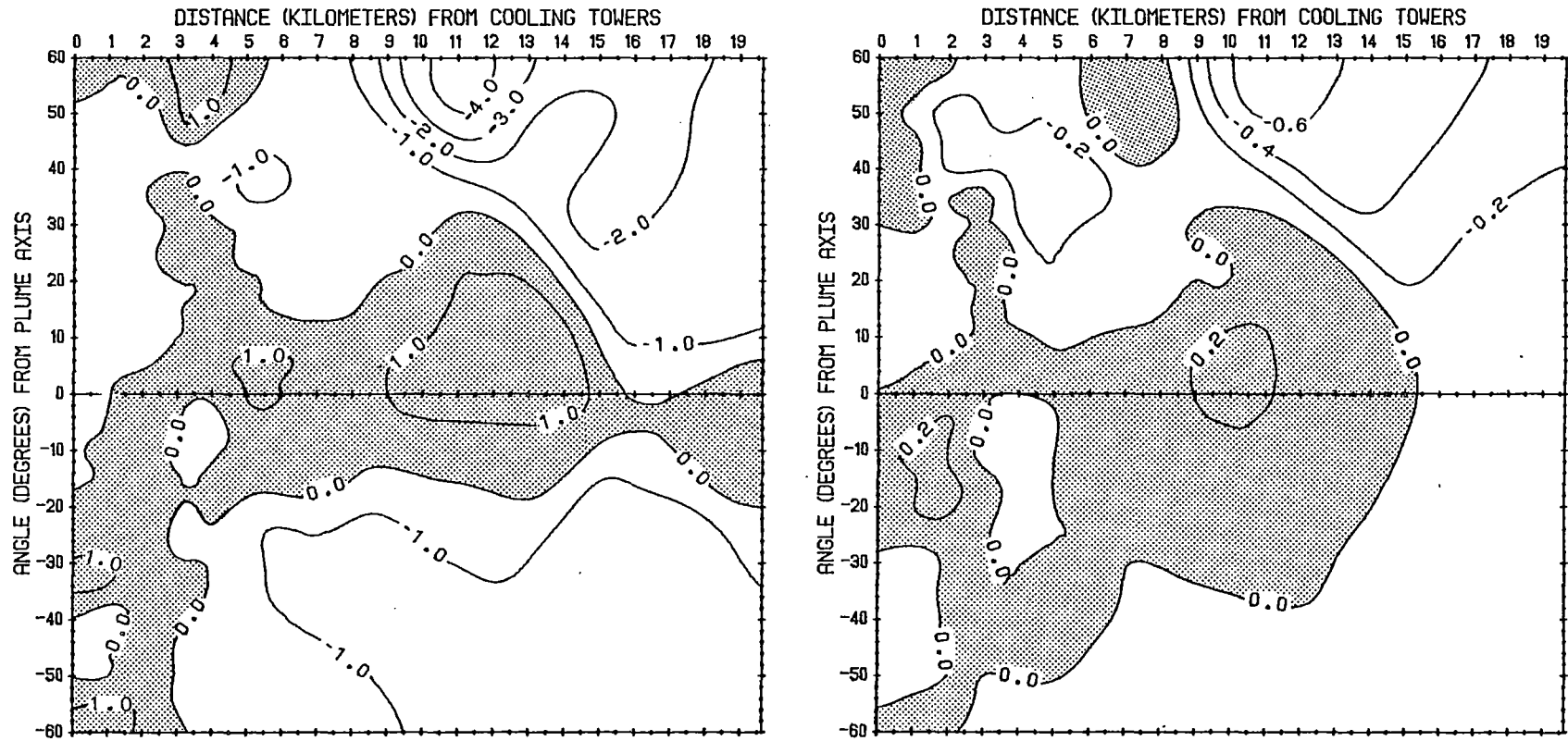


Fig. 6.24: Average 0100 EST winter operational minus nonoperational relative humidity (left) and dew point (right) as a function of distance from cooling towers and angle from plume axis. Regions with a positive difference are shaded.

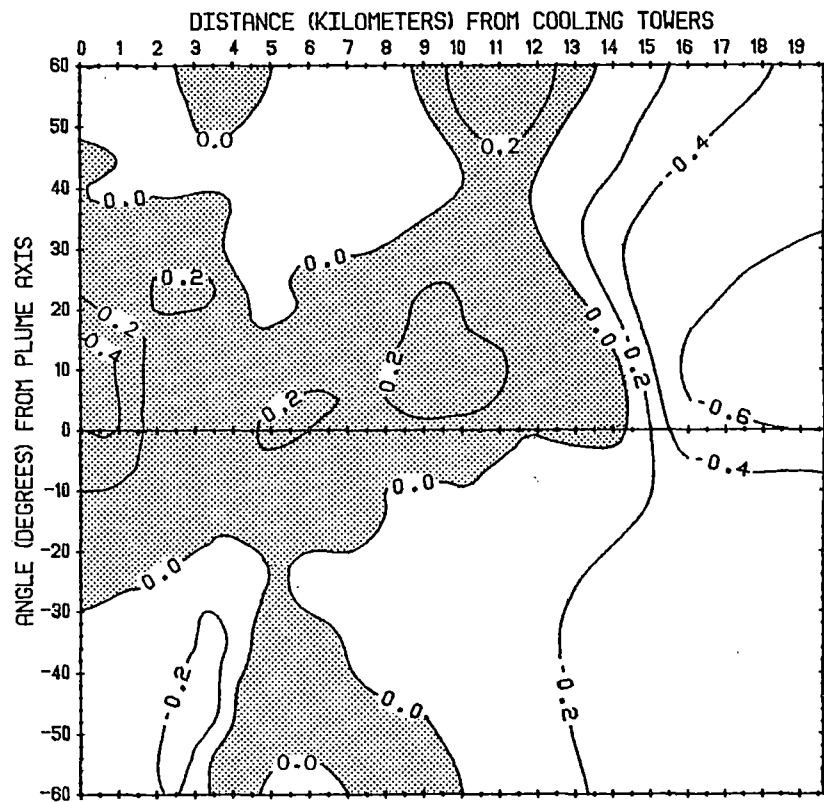
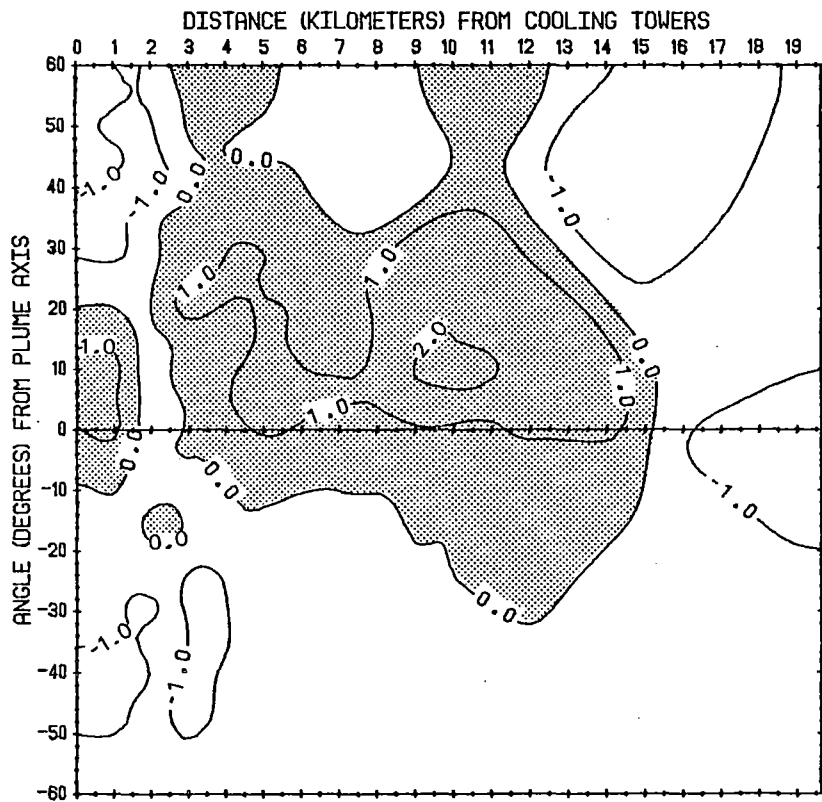


Fig. 6.25: As in Fig. 6.24, for 1900 EST.

In most areas of Figs. 6.22 and 6.23 the near-axis probabilities have magnitudes which indicate only marginal significance that more saturated conditions are present in the operational data set than the nonoperational. In only a few places does the probability exceed the classical level of 0.90 (heavier shaded areas). However, in several of the figures, the off-axis probabilities are considerably less than 0.5, implying that the "background" situation is one of drier conditions during the operational period. Hence, the likelihood that the plume is being detected is higher than the magnitude of these probabilities indicates.

In three of the four analyses there is a gap in the area with the probabilities equal to or greater than 0.6 near the plant. In fact, the region with greatest probabilities is approximately 11 km from the cooling towers. At 0100 EST the shaded area does not even begin at the cooling towers. This pattern may be due partly to the method of analysis, but it may also result from the plume rising as it leaves the plant area and then being brought down to the ground by diffusion and turbulent mixing at some distance inland. In this situation, the effects of the plume would be greater at stations farther from the plant than at those close by. Such a scenario was hypothesized by Koss and Altomare (1971) for the Palisades cooling towers. Since there are no direct data available indicating a cause and effect relationship, the present analysis may only be considered as evidence that such a relationship may exist.

At 1900 EST the shaded area, even though suggestive of a plume, is off-axis by around 10° . Such a deviation may be due to meteorological factors as discussed above or may be indicative of a systematic error of approximately 10° in the wind direction measurements (which is roughly their inherent accuracy). Since the plume appears to be exactly on-axis at 0100 EST, the former explanation is more likely correct.

Figs. 6.24 and 6.25 indicate that the magnitudes of the increase in relative humidity and dew point on the plume axis are on the order of 1% and 0.2°C , respectively. Taking into account the off-axis negative differences, the effect of the plume is generally less than 2% and 0.5°C . These represent the maximum differences being detected. In much of the analysis area the differences are less and the corresponding significance levels are marginal. In fact, this analysis failed to show any effects of the plume except during the two nighttime hours for the moisture variables shown above.

Conclusions

The analyses above have examined diurnal and spatial variations of average temperature, relative humidity and dew point data for stations in the vicinity of the Palisades nuclear plant. The diurnal analysis showed that differences between data from the operational and nonoperational periods on the order of 0.3°C for temperature, 1.4% for relative humidity and 0.4°C for dew point are detectable with 95% confidence (i.e., statistically significant at

the .05 level). The largest difference between operational and nonoperational data occurred in spring, where daytime ΔT averaged 0.5-1.3°C lower during the operational period. That difference was related to differences in cloud cover between the operational and nonoperational periods, and served to show that significant differences between the two data sets could exist which were totally unrelated to the operation of the cooling towers.

The only season which showed possible cooling tower effects was winter. Onsite, at P01A, operational temperatures and dew points were significantly higher (at the .05 level) than nonoperational with onshore winds. Offsite, marginal significance was attached to nighttime increases in relative humidity and dew point during the operational period. These increases appeared to be most significant under the plume centerline, at a distance of about 11 km from the cooling towers. The magnitudes of these increases were small: 0.5°C for temperature and dew point and 1.5% for relative humidity.

VII. PRECIPITATION

Introduction

Of the possible meteorological effects of the cooling towers, a modification of precipitation is one of the most difficult to detect because of the high natural variability of precipitation in time and space. As discussed in the Fifth (1977) and the Sixth (1978) Annual Reports, detection of any modification is further hampered by the fact that, like other meteorological variables, precipitation amounts are not normally distributed statistically. According to Huff (1971) and Brooks and Carruthers (1953), the distribution is approximately a log-normal or a gamma type. Because of this non-normality, classical statistical methods which assume normality (such as "Student's" t -test) cannot be used on precipitation data. Numerous techniques which have been applied in attempts to normalize precipitation data have been unsuccessful in doing so.

To test for changes which may be caused by the cooling towers required a statistical test which was independent of the sample distribution. The Wilcoxin-Mann-Whitney statistical test was chosen here because it:

- (1) is independent of the sample distribution,
- (2) can be used on samples of unequal sizes,
- (3) abstractly uses magnitude by its utilization of ranks, and

- (4) is as powerful as the t -test when dealing with non-normal distributions (Lehmann, 1975).

Other researchers are currently employing the Wilcoxin-Mann-Whitney statistic in assessing possible precipitation modification. Patrinos and Hoffman (1979) are currently developing and testing new statistical methods for assessing possible precipitation modification near the Bowen plant's natural draft cooling towers. These new techniques test for a change in the distributional properties of the skewness and kurtosis of the precipitation data in addition to change in the mean.

In the present study, daily precipitation data for the period September, 1972, through March, 1979, were analyzed for both the Palisades stations and nearby National Weather Service stations. The Wilcoxin-Mann-Whitney statistic from this data set was obtained by applying the following steps to each station's data:

- (1) All days with precipitation less than .005 inches (trace) were ignored. This removed the obvious bias of no effect, since there must be precipitation in order for it to be modified.
- (2) The precipitation days were grouped by season.
- (3) The precipitation days were coded either "operational" or "nonoperational" depending on the cooling tower status.
- (4) The days with precipitation were ranked in order of increasing amount without regard to cooling tower status.

- (5) The ranked data were separated according to the operational status of the cooling towers.
- (6) The number of observations in each group was counted and the ranks were summed.
- (7) The Wilcoxin-Mann-Whitney statistic was computed from the following equation:

$$WMWS = N_1 N_2 + \frac{N_1 (N_1 + 1)}{2} - \sum R_1$$

where: WMWS is the Wilcoxin-Mann-Whitney statistic,

N_1 is the size of sample,

N_2 is the size of sample 2, and

$\sum R_1$ is the summation of the ranks pertaining to sample 1 (Hewlett-Packard, 1975).

- (8) A significance level was determined from this statistic and compared to a predetermined confidence level after which a decision was made. The null hypothesis tested by the Wilcoxin-Mann-Whitney statistic was H_0 : the mean daily operational precipitation equals the mean daily nonoperational precipitation (e.g., $H_0: \mu_1 = \mu_2$).

This hypothesis was rejected if either of the following conditions occurred:

$$WMWS (\text{Sample}) > WMWS (1-\alpha/2) \text{ or}$$

$$WMWS (\text{Sample}) < WMWS (\alpha/2)$$

where α is a significance level.

Recent research has shown that an interpretation of this statistic in terms of its classical use is not always required to determine a modification. Instead, the

relative magnitude of the significance level can be interpreted as an indicator of a possible difference (Lindmann, 1974). In the following discussion, both interpretations are used and to aid in showing the results, the significance level α is given as a percentage. This percentage refers to the probability of rejecting the null hypothesis. Moreover, a difference is considered significant whenever this probability is 90% or greater.

Discussion

The figures given below show differences and rejection probabilities by season. In the figures, positive differences between precipitation means indicate that the mean daily precipitation for the operational period was greater than that for the nonoperational period. Also, stations with an M (missing) symbol have precipitation data, but these data for late 1978 and early 1979 were not available from the National Climatic Center in time for inclusion in this analysis. Finally, stations which are just beyond the map perimeter are also included to extend the region analyzed. The stations are Holland, Kalamazoo, Eau Claire, Dowagiac, and Three Rivers.

Winter. The mean differences and rejection probabilities for the winter season are given in Fig. 7.1. The only significant probabilities are those near stations P03A, P05A, P09A, P10A and Benton Harbor. The differences corresponding

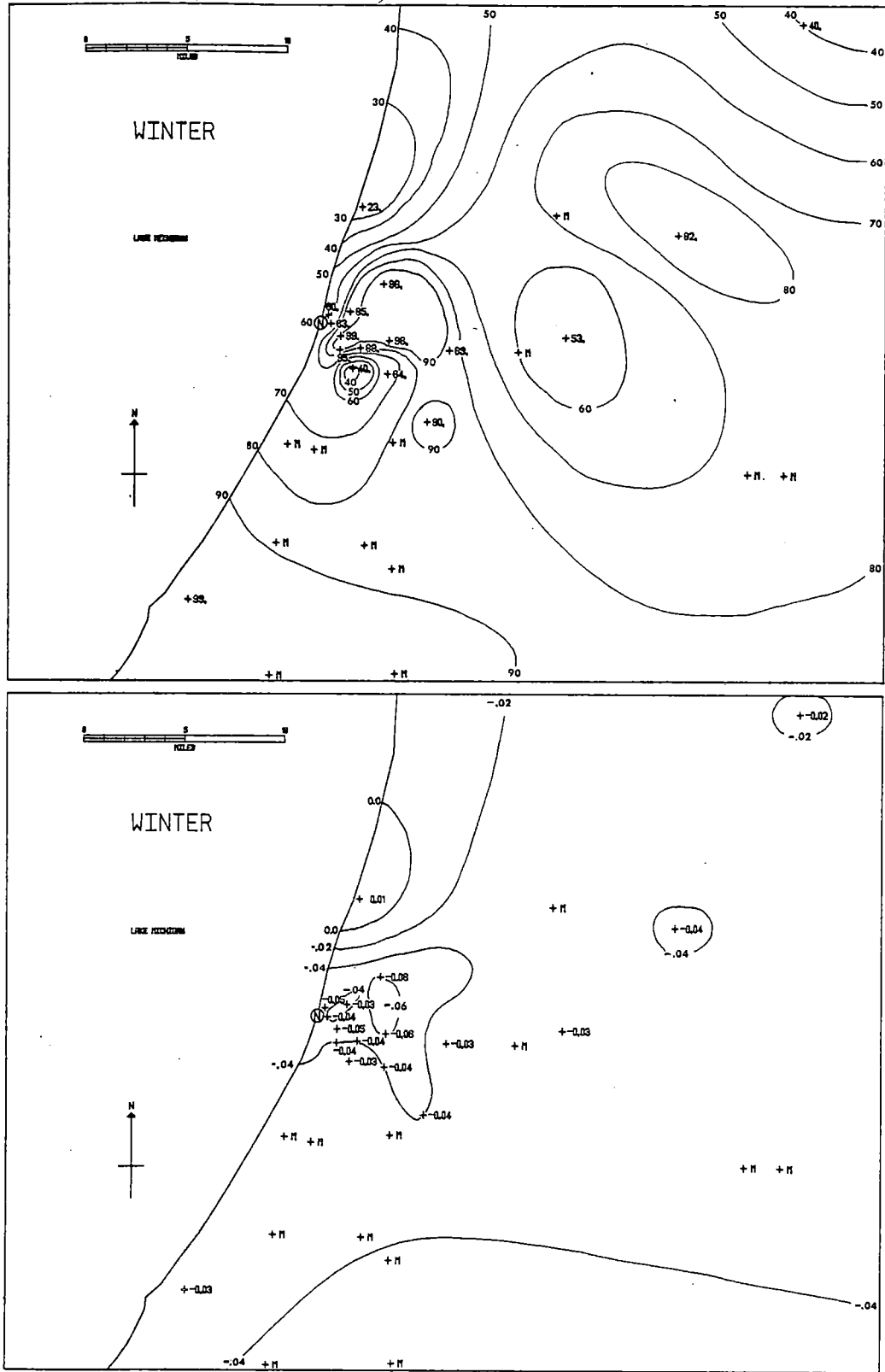


Fig. 7.1: Winter mean daily precipitation differences in inches between operational and nonoperational periods (top) and percent probability of rejecting the hypothesis that mean daily amounts for the two periods are equal (bottom).

to these probabilities are negative, which means that on the average, less precipitation occurred during the operational period than during the nonoperational period.

Spring. The difference and probability patterns for the spring season are quite variable as shown in Fig. 7.2. Only one station, South Haven, has a marginal significance.

Summer. The values for the summer months reveal a more orderly pattern as shown in Fig. 7.3. The area of highest probabilities for rejecting the hypothesis of equal means includes the entire network and extends east-southeast toward Kalamazoo. The magnitude of these probabilities (>95%), as well as the fact that the differences are positive, indicate that precipitation for the operational period is much higher than for the nonoperational period.

The following two factors indicate that this pattern is due to natural causes and not to the cooling towers:

- (1) There is relatively little spatial change of rejection probabilities with distance from the towers. In fact, with the exception of Benton Harbor, all probabilities are greater than or equal to 79%, and all differences are highly positive. If the cooling towers were the cause for the increase in precipitation, some evidence of this in the form of a region of lower rejection probability should be discernible.

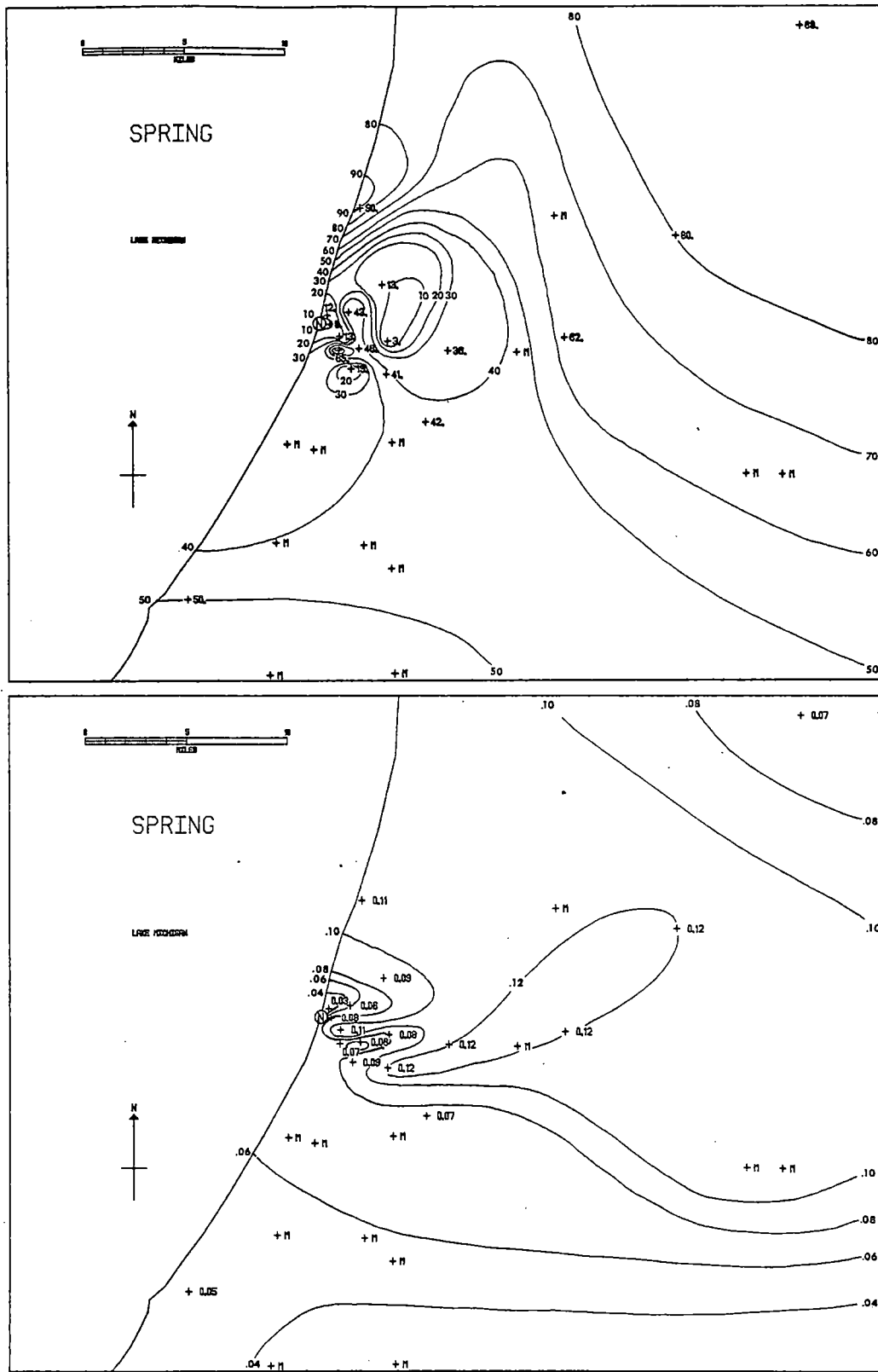


Fig. 7.2: As in Fig. 7.1, but for spring.

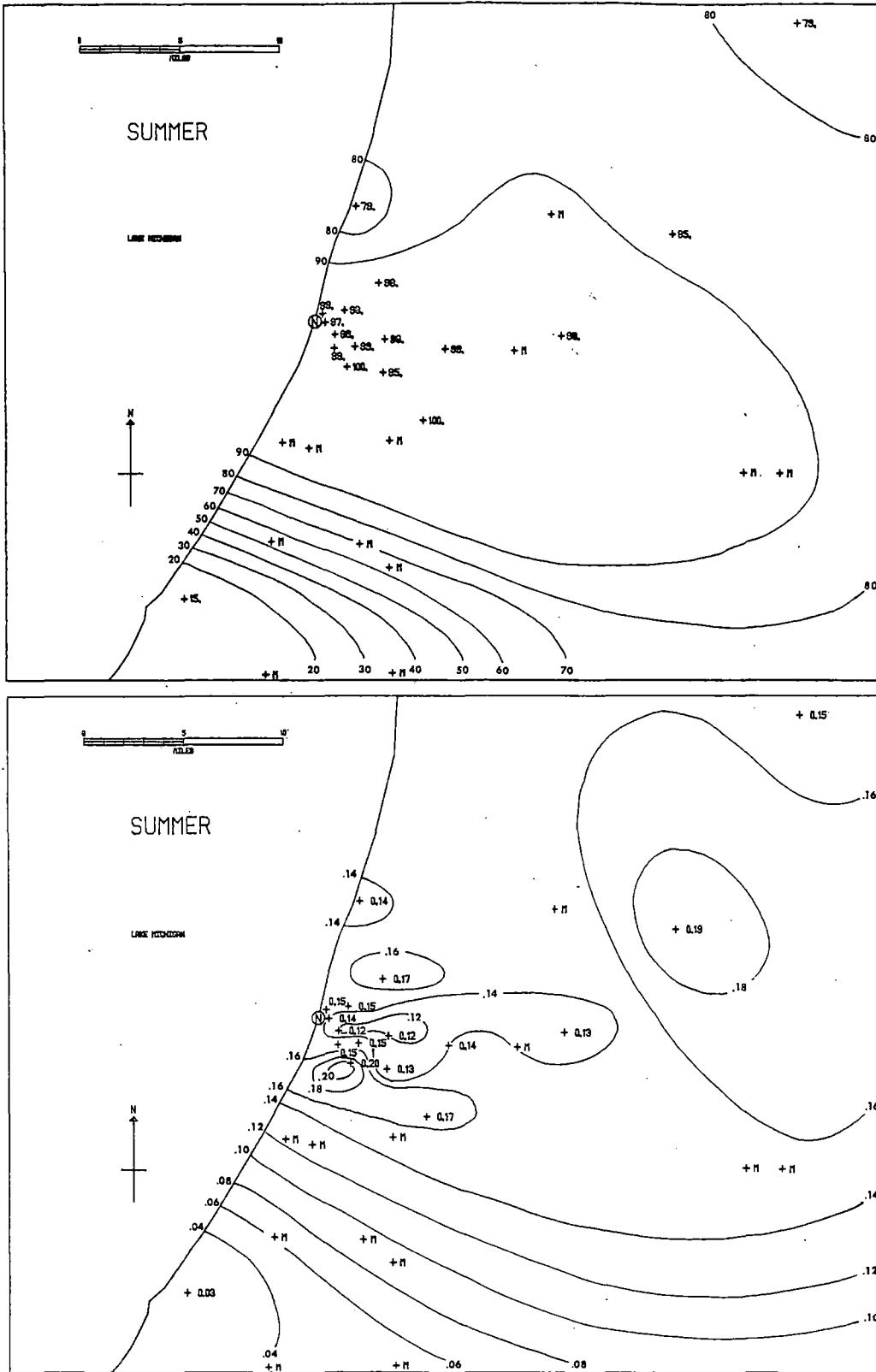


Fig. 7.3: As in Fig. 7.1, but for summer.

(2) The rejection probabilities were insensitive to changes in the lower precipitation cutoff limit. For this analysis, the limit below which precipitation amounts were ignored was intentionally varied from the original .005 inches to .05, .10, .15, .20, and .25 inches and new probabilities computed to determine if sensitivity to new values existed. No change occurred up to 0.25 inches. It is highly unlikely that the cooling towers could influence precipitation by more than this amount.

Both of these factors indicate that large (>0.25 inch) rainfalls are affecting the means. To test this possibility, histograms of operational and nonoperational precipitation amounts were prepared as shown in Fig. 7.4. It can be noted that the operational data set contains a larger percentage of rainfalls greater than 0.25 inches than does the nonoperational set.

Autumn. The statistics for the autumn season are shown in Fig. 7.5. The patterns are quite variable, with Benton Harbor displaying the only critical value. Because the corresponding difference is negative, however, no cooling tower influence is indicated.

Conclusions

The Wilcoxin-Mann-Whitney statistic was applied to daily precipitation data from both network and National

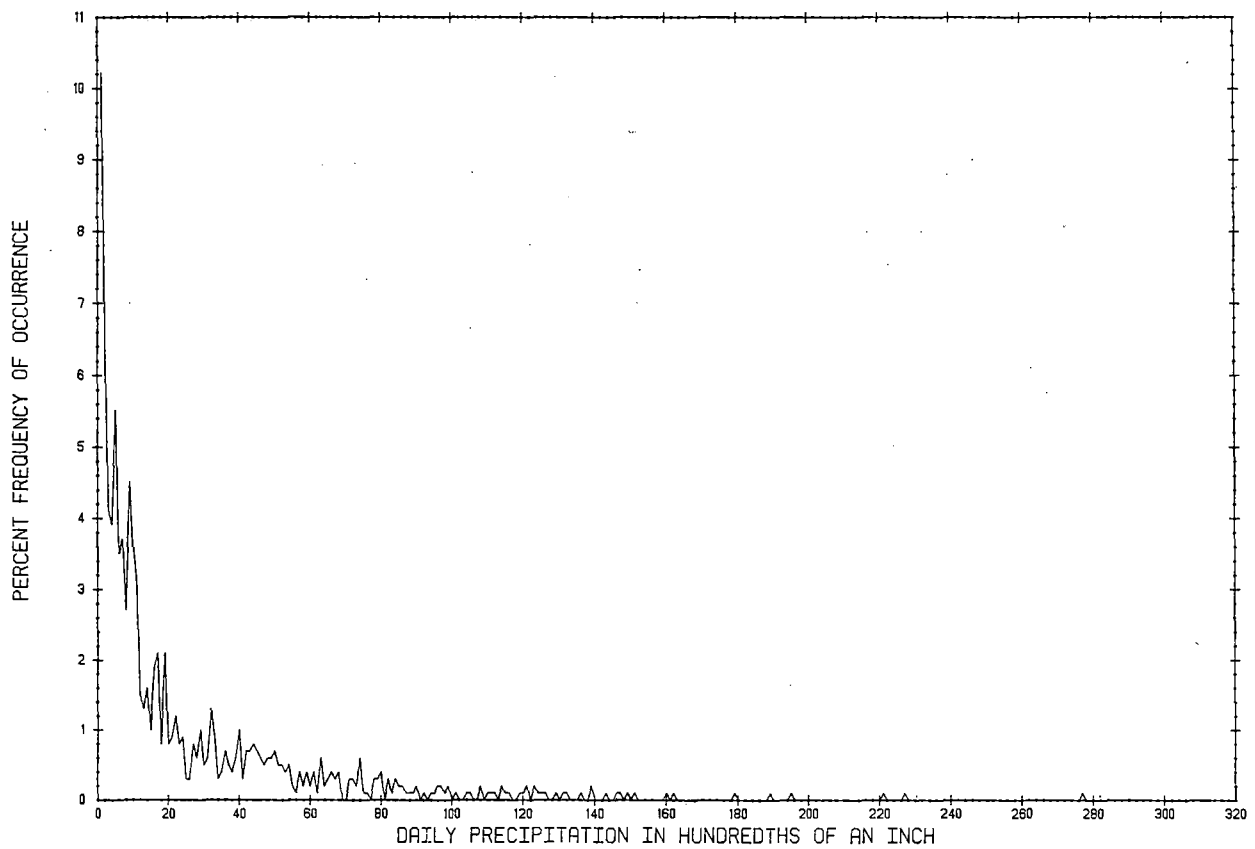
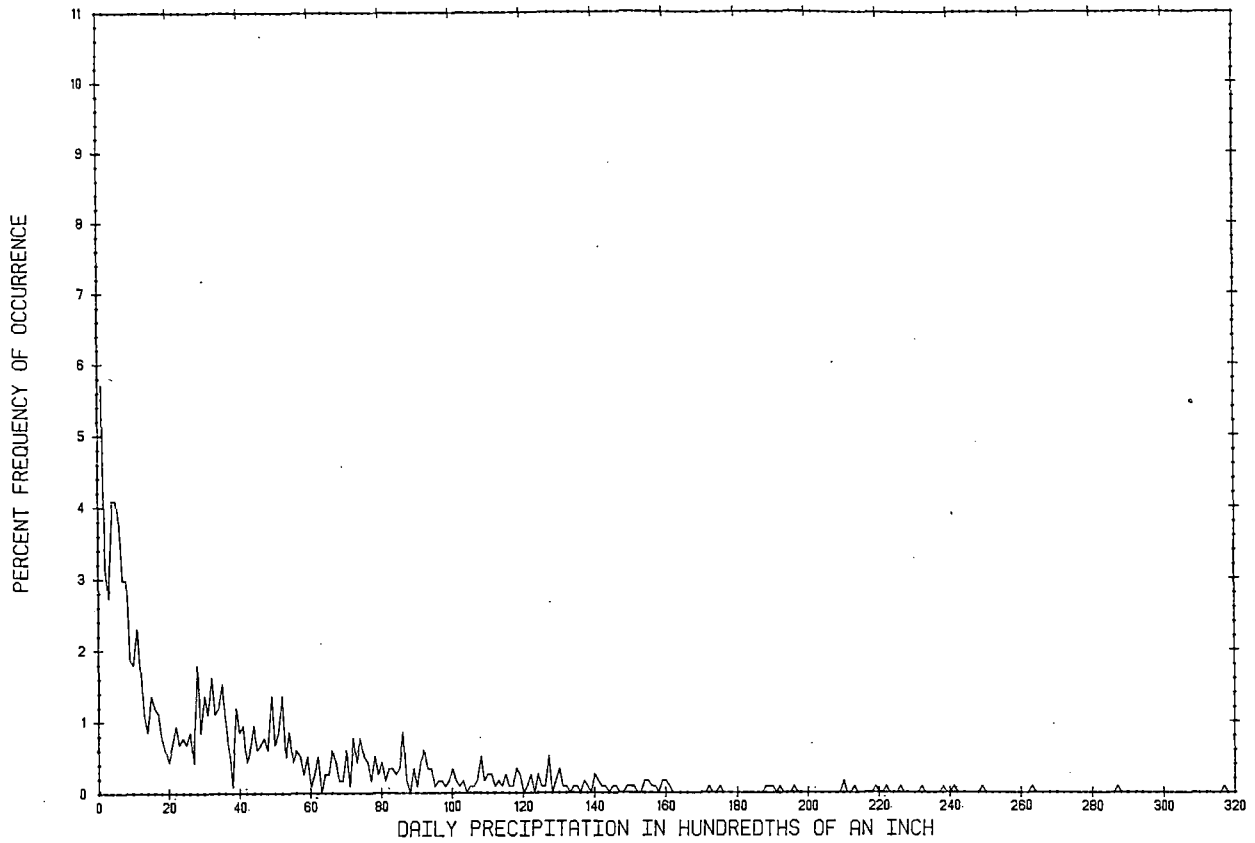


Fig. 7.4: Percent frequency of occurrence of mean daily operational (top) and nonoperational (bottom) precipitation amounts for summer.

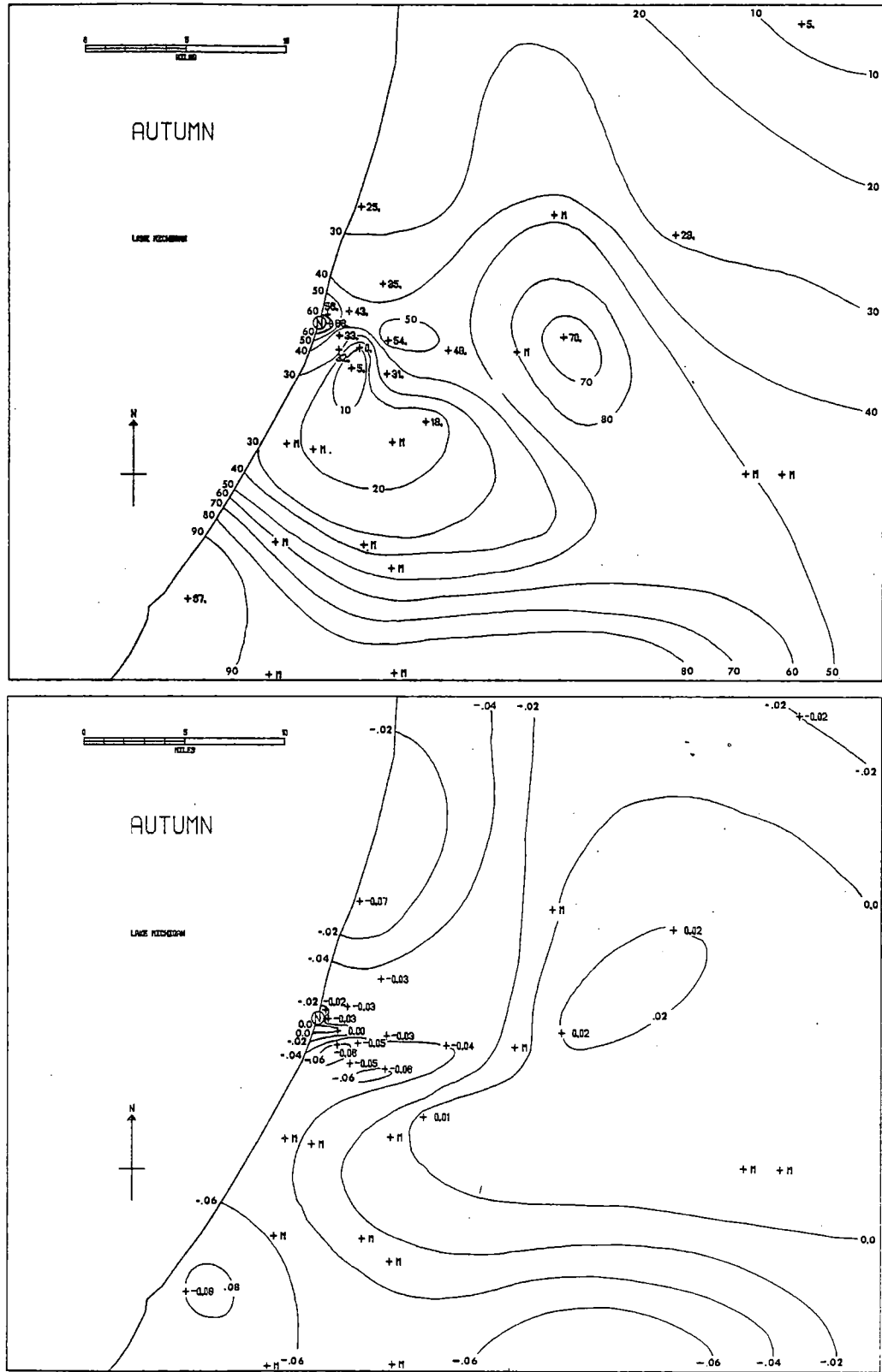


Fig. 7.5: As in Fig. 7.1, but for autumn.

Weather Service stations to determine if significant differences occurred between operational and nonoperational periods. In the winter and autumn seasons, some stations indicated negative differences, meaning that the operational mean was significantly less than the nonoperational mean and that there was no cooling tower effect. In the spring season, only one station indicated a positive difference. This difference was only marginally significant, however, and inconclusive in determining any cooling tower influence. For the summer season, significant positive difference occurred in an orderly pattern, but further analysis of the precipitation distribution showed that the differences were the result of natural causes. In summary, the statistical method applied did not disclose a modification of precipitation by the cooling towers.

VIII. POTENTIAL APPLE SCAB INFECTION CONDITIONS

Introduction

The release of large amounts of heat and moisture into the atmosphere by the cooling towers has caused concern that an increase in occurrences of apple scab infections may result. Apple scab is a parasitic fungus disease which can cause major damage to both leaves and fruit of apple orchards (Jones, 1971). Because the raising of apples and other fruit is one of the main industries in southwestern Lower Michigan, the concern centers around the possibility that the cooling towers could cause an increase in occurrences of certain combinations of temperature, humidity and precipitation conditions conducive to potential apple scab infections. A study of occurrences of these conditions, therefore, has been an ongoing part of this investigation. Final results are described below.

The study consists of a comparison of occurrences computed using meteorological data for several Palisades stations with those computed using data for Muskegon, which serves as a representative control station. As mentioned previously, the National Weather Service Station at Muskegon is as close to Lake Michigan as several Palisades stations are, but because it is about 112 km north of the cooling towers, it is out of range of their effects.

Conditions for Formation

Germination leading to apple scab infections begins as soon as disease-carrying spores, which are released from perithecia on dead leaves on the orchard floor during temperatures above freezing, land on new green leaves or fruit which are also wet. As shown in Table 8.1, the meteorological conditions most conducive to apple scab germination and infection are temperatures between 63°F and 75°F accompanied by or immediately following rain (Jones, 1971). In this temperature range, Table 8.1 shows that it takes only 9 hours for a light infection and 18 hours for a heavy infection to take place after the start of rain. If a protective spray is not applied before or within this critical 9-hour period, a spray with eradicative properties must be used. At colder temperatures, longer times are required for infections to occur. None occurs at temperatures below freezing.

Because an infection period begins only with the start of rain, the criteria used here to determine the potential severity of an infection were that the temperature remain above freezing during precipitation and that the relative humidity remain at least 85% following the end of precipitation. The precipitation criterion chosen was that it must exceed 0.005 inch per hour. The reason for adding relative humidity to the precipitation-temperature requirement (for the temperature range conducive to infections) is that leaves, bark and fruit which are wet from rain

are likely to remain wet as long as the relative humidity is at least 85%, even though the rain has ended. The period of infection and, therefore, its severity are likely to be increased.

Table 8.1

Number of hours of wetting required for primary apple scab infection at different air temperatures.*

Average Temperature	Degree of Infection		
	Light	Moderate	Heavy
<u>°F</u>	<u>hrs</u>	<u>hrs</u>	<u>hrs</u>
78	13	17	26
77	11	14	21
76	9 1/2	12	19
63 to 75	9	12	18
62	9	12	19
61	9	13	20
60	9 1/2	13	20
59	10	13	21
58	10	14	21
57	10	14	22
56	11	15	22
55	11	16	24
54	11 1/2	16	24
53	12	17	25
52	12	18	26
51	13	18	27
50	14	19	29
49	14 1/2	20	30
48	15	20	30
47	17	23	35
46	19	25	38
45	20	27	41
44	22	30	45
43	25	34	51
42	30	40	60
33 to 41	2 days		

*taken from Jones (1971).

A computer program was written which totaled the number of hours fulfilling the above criteria for several Palisades stations for February through August, 1974 through 1978. Each occurrence was categorized as being conducive to either light, moderate or heavy infection according to the data in Table 8.1, and the number of occurrences was totaled by month.

Climatological information necessary to determine natural occurrences was obtained by performing similar computations using data for Muskegon for the period 1948-1952, which was chosen on the basis of completeness of hourly weather observations on magnetic tape. Muskegon occurrences for 1974 through 1978 were obtained by manually screening hourly weather observations and tabulating these data according to the criteria of Table 8.1.

Nonoperational and operational occurrences

Results of the computations of occurrences of apple scab infection conditions are given in Table 8.2. The top half gives the number of occurrences by month and year for Muskegon and for station P05A, located in an orchard about 5 km from the cooling towers. Because station P05A was not in operation in 1978, data for station P07A were used. The average number of occurrences for Muskegon for the period 1948-52 is also given. The bottom half of Table 8.2 lists total occurrences for Muskegon and for several network stations by degree of potential infection and by year.

Table -8.2

Number of Occurrences of Potential Apple Scab Infection Conditions

<u>Muskegon County Air (MKG)</u>																								
	LIGHT (L)						MODERATE (M)						HEAVY (H)											
	F	M	A	M	J	J	A	TOT	F	M	A	M	J	J	A	TOT	F	M	A	M	J	J	A	TOT
1974 (non-op)	0	0	1	0	5	1	0	7	0	0	1	2	3	1	1	8	0	1	1	2	0	1	0	5
1975 (op)	0	0	1	2	3	1	1	8	0	0	1	3	3	2	2	11	0	0	0	0	1	0	3	4
1976 (op)	0	1	0	0	1	2	0	4	0	1	0	1	2	2	0	6	0	0	0	2	2	1	1	6
1977 (op)	0	1	1	1	1	1	2	7	0	0	2	0	4	1	1	8	0	2	0	0	1	3	5	11
1978 (op)	0	0	2	1	3	0	2	8	0	0	0	2	2	1	0	5	0	0	0	1	1	3	2	7
AVE (climo)	(1948-1952)						7								8								3	

<u>Station P05A</u>																								
	F	M	A	M	J	J	A	TOT	F	M	A	M	J	J	A	TOT	F	M	A	M	J	J	A	TOT
1974	0	0	1	2	0	1	2	6	0	0	1	0	5	0	2	8	0	0	0	1	1	1	2	5
1975	0	0	1	3	3	4	1	12	0	0	0	3	3	1	3	10	0	0	0	2	0	0	2	4
1976	0	0	2	0	0	0	0	2	0	0	0	1	2	6	0	9	0	0	0	2	2	0	0	4
1977	0	0	1	0	2	0	4	7	0	0	1	1	2	0	4	8	0	1	1	1	2	1	2	8
1978 (P07A)	0	0	1	1	0	1	2	5	0	0	1	0	2	2	1	6	0	0	0	2	0	2	0	4

<u>Totals</u>																				
Station	1974				1975				1976				1977				1978			
	L	M	H	TOT	L	M	H	TOT	L	M	H	TOT	L	M	H	TOT	L	M	H	TOT
MKG	7	8	5	20	8	11	4	23	4	6	6	16	7	8	11	26	8	5	7	20
P03A	4	9	2	15	4	15	3	22	4	10	3	17	12	4	4	20	6	3	4	13
P04A	3	12	3	18	3	15	3	21	4	8	4	16	10	5	8	23				
P05A	6	8	5	19	12	10	4	26	2	9	4	15	7	8	8	23				
P06A	4	11	5	20	7	13	5	25	5	6	5	16	11	7	6	24				
P07A	5	10	3	18	9	12	3	24	5	6	5	16	7	7	5	19	5	7	4	16

The results show that

- (1) For Muskegon, whose results are representative of those for a control station, meteorological conditions conducive to some degree of apple scab infection occur most frequently in June, with an average of about six occurrences. There are usually no occurrences in February, one in March, two in April, three in May and four both in July and August. In the five-year period shown, 1977 had the largest total occurrences with 26, and 1976 had the smallest with 16.
- (2) Similar results can be noted for station P05A. May, June, July and August each have four or five occurrences on the average, February has none, March has one and April has two. Like the Muskegon results, the fewest occurrences at P05A were in 1976 when there were 15. The most were in 1975 when there were 26, which was two greater than at Muskegon.
- (3) Although it is not shown explicitly at the bottom of Table 8.2, the average of the total occurrences for each year for the five Palisades stations was equal to or less than that of the Muskegon control data for each year except 1975 when it was one greater.

These results show that for the stations used in the analysis there was no increase in occurrences of potential apple scab infection conditions due to the

operation of the cooling towers. Most changes in occurrences which took place in the network data from month to month and from year to year also took place in the control data, which indicates that weather patterns on the scale of migratory pressure systems are the dominating influence on occurrences of potential apple scab infection conditions.

PART C. CONCLUSIONS

IX. SUMMARY OF FINDINGS

1) The most serious effect of the cooling towers is icing caused by the freezing of both drift and plume in downwash conditions. For temperatures less than about -3°C , both drift and plume freeze as dense glaze ice on impact with natural surfaces. For wind speeds greater than 6 m sec^{-1} , icing may extend as far as 200 m downwind. Because the heaviest drift droplets are the first to fall out and freeze, beyond about 200 m freezing of only the plume produces a less dense type of icing on only tall objects. This type of icing may extend as far as 400 m downwind if the wind speed exceeds 8 m sec^{-1} . In general, wind directions from the southwest and northwest quadrants produce the most frequent and longest lasting icing episodes. Reports of icing were received as early in the autumn as 12 November and as late in the spring as 9 April.

2) Based on observations reported by personnel at the plant site, damage to vegetation and slippery driving conditions are the main impacts of the icing. Their severity decreases with distance downwind, but the longer the duration of subfreezing temperatures with a steady wind direction, the greater will be the accumulation of ice, the narrower will be the zone of icing and the more severe will be the impact of the icing. The damage to vegetation and slippery driving conditions were reported at locations on the plant site itself.

3) Cooling tower effects on humidity, temperature and fog are minimal except for locations within about 200 m of the towers which are occasionally affected by plume downwash. For wind speeds greater than 4 m sec^{-1} downwash occurs which often reaches ground level and causes an increase in temperature and humidity and a reduction in visibility. The higher the wind and natural humidity, the farther downwind the plume remains dense and in contact with the ground before lifting. Six observations reported the plume remaining at ground level near the 0.7-km inland distance of the plant site boundary from the cooling towers.

4) Statistical analyses of visibility and precipitation data for the operational and nonoperational periods show that there are a few significant differences between these periods. None of the observed differences, however, is attributable to cooling tower effects. Instead natural meteorological processes and variabilities are believed to be responsible.

5) Statistical analyses of temperature, relative humidity and dew point data show no differences between the nonoperational and operational periods which are attributable to cooling tower effects in spring, summer and autumn. A few statistically significant, but small, increases in the values of these variables were found in winter both near the plant and downwind under the plume centerline. The overall impact of the cooling towers on these variables at any point in the network, however, is negligible.

6) The occurrences of combinations of precipitation, temperature and humidity which are conducive to apple scab infections are not increased by cooling tower operation over those which occur naturally.

7) Shadowing effects of the cooling tower plume are minor compared to shadowing by natural cloudiness except for mornings in the summer season at locations within a few km of the cooling towers. Summer mornings are normally cloudless except for the plume, so shadowing is significant near the towers until rapid evaporation of the plume occurs near midday. In cloudless conditions with a dense plume, solar radiation is decreased where the plume's shadow falls, but it is increased above clear sky values on either side of the shadow due to reflections from the sides of the plume. Because the average amount of sky covered by natural cloudiness during daytime is 6/10 in spring, 7/10 in autumn and 8/10 in winter, it is concluded that the plume does not add significantly to the natural shadowing produced by clouds in those seasons.

REFERENCES

- Baten, W.D. and A.H. Eichmeier, 1955: A summary of weather conditions at South Haven, Michigan from 1926 to 1952. Michigan State College Experiment Station Report, 52 pp.
- Brooks, C.E.P. and N. Carruthers, 1953. Handbook of Statistical Methods in Meteorology. Her Majesty's Stationery Office, London.
- Carson, J.E., 1976: Atmospheric impacts of evaporative cooling systems. Argonne National Laboratory Report ANL/ES-53, 48 pp.
- Dixon, W.J. and F.J. Massey, 1969: Introduction to Statistical Analysis. McGraw-Hill Book Company, 638 pp.
- Hewlett-Packard Co., 1975: Statistical Applications; from J.L. Freund, 1962, Mathematical Statistics, Prentice-Hall.
- Huff, F.A., 1971: Evaluation of Precipitation Records in Weather Modification Experiments, Advances in Geophysics 15, Academic Press, New York.
- Jones, A.L., 1971: Diseases of tree fruits in Michigan. Michigan State University Extension Bulletin E-714, 31 pp.
- Koss, T.C. and P.M. Altomare, 1971: Evaluation of environmental effects of evaporative heat dissipation systems at the Palisades Plant. Report for Consumers Power Company, NUS - 785, NUS Corporation, Rockville, Maryland, 68 pp.
- Larson, H.J., 1969: Introduction to Probability Theory and Statistical Inference, John Wiley & Sons, 387 pp.
- Lehmann, E.L., 1975: Nonparametrics: Statistical Methods Based on Ranks. Holden-Day, Inc., San Francisco.
- Lindman, H.R., 1974: Analysis of Variance in Complex Experimental Designs. W.H. Freeman & Company, San Francisco.
- Lowry, W.P., 1977: Empirical estimation of urban effects on climate: a problem analysis. J. Appl. Meteor., 16, 129-135.
- Michigan Department of Agriculture, Michigan Weather Service, 1971: Climate of Michigan by Stations.
- Patrinos, A.A.N. and H.W. Hoffman, 1979: Meteorological Effects of Thermal Energy Releases (METER). Annual Progress Report, 1977-78, Oak Ridge National Laboratory.

REFERENCES (cont.)

- Rochow, J.J., 1978a: Compositional, structural and chemical changes to forest vegetation from fresh water wet cooling tower drift. In Proceedings of Cooling Tower Environment - 1978 Symposium, May 2-4 1978, University of Maryland, College Park.
- _____, 1978b: Measurements and vegetational impact of chemical drift from mechanical draft cooling towers. Env. Sci. and Tech., 12, 1379-1383.
- Ryznar, E., 1978: An observation of cooling tower plume effects on total solar radiation. Atmos. Env., 12, 1223-1224.
- _____, D.G. Baker, and H. Moses, 1976: Coastal meteorological networks to determine effects of nuclear plant cooling systems. Bull. Am. Meteor. Soc., 56, 1441-1446.
- Sampson, R.J., 1978: Surface II Graphic System. Kansas Geological Survey.
- Snedecor, G.W., 1956: Statistical Methods. Iowa State College Press, Ames, Iowa, 534 pp.
- U.S. Atomic Energy Commission, 1972: Environmental Statement for Palisades Nuclear Generating Plant. Docket No. 50-255.
- U.S. Atomic Energy Commission, 1973: Environmental Statement for Donald C. Cook Nuclear Generating Plant. Docket No. 50-315 and 50-316.
- Weber, M.R., 1978: "Average diurnal wind variation in southwestern lower Michigan." J. Appl. Meteor., 17, 8, 1182-1189.

APPENDIX A
PROJECT PUBLICATIONS AND REPORTS

Journal Articles and Papers

Ryznar, E., D.G. Baker and H. Moses, 1976: "Coastal meteorological networks to determine effects of nuclear plant cooling systems". Bull. Amer. Meteor. Soc., 57, 1441-1446.

_____, 1977: "Advection-radiation fog near Lake Michigan." Atmos. Env., 11, 427-430.

_____, 1978: "An observation of cooling tower plume effects on total solar radiation." Atmos. Env., 12, 1223-1224.

Weber, M.R., 1978: "Average diurnal wind variation in southwestern lower Michigan." J. Appl. Meteor., 17, 8, 1182-1189.

Weber, M.R., 1978: "Seasonal variations in temperature in the vicinity to two nuclear power plants: a comparison of operational and preoperational data." Presented at the American Meteorological Society Conference on Climate and Energy, May 1978, and published in proceedings:

Moses, H., D.G. Baker, E. Ryznar, and D. Young: "A comparison of the amounts of solar and wind energy available." Presented at the American Meteorological Society Conference on Climate and Energy, May 1978, and published in proceedings.

Annual Reports

All annual reports come under the general heading of "An investigation of the meteorological impact of mechanical-draft cooling towers at the Palisades Nuclear Plant", DRDA Project 320158, University of Michigan.

1973 Ryznar, E. and D.G. Baker: First Annual Progress Report, 42 pp.

1974 _____ and D.G. Baker: Second Annual Report, 78 pp.

1975 _____ M. R. Weber, and D.G. Baker: Third Annual Report, 59 pp.

1976 _____ M. R. Weber, D.G. Baker and D.F. Kahlbaum, Fourth Annual Report, 102 pp.

1977 _____ M.R. Weber, D.F. Kahlbaum and W.G. Snell, Fifth Annual Report, 103 pp.

1978 _____ D.G. Baker, M.R. Weber and D.F. Kahlbaum, Sixth Annual Report, 196 pp.

Data Reports

1975 Ryznar, E., D.G. Baker, M.R. Weber, R. Kessler, and J.A. Baron: Data Report No. 1: Summary of Meteorological Measurements for the Period October 1972 through June 1973. 99 pp.

- 1975 Weber, M.R., R. Kessler, W.G. Snell, D.C. Dismachek, and D.F. Kahlbaum: Data Report No 2: Summary of Meteorological Measurements for the Period July 1973 through December 1973. 100 pp.
- 1976 Weber, M.R., R. Kessler, W.G. Snell, D.F. Kahlbaum: Data Report No. 3: Summary of Meteorological Measurements for the Period January 1974 through December 1974. 172 pp.
- 1976 Snell, W.G. and D.F. Kahlbaum: Data Report No. 3.1: Summary of Temperature and Humidity Measurements for the Period January 1974 through December 1974. 37 pp.
- 1977 Weber, M.R., D.F. Kahlbaum, R. Kessler and C.R. Wilkes: Data Report No. 4: Summary of Meteorological Measurements for the Period January 1975 through December 1975. 215 pp.
- 1977 Weber, M.R., D.F. Kahlbaum, R. Kessler, G.J. Rizzo, M. St. Peter and C.R. Wilkes: Data Report No. 5: Summary of Meteorological Measurements for the Period January 1976 through December 1976.
- 1978 Weber, M.R., D.F. Kahlbaum, M.J. St. Peter, W.W. Beaton and J.N. Deaconson: Data Report No. 6 Summary of Meteorological Measurements for the Peirod January 1977 through December 1977. 221 pp.

Appendix B. Percent Data Recovery By Month and Variable

1973	Precip.	Temp.	Rel. Hum.	Solar Radiation		Wind Direction		Wind Speed		Visibility	
	(Network)	(Network)	(Network)	P03A	P07A	P03A	P07A	P03A	P07A	P03A	P07A
APR	91	58	-	-	-	76	96	87	59	-	-
MAY	95	50	-	-	-	98	99	98	99	100 (a)	100 (b)
JUN	98	49	-	-	-	99	99	99	99	100	90
JUL	98	96	-	100	100	92	99	92	99	100	97
AUG	98	84	-	100	93	99	60	99	86	97	61
SEP	96	89	-	99	99	99	0	99	0	100	60
OCT	98	94	-	99	99	100	0	92	17	98	100
NOV	99	89	-	100	100	75	51	99	94	100	100
DEC	95	80	-	95	100	49	99	88	96	97	100
1974											
JAN	97	84	86	100	25	98	98	79	99	0	96
FEB	97	84	85	98	61	97	99	89	98	55	94
MAR	99	97	97	98	88	96	99	74	96	59	66
APR	98	99	98	91	100	50	99	99	99	0	0
MAY	96	98	94	100	100	98	99	98	99	43	75
JUN	98	97	92	99	100	99	89	98	96	100	99
JUL	97	99	97	100	99	99	99	100	99	100	100
AUG	99	100	99	100	91	99	99	99	79	86	67
SEP	98	98	98	98	100	99	99	99	99	93	0
OCT	98	100	99	100	100	99	99	99	99	100	0
NOV	86	99	99	100	100	99	99	99	99	100	0
DEC	98	99	99	17	17	100	98	99	100	100	0

Appendix B. Percent Data Recovery By Month and Variable (cont.)

1975	Precip.		Rel. Hum. (Network)	Solar Radiation		Wind Direction		Wind Speed		Visibility	
	(Network)	(Network)		P03A	P07A	P03A	P07A	P03A	P07A	P03A	P07A
JAN	96	99	99	88	98	77	98	62	99	99	0
FEB	96	99	100	99	100	4	98	4	99	99	33
MAR	98	96	96	100	99	99	99	95	99	100	100
APR	99	90	90	100	76	99	58	99	79	100	73
MAY	99	100	99	99	89	99	95	99	84	77	100
JUN	100	98	97	99	100	98	99	99	99	93	100
JUL	99	99	99	100	95	87	99	99	99	81	100
AUG	100	99	99	100	98	99	99	100	99	95	88
SEP	100	99	99	100	66	99	79	99	99	86	95
OCT	100	100	100	99	99	100	100	100	99	100	100
NOV	100	99	99	100	99	56	99	56	99	88	67
DEC	99	99	99	99	100	96	97	91	89	86	0
1976											
JAN	100	93	93	100	100	99	99	96	99	100	0
FEB	99	97	97	100	100	99	90	100	83	100	0
MAR	99	98	98	100	99	81	80	99	80	92	85
APR	100	98	98	96	100	72	98	100	98	89	100
MAY	99	100	100	97	92	99	99	99	99	91	100
JUN	99	99	99	94	60	90	99	99	99	98	100
JUL	100	95	94	97	14	94	99	92	99	81	88
AUG	99	99	99	86	100	99	99	99	99	100	100
SEP	99	98	98	100	100	99	99	99	100	100	89
OCT	99	94	94	100	100	95	99	94	99	90	100
NOV	96	99	99	100	100	99	99	93	99	96	97
DEC	96	94	94	99	99	99	100	92	100	20	81

Appendix B. Percent Data Recovery By Month and Variable (cont.)

	Precip.	Temp.	Rel. Hum.	Solar Radiation		Wind Direction		Wind Speed		Visibility	
	(Network)	(Network)	(Network)	P03A	P07A	P03A	P07A	P03A	P07A	P03A	P07A
1977											
JAN	85	94	94	80	99	71	74	71	74	20	80
FEB	90	93	93	91	98	91	98	86	95	40	93
MAR	99	99	99	99	100	99	99	99	99	77	100
APR	99	99	99	89	100	100	99	100	99	87	99
MAY	98	97	97	98	99	96	100	99	80	100	98
JUN	96	97	97	100	69	99	94	72	94	96	92
JUL	96	94	92	100	68	93	93	93	65	100	98
AUG	97	94	92	100	78	99	99	100	99	90	100
SEP	98	97	97	99	73	99	99	99	99	100	100
OCT	99	97	97	100	97	100	99	99	100	83	100
NOV	96	97	98	100	99	100	99	87	99	96	95
DEC	90	99	99	99	98	99	90	67	41	78	71
1978											
JAN	83	93	93	97	98	58	14	70	1	33	17
FEB	82	91	93	100	20	0	83	7	65	86	0
MAR	96	99	99	99	59	0	99	0	96	100	0
APR	100(c)	96(c)	94(c)	100	100	58	100	58	96	100	0
MAY	100(c)	100(c)	100(c)	100	91	97	99	100	96	100	95
JUN	100(c)	90(c)	90(c)	96	85	91	96	96	96	92	80
JUL	100(c)	93(c)	93(c)	99	99	86	87	77	85	99	100
AUG	100(c)	89(c)	89(c)	100	100	100	99	99	99	86	99
SEP	100(c)	94(c)	94(c)	100	94	99	99	99	99	88	98
OCT	100(c)	99(c)	99(c)	86	94	86	99	86	99	83	100
NOV	100(c)	95(c)	95(c)	99	90	99	96	100	81	100	100
DEC	88(d)	76(d)	69(d)	100	100	73	75	94	78	92	83

Appendix B. Percent Data Recovery By Month and Variable (cont.)

1979	Precip.	Temp.	Rel. Hum.	Solar Radiation		Wind Direction		Wind Speed		Visibility	
	(Network)	(Network)	(Network)	P03A	P07A	P03A	P07A	P03A	P07A	P03A	P07A
JAN	52	67	61	100	87	69	61	80	73	77	58
FEB	80	84	84	99	99	97	97	99	90	100	98
MAR	85(e)	96(e)	96(e)	100(f)	100(g)	99(f)	100(g)	93(f)	81(g)	98(f)	92(g)

(a) beginning 10 May

(b) beginning 17 May

(c) P03A & P07A only

(d) P03A & P07A only through 10 Dec

(e) ending 27 Mar

(f) ending 26 Mar

(g) ending 28 Mar